

604599

ASD-TDR-62-509
VOLUME V

— 107p —

COPY	2	OF	3
HARD COPY	\$.400		
MICROFICHE	\$.075		

BERYLLIUM RESEARCH AND DEVELOPMENT PROGRAM
METALLURGICAL FACTORS AFFECTING THE DUCTILE-BRITTLE
TRANSITION IN BERYLLIUM

TECHNICAL DOCUMENTARY REPORT No. ASD-TDR-62-509, VOL. V

JULY 1964



AIR FORCE MATERIALS LABORATORY
RESEARCH AND TECHNOLOGY DIVISION
AIR FORCE SYSTEMS COMMAND
WRIGHT-PATTERSON AIR FORCE BASE, OHIO

Project No. 7351, Task No. 735104

(Prepared under Contract No. AF 33(616)-7065 by
Lockheed Missiles and Space Company, Palo Alto, California
Dr. M. I. Jacobson, author)

NOTICES

When Government drawings, specifications, or other data are used for any purpose other than in connection with a definitely related Government procurement operation, the United States Government thereby incurs no responsibility nor any obligation whatsoever; and the fact that the Government may have formulated, furnished, or in any way supplied the said drawings, specifications, or other data, is not to be regarded by implication or otherwise as in any manner licensing the holder or any other person or corporation, or conveying any rights or permission to manufacture, use, or sell any patented invention that may in any way be related thereto.

Qualified requesters may obtain copies of this report from the Defense Documentation Center (DDC), (formerly ASTIA), Cameron Station, Bldg. 5, 5010 Duke Street, Alexandria, Virginia, 22314.

This report has been released to the Office of Technical Services, U.S. Department of Commerce, Washington 25, D. C., in stock quantities for sale to the general public.

Copies of this report should not be returned to the Research and Technology Division, Wright-Patterson Air Force Base, Ohio, unless return is required by security considerations, contractual obligations, or notice on a specific document.

FOREWORD

This report was prepared under USAF Contract No. AF 33(616)-7065 with Nuclear Metals, Inc., West Concord, Massachusetts, as the prime contractor. The contract was initiated under Project No. 7351, "Metallic Materials," Task No. 735104, "Beryllium and Beryllium Alloys." The work was administered under the direction of the Metals and Ceramics Division, Air Force Materials Laboratory, Research and Technology Division, with Mr. K. L. Kojola and Capt. P. S. Duletsky acting as project engineers.

The portion of the work covered by this volume was performed under Subcontract No. 5, "Metallurgical Factors Affecting the Ductile-Brittle Transition in Beryllium," by the Metallurgy and Ceramics Laboratory, Lockheed Missiles and Space Company, Palo Alto, California. The author of this volume is Dr. M. I. Jacobson of Lockheed Missiles and Space Company.

This report covers work conducted from 1 October 1961 to 31 March 1963.

The Air Force gratefully acknowledges the assistance provided by Dr. A. R. Kaufmann of Nuclear Metals in editing this report.

Several persons at Lockheed Missiles and Space Company are deserving of thanks for the contributions they made to this project. Professor J. E. Dorn and the late A. N. Stroh acted as consultants. E. E. Underwood selected the techniques to be used for measuring grain size. Pole figure and X-ray diffraction studies were performed by R. H. Bragg, C. M. Packer, J. C. Robinson, and P. Lindquist. W. Coons prepared the photomicrographs. Special thanks are due to R. J. Huber, who performed the majority of the mechanical tests. The helpful discussions with J. L. Lytton and M. P. Gomes of the Metallurgy Laboratory are also acknowledged.

ABSTRACT

An investigation was made of the factors controlling the ductile-brittle behavior of two grades of commercial purity beryllium, Brush QMV and Pechiney CR. Tensile tests were made on randomly oriented samples at temperatures from 23°C to 500°C. Extrusions were tested in the longitudinal and transverse directions in the range -195°C to 200°C. Three grain sizes of each material were investigated, and comparisons made between specimens tested in the aged and unaged condition. The aging treatment was 900°C for 6 hours followed by 48 hours at 700°C. Mechanical properties of both materials were very similar after this heat treatment and no advantage could be claimed for the higher purity Pechiney beryllium. Aging reduced the amount of impurities in solid solution and contributed to improved ductility in certain temperature ranges. In general, the transition temperature was lower the smaller the grain size, the slower the strain rate, and the purer the material. Lower transition temperatures were observed for the longitudinal and transverse directions of the extrusions than for the hot-pressed, randomly oriented specimens.

The ductile-brittle transition could not be described in terms of the dislocation pileup theories for body-centered-cubic metals. A theory of the ductile-brittle transition based on the thermally activated cross slip of screw dislocations from the basal plane into pyramidal or prismatic planes was proposed. The data could be described reasonably well in terms of this theory.

This technical documentary report has been reviewed and is approved.



I. PERLMUTTER

Chief, Physical Metallurgy Branch
Metals and Ceramics Division
Air Force Materials Laboratory

TABLE OF CONTENTS

<u>Section</u>	<u>Page</u>
1 INTRODUCTION	1
1.1 Nature of the Investigation	1
1.2 Results of Previous Investigations	2
2 EXPERIMENTAL PROCEDURE	3
2.1 Material	3
2.2 Specimen Preparation	3
2.3 Mechanical Testing	8
2.4 Metallographic and X-Ray Analysis	9
3 RESULTS	13
3.1 Grain Size Measurements	13
3.2 Pole Figures	13
3.3 Tensile Tests	13
3.3.1 Tests on Hot-Pressed Material	17
3.3.2 Tests on Extruded Material	27
4 DISCUSSION OF RESULTS	45
4.1 General Discussion of Tensile Data	45
4.1.1 Hot-Pressed Material	45
4.1.2 Extruded Material	50
4.2 Ductile-Brittle Transition Theory	52
4.2.1 Theory of Cottrell	53
4.2.2 Stroh's Theory of Probability of Brittle Fracture	54
4.2.3 Proposed Theory of the Ductile-Brittle Transition in Beryllium	58
5 SUMMARY AND CONCLUSIONS	66
6 REFERENCES	67
APPENDIX I - EFFECT OF STRAIN RATE ON MECHANICAL PROPERTIES OF HOT-PRESSED PLOCK	71

LIST OF ILLUSTRATIONS

<u>Figure</u>	<u>Page</u>
1 Dimensions of tensile specimens	6
2 Location of test specimens in extruded bar	7
3 Microstructure of hot-pressed Pechiney, $d = 11$ microns. 500X. Polarized light	10
4 Microstructure of hot-pressed Brush, $d = 18.9$ microns. 500X. Polarized light	10
5 Transverse section of Brush extrusion, $d_1 = 6.07$ microns. Black line used for orientation purposes in grain size measurements. 500X. Polarized light	11
6 Longitudinal section of Brush extrusion, $d_1 = 6.07$ microns. 500X. Polarized light	11
7 Transverse section of Pechiney extrusion, $d_1 = 6.57$ microns. 500X. Polarized light	12
8 Longitudinal section of Pechiney extrusion, $d_1 = 6.57$ microns. 500X. Polarized light	12
9 (0002) pole figure for extrusion fabricated from -150 +200 mesh Brush QMV powder. Numbers indicate intensity, times random	15
10 (10 $\bar{1}$ 0) pole figure	16
11 Tensile strength of hot-pressed beryllium	19
12 Yield strength of hot-pressed beryllium	20
13 Elongation of hot-pressed beryllium	21
14 Reduction in area of hot-pressed beryllium	22
15 Comparison of mechanical properties of hot-pressed Brush and Pechiney beryllium in the aged condition	24
16 True stress vs. true strain curves for hot-pressed Brush	25
17 True stress vs. true strain curves for hot-pressed Pechiney	26
18 Effect of strain rate on mechanical properties of unaged, hot-pressed Brush, $d = 9.7$ microns	28

LIST OF ILLUSTRATIONS (Continued)

<u>Figure</u>		<u>Page</u>
19	Effect of strain rate on mechanical properties of aged, hot-pressed Brush, $d = 9.7$ microns	29
20	Effect of strain rate on mechanical properties of unaged, hot-pressed Pechiney, $d = 10.3$ microns	30
21	Effect of strain rate on mechanical properties of aged, hot-pressed Pechiney, $d = 10.3$ microns	31
22	Tensile strength of Brush extrusions	34
23	Tensile strength of Pechiney extrusions	35
24	Yield strength of Brush extrusions	36
25	Yield strength of Pechiney extrusions	37
26	Elongation of Brush extrusions	38
27	Elongation of Pechiney extrusions	39
28	Comparison of mechanical properties of aged Brush and Pechiney extrusions tested in the transverse direction	41
29	True stress vs. true strain curves for unaged Brush extrusions tested at 23°C	42
30	True stress vs. true strain curves for unaged Brush extrusions tested at -195°C	43
31	Twinning in central portion of longitudinal Brush specimen tested at -195°C . 100X. Polarized light	44
32	Central portion of transverse Brush specimen tested at -195°C . 100X. Polarized light	44
33	True stress vs. true strain curves for Brush extrusions at various temperatures, $d_1 = 6.07$ microns	46
34	True stress vs. true strain curves for Pechiney extrusions at various temperatures	47
35	Region adjacent to fracture surface of unaged, hot-pressed Pechiney specimen tested at 300°C , $d = 10.3$. 100X	49
36	Region adjacent to fracture surface of aged, hot-pressed Pechiney specimen tested at 300°C , $d = 10.3$. 100X	49

LIST OF ILLUSTRATIONS (Continued)

<u>Figure</u>		<u>Page</u>
37	Effect of grain size on yield strength of hot-pressed Brush tensile specimens	55
38	Effect of grain size on yield strength of extruded Brush tensile specimens	56
39	$\ln d$ vs. $1/T_c$ plots for Brush beryllium	59
40	Work hardening rates at 1 per cent strain for hot-pressed beryllium	60
41	Flow stress at 0.05 and 1.0 per cent strain for hot-pressed Brush, $d = 9.7$ microns	61
42	Work hardening rates at 1 per cent for extrusions tested in the transverse direction	63

LIST OF TABLES

<u>Table</u>		<u>Page</u>
1	COMPOSITION AND SIZE DISTRIBUTION OF BRUSH QMV POWDER	4
2	COMPOSITION OF PECHINEY CR POWDER	5
3	GRAIN SIZE FOR HOT-PRESSED BLOCKS	14
4	GRAIN SIZE FOR EXTRUDED FLATS	14
5	EFFECTS OF AGING TREATMENTS ON PROPERTIES OF HOT-PRESSED BLOCK	18
6	EFFECT OF PRESTRAIN AT ELEVATED TEMPERATURE ON ROOM TEM- PERATURE MECHANICAL PROPERTIES OF UNAGED HOT-PRESSED BLOCK	32
7	EFFECT OF STRAIN RATE ON MECHANICAL PROPERTIES OF BRUSH HOT-PRESSED BLOCK	72
8	EFFECT OF STRAIN RATE ON MECHANICAL PROPERTIES OF PECHINEY HOT-PRESSED BLOCK	74

Section 1

INTRODUCTION

Nature of the Investigation

Ductility in beryllium is controlled by two primary factors: (1) conditions imposed in testing, and (2) processing variables. These may be further subdivided as follows:

1. Conditions imposed in testing
 - (a) temperature
 - (b) strain rate
 - (c) environment, i.e., air, inert gas, or vacuum
2. Processing variables
 - (a) orientation (controlled by fabrication procedure)
 - (b) grain size
 - (c) purity
 - (d) thermal treatments
 - (e) surface condition
 - (f) method of consolidation (i.e., powder, cast)

The purpose of this investigation was to determine the effects of some of these variables on the ductile-brittle transition and to consider the transition from a theoretical viewpoint. Two grades of commercial purity powder metallurgy beryllium were studied, Brush QMV and Pechiney CR, the latter being of higher purity. Tensile specimens with randomly oriented grains were machined from hot-pressed blocks of each material, and specimens with preferred orientations from extruded flats. Grain size was varied by using three different mesh sizes of powder for fabricating the hot-pressed blocks and the extrusions. Thermal treatment consisted of a solution treatment at 900°C for 6 hours, followed by precipitation for 48 hours at 700°C. Samples given this treatment are referred to as "aged", while those not so treated are "unaged". Test temperature varied from room temperature to 500°C for the randomly oriented samples, and from -195°C to 200°C for the extrusions. Strain rate was varied for the hot-pressed samples only, with tests being made at strain rates of 0.0033, 0.033, and 0.33 per minute. A limited investigation was made of the effects of prior strain at elevated temperature on the room temperature properties of hot-pressed material.

This would be effective in improving ductility if dislocations, locked by impurity atmospheres at low temperature, could be freed from their atmospheres at high temperature.

Environment, surface condition, and method of consolidation were not variables in this study. As it was, mechanical property data were obtained on some 400 tensile specimens. Analysis of the data led to a proposed mechanism for the ductile-brittle transition in beryllium.

1.2 Results of Previous Investigations

For any given temperature, ductility (as measured by elongation and/or reduction in area in a tensile test) is affected by strain rate and all of the processing variables previously listed. This has led to the publication of numerous curves of elongation vs. temperature that show one feature in common, a ductile-brittle transition in the region 0-150°C, and a maximum in the ductility vs. temperature curve at about 300-500°C (Refs. 1-13).

The effects of strain rate on beryllium are rather well known. In general, under conditions producing transcrystalline fracture, ductilities increase with decreasing strain rate (Refs. 1, 6, 8), and transition temperature increases with increasing strain rate. The role of test environment has not been studied extensively, although it has been mentioned as one factor that might influence the shape of the temperature-elongation curve (Ref. 1).

The relation of crystallographic orientation to ductility has been adequately covered by several authors (Refs. 11-20) and no attempt will be made to review this subject here. The general conclusion is that when basal planes are oriented so that little or no basal slip takes place, suitable ductilities can be obtained in one or two dimensions. Limited three-dimensional ductility has been attained in hot-upset sheet (Refs. 20, 21) in which the basal plane texture (planes parallel to the plane of the sheet) is relatively low, and in which there is no preferred crystallographic direction in the plane of the sheet, as there is in normal cross-rolled sheet.

Grain size was studied by Beaver and Wickle (Ref. 1), who found that small grain size produces better elongation when fracture is primarily transgranular. Greenspan (Ref. 19) showed that the room temperature strength of basal-plane-layered beryllium increased as grain size decreased. Bunce and Evans (Ref. 12) found that the transition temperature decreased as grain size decreased.

Considerable controversy exists as to the exact role of impurities in beryllium, although recent evidence supports the conclusion that ductility can be affected by impurities over a wide range of temperature. Mash (Ref. 22) investigated the use of aging effects to improve the ductility of beryllium, as did Bennett (Ref. 5), Gelles, et al (Ref. 23), and Wolff, et al (Ref. 24). Bunce and Evans (Ref. 12) found that aging at 700°C for 200 hours improved the ductility of extruded beryllium tested in the 20-400°C range. The purification of beryllium by zone refining has resulted in a lowering of the critical resolved shear stress for both basal and prismatic slip (Refs. 11, 25), with

basal slip far more sensitive to impurity content. Sheet prepared from vacuum distilled beryllium has also shown improved ductility in the 20-400°C range (Ref. 26).

Another factor affecting the ductility is surface condition. Several authors have shown that elimination of the twins and cracks produced in the machining of test samples results in considerable improvement in ductility (Refs. 2, 27, 28).

The ductility of beryllium is thus seen to be governed by a number of variables, making it a difficult subject for study.

Section 2

EXPERIMENTAL PROCEDURE

2.1 Material

The powder for this investigation was acquired from the Brush Beryllium Company and the Pechiney Company, each of which supplied three mesh sizes attritioned from a single ingot. Analyses and mesh sizes as supplied by the manufacturers are shown in Tables 1 and 2. Where direct comparisons of metallics are available, the Pechiney powder is an order of magnitude purer, although the BeO content is similar for both materials. Of the impurities present in relatively large amounts (namely, aluminum, iron, nickel, and BeO), the percentages increased as mesh size decreased. This factor will be taken into account in the final analysis of the data.

Each batch of powder was fabricated at Nuclear Metals into one hot pressing (4-inch diameter by 3 inches high) and one extruded flat (approximately 3 inches wide by $\frac{1}{2}$ inch thick by 20 inches long). The hot pressed cylinders and the extrusion billets were both prepared by compacting the powder in mild steel cans, evacuating the cans, and heating to 1950°F. Reduction in area on extrusion was 8:1. Some of the extrusions required excessive cropping to assure sound material and, as a result, fewer than the planned number of tensile specimens could be machined.

2.2 Specimen Preparation

Round bar tensile specimens with tapered ends, as shown in Figure 1, were machined from the hot-pressed blocks with the axes of the specimens parallel to the pressing direction. Specimens cut from the extrusions were in two orientations: (a) longitudinal, with the specimen axis parallel to the extrusion direction, and (b) transverse, with the specimen axis at 45 degrees to the extrusion direction (Figure 2). These orientations were such that the longitudinal samples would deform primarily by slip on the {1010} prism plane, and the transverse samples by slip on the basal plane.

Table 1

COMPOSITION AND SIZE DISTRIBUTION OF BRUSH QMV POWDER

Element	<u>Analysis, ppm</u>		
	<u>-60 + 80 mesh</u>	<u>-150 + 200 mesh</u>	<u>-325 mesh</u>
Al	500	600	1300
Fe	1300	1500	1500
Mg	200	200	200
Si	400	400	400
C	800	900	800
BeO	0.41%	0.57%	1.4%

<u>Nominal mesh size</u>	<u>Actual Distribution</u>	
	<u>mesh</u>	<u>%</u>
-60 + 80	+60	0.4
	-60 + 70	38.5
	-70 + 80	46.5
	-80 + 100	10.6
	-100	4.0
150 + 200	+140	8.7
	-140 + 170	30.7
	-170 + 200	34.3
	-200	26.3
-325	+325	1.2
	-325 + 400	14.3
	-400	84.3

Table 2

COMPOSITION OF PECHINEY CR POWDER

<u>Element</u>	<u>Analysis, ppm</u>		
	<u>-50 + 120 mesh</u>	<u>-120 + 200 mesh</u>	<u>-200 + 350 mesh</u>
Al	70	100	190
Ag	< 3	< 3	< 3
B	1	1	1
Cd	< 2	< 2	< 2
Ca	100	90	75
C	260	210	280
Cr	10	< 10	30
Cu	60	90	35
Fe	155	195	300
Cl	< 20	< 20	< 20
Mg	< 10	< 10	< 10
Mn	7	5	9
Mo	< 15	< 15	< 15
Ni	152	205	230
Pb	< 15	< 15	< 15
BeO	0.42%	0.68%	1.17%

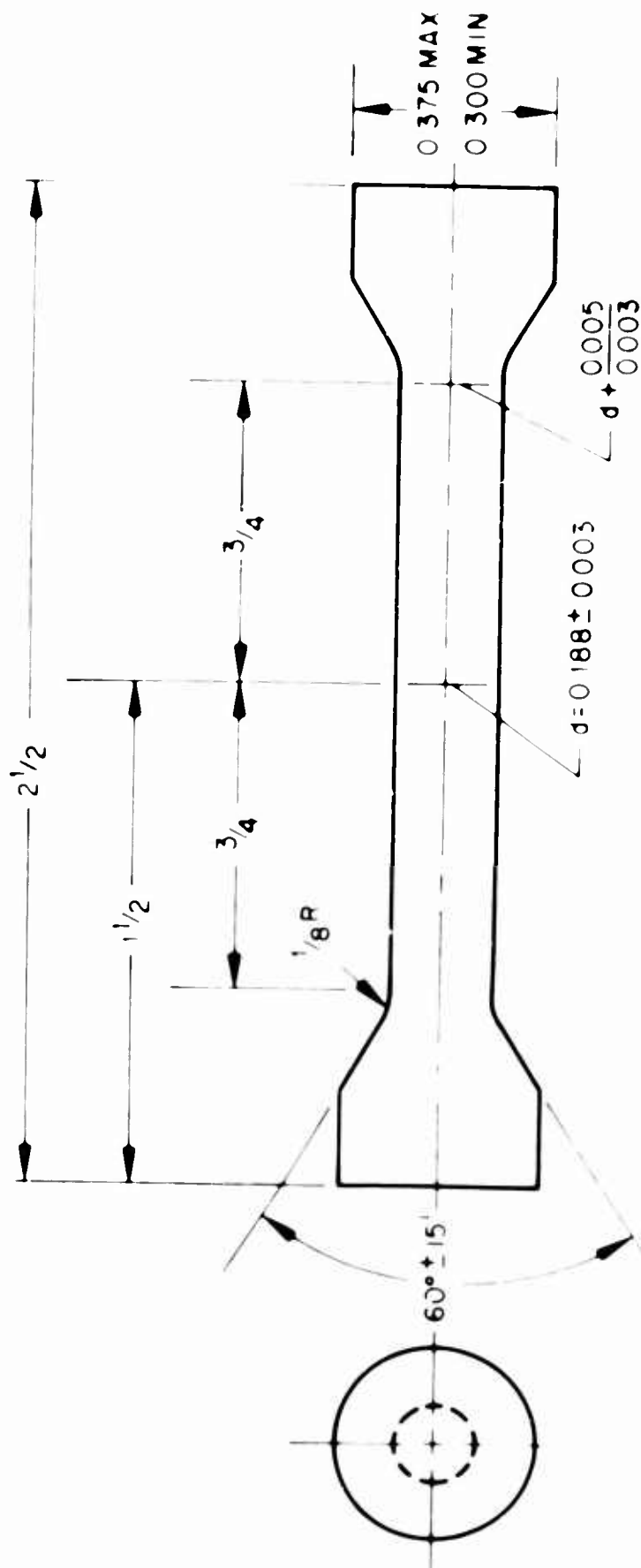


Figure 1 - Dimensions of tensile specimens.

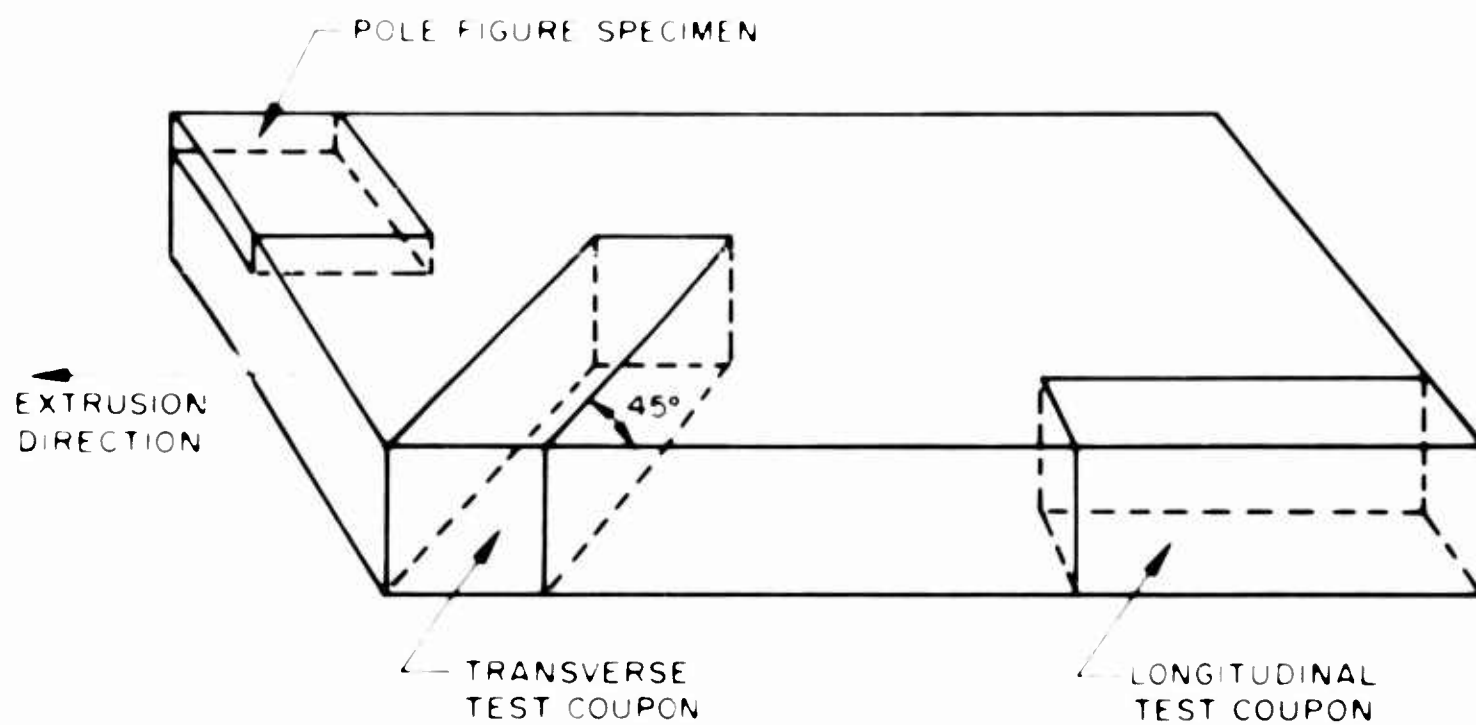


Figure 2 - Location of test specimens in extruded bar.

Previous work by Greenspan (Ref. 19) had indicated that in an extruded flat, basal planes would be aligned parallel to the extrusion direction, with the poles of the basal plane concentrated at approximately 75 to 90 degrees from the large surface of the extrusion. Thus, the transverse test samples cut at 45 degrees to the extrusion direction, as shown in Figure 2, were expected to have the basal planes aligned in the direction of maximum shear stress in a tensile test, i.e., at 45 degrees to the tensile axis. As will be shown subsequently, basal planes in the current extrusions were parallel to the extrusion direction, but concentrated at 45 degrees to the large surface, so that the resulting angle between the tensile axis and the basal planes was only 30 degrees. However, flow would still be expected to occur preferentially on the basal planes because of the large difference in flow stress between the basal and prismatic planes at low temperatures.

The specimens machined from hot-pressed block were annealed for 1 hour at 700°C to remove residual stresses introduced in machining. Since the blocks had been slow cooled after sintering, this treatment should have had little, if any, effect on redistribution of impurities. On the other hand, the extruded specimens were cooled at a comparatively rapid rate after extrusion, and heating for 1 hour at 700°C might have constituted an aging treatment. For reasons to be discussed subsequently, residual machining stresses were not a problem in the extruded material. All samples were chemically polished to remove 4 to 5 mils from the surface in a solution of 450 ml H_3PO_4 , 25 ml H_2SO_4 , and 53 g chromium trioxide at 100-120°C. Finally, the samples were electropolished to remove an additional 1 to 2 mils in a solution of 1000 ml ethylene glycol, 100 ml HNO_3 , 20 ml HCl , and 20 ml H_2SO_4 .

2.3 Mechanical Testing

Tensile tests were performed on a 10,000 lb. Instron machine operated at a basic crosshead speed of 0.005 inch/min. The grips were split and machined with a tapered recess to match that on the tensile specimens. Initially, tests on hot-pressed block in the region 100-200°C were made with the specimens immersed in a stirred silicone oil bath. At 300°C, a Marshall, creep-type, solid shell tube furnace was used. In either case, inserting and removing specimens from the machine was inconvenient and time consuming. All subsequent elevated temperature tests were made in a split-tube furnace, with a heating section 12 inches long and 2 inches diameter. It was mounted so that both halves swung away from the specimen, permitting easy access. A chromel-alumel thermocouple wired to the specimen acted as the temperature-controlling thermocouple. Temperature was maintained to $\pm 5^\circ\text{C}$ by a Leeds and Northrup Speedomax controller, and specimens were held at temperature for 10 minutes prior to testing.

Subzero tests were made by immersing the specimens in various media. Liquid nitrogen was used at -195°C . Initially, dry ice - acetone was used for -75°C , but some anomalously low ductilities were observed and it was thought that the acetone might in some way be embrittling. Therefore, subsequent tests in the region -75°C to -150°C were made in isopentane cooled with a copper coil containing liquid nitrogen. Temperatures were measured with a chromel-alumel thermocouple wired to the specimens.

Load extension curves were obtained for each specimen, with crosshead motion serving as a measure of the extension. The assumption was made that deformation was confined to the 1.5 inch reduced section of the samples and elongation is thus reported as percent in 1.5 inches. Several samples were tested with an extensometer attached to the gage section and the elongations agreed closely with those obtained by measuring crosshead separation. As an additional check, overall sample length was measured before and after testing and the change in sample length was found to agree favorably with the amount of plastic deformation indicated on the load-extension chart.

2.4 Metallographic and X-Ray Analysis

Metallographic sections were prepared for each hot-pressed block and each extrusion so that the structure could be examined and the grain size measured. The polishing procedure was similar to that used previously (Ref. 28), and typical structures are shown in Figures 3 through 8.

For the randomly oriented hot-pressed block, three 500x photographs were made of each specimen. Ten 5 cm traverses were made at various angles across each photograph, and the number of grain boundaries intersected per unit length of this random line, N_L , was recorded. The reciprocal, d , is the mean intercept diameter of the polycrystalline aggregate, and, for equiaxed grains, is the true three-dimensional intercept grain diameter.

Since the grains for the extruded material were not equiaxed, it was necessary to make measurements in more than one plane. Three 500x photographs were made at random locations on each of the three mutually perpendicular faces of an extruded flat, as shown in the sketch accompanying Table 4. On each photograph, three traverses of 20 cm each were made in the direction indicated and N_L measured. From these, values of d_1 , d_2 , and d_3 were calculated, characterizing the dimensions of the grains in relation to the extrusion axes.

A (0002) and $\{10\bar{1}0\}$ pole figure were made for the Brush extrusion fabricated from -150 +200 mesh powder. The basic techniques for obtaining quantitative measurements are described in Refs. 29, 30, and 31. The pole figure specimen was about 1 inch square and 0.3 inch thick, and was cut from the extrusion as shown in Figure 2. A GE pole figure device was used in conjunction with a GE XRD-5 diffraction unit to measure diffracted intensities.

As mentioned in Ref. 28, certain problems arise because of the deep penetration of X-rays in beryllium. Among these are the overlapping of the (0002) and $\{10\bar{1}1\}$ reflections, and the "blind" regions in the pole figure caused by the diffracted beam being blocked by the specimen holder. Special analyses were applied to the data to correct for the low absorption effects and to resolve the (0002) and $\{10\bar{1}1\}$ lines. Both the (0002) and (0004) reflections (which have different blind regions) were measured and matched to overcome the limitations imposed by the specimen holder. Copper $K\alpha$ radiation was used for both the transmission and reflection portions of the pole figure.

Admittedly, it would have been desirable to have completed the pole figure prior to machining the specimens. However, the program would have been unduly delayed if this had been done.

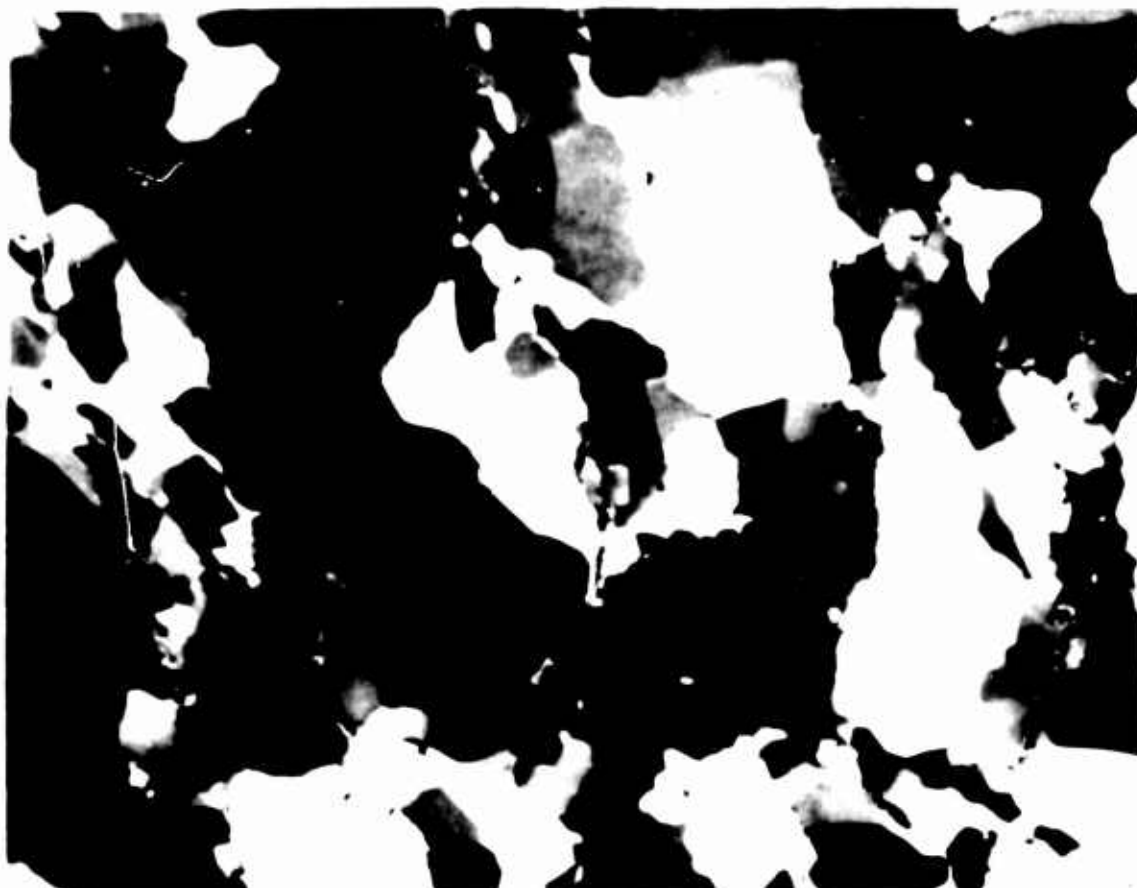


Figure 3 - Microstructure of hot pressed Pechiney, $d = 11$ microns.
500X. Polarized light.

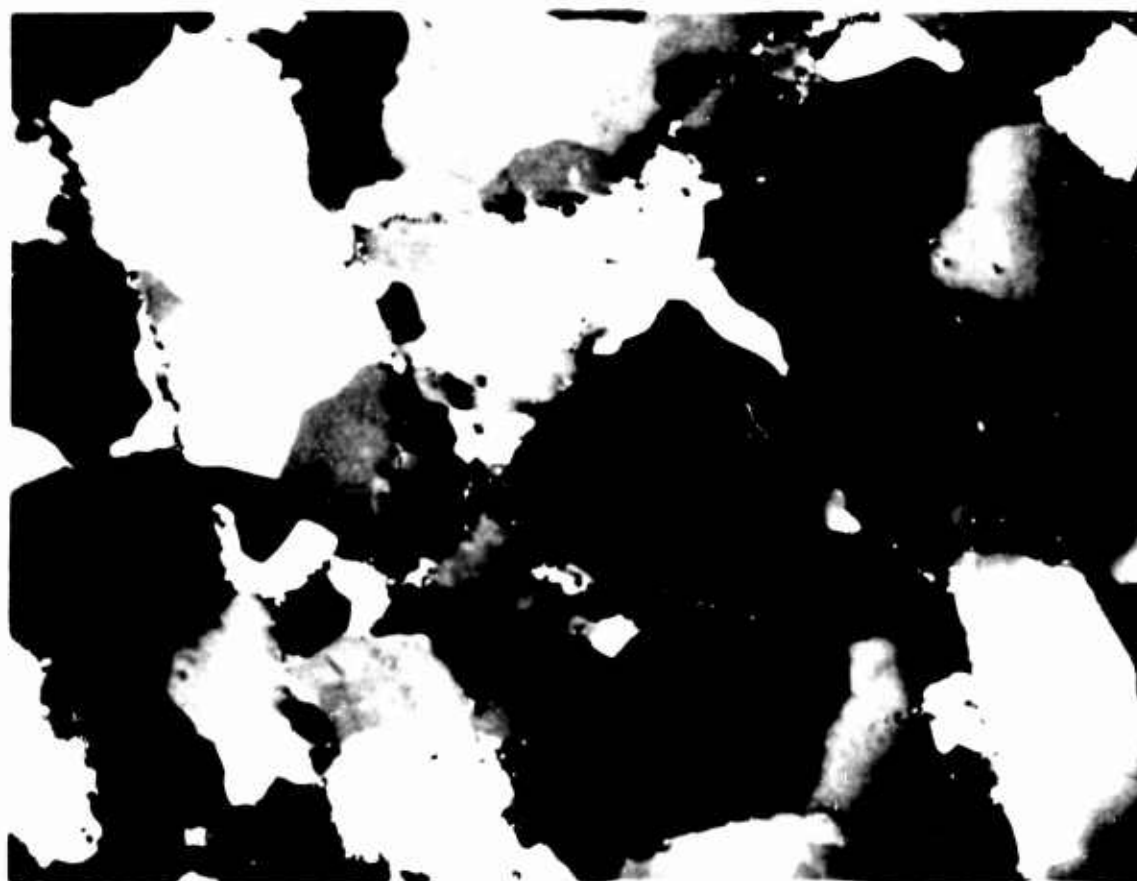


Figure 4 - Microstructure of hot pressed Brush, $d = 18.9$ microns.
500X. Polarized light.

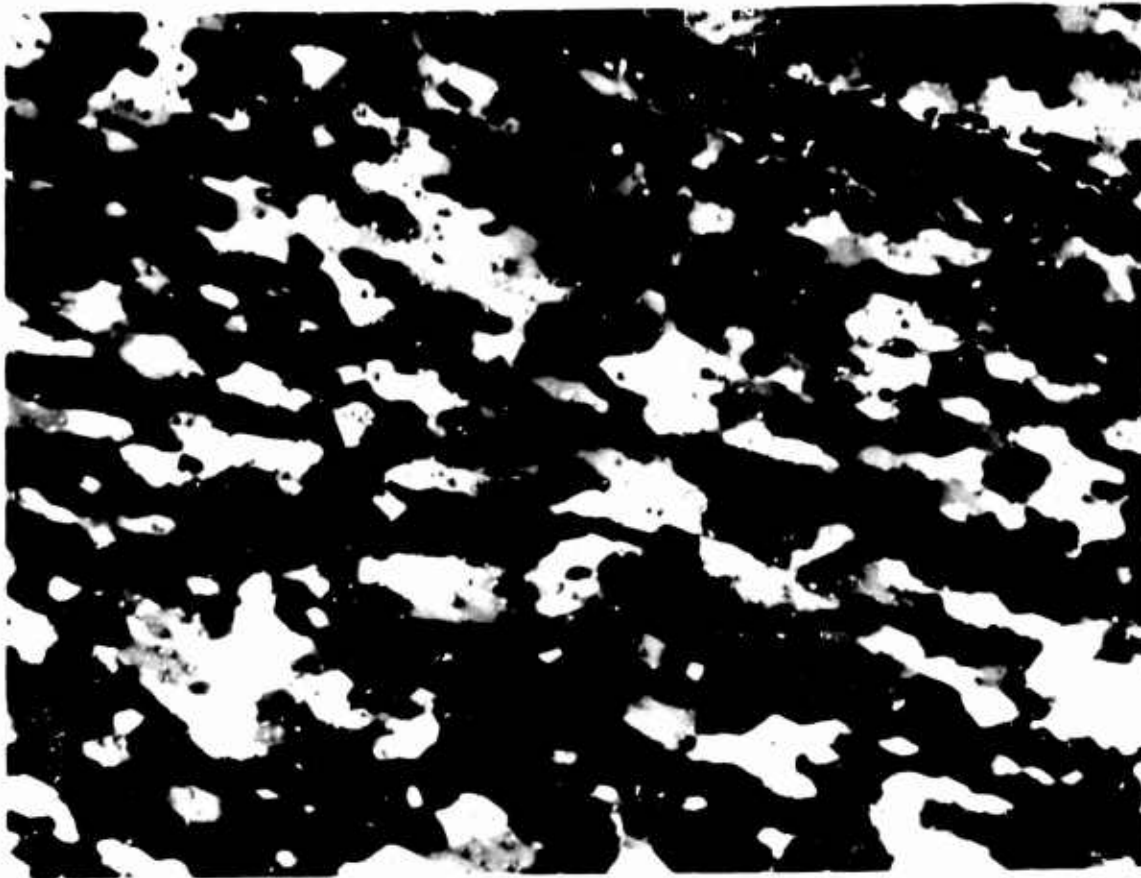


Figure 5 - Transverse section of brush extrusion, $d_1 = 6.07$ microns. Black line used for orientation purposes in grain size measurements. 500X. Polarized light.

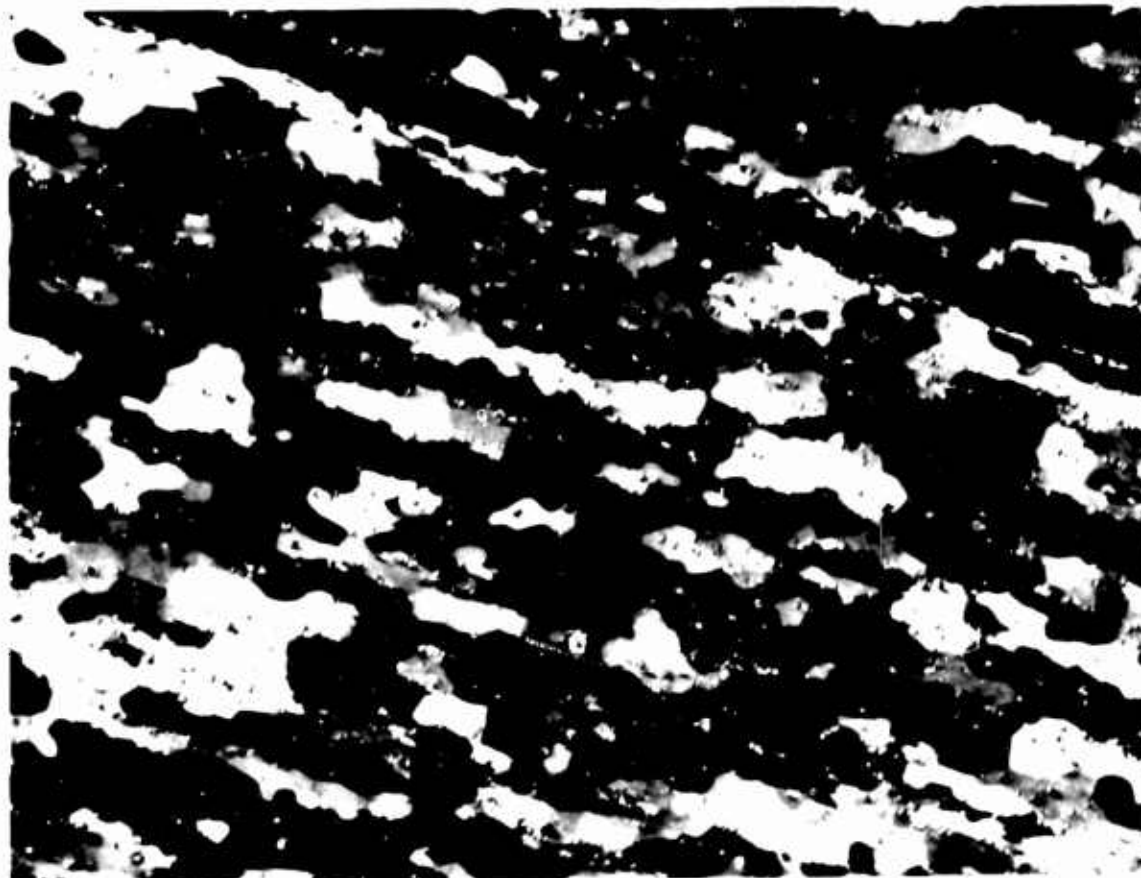


Figure 6 - Longitudinal section of brush extrusion, $d_1 = 6.07$ microns. 500X. Polarized light.

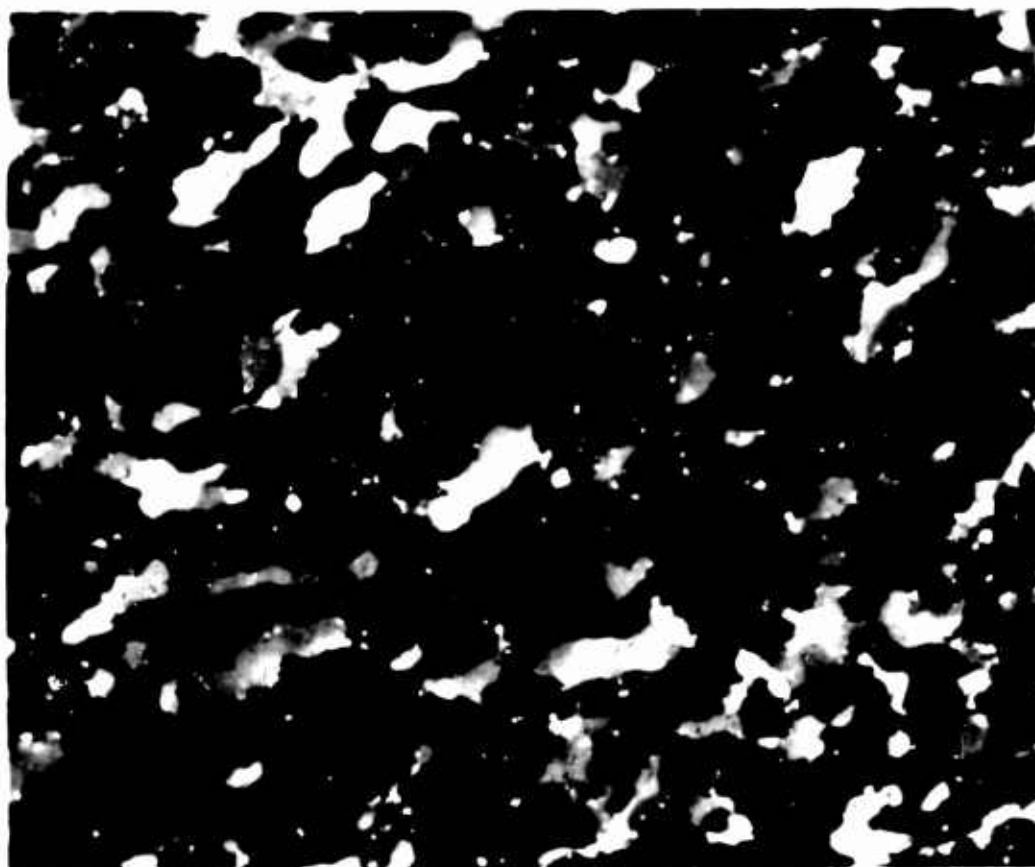


Figure 7 - Transverse section of Pechiney extrusion, $d_1 = 6.57$ microns. 500X. Polarized light.

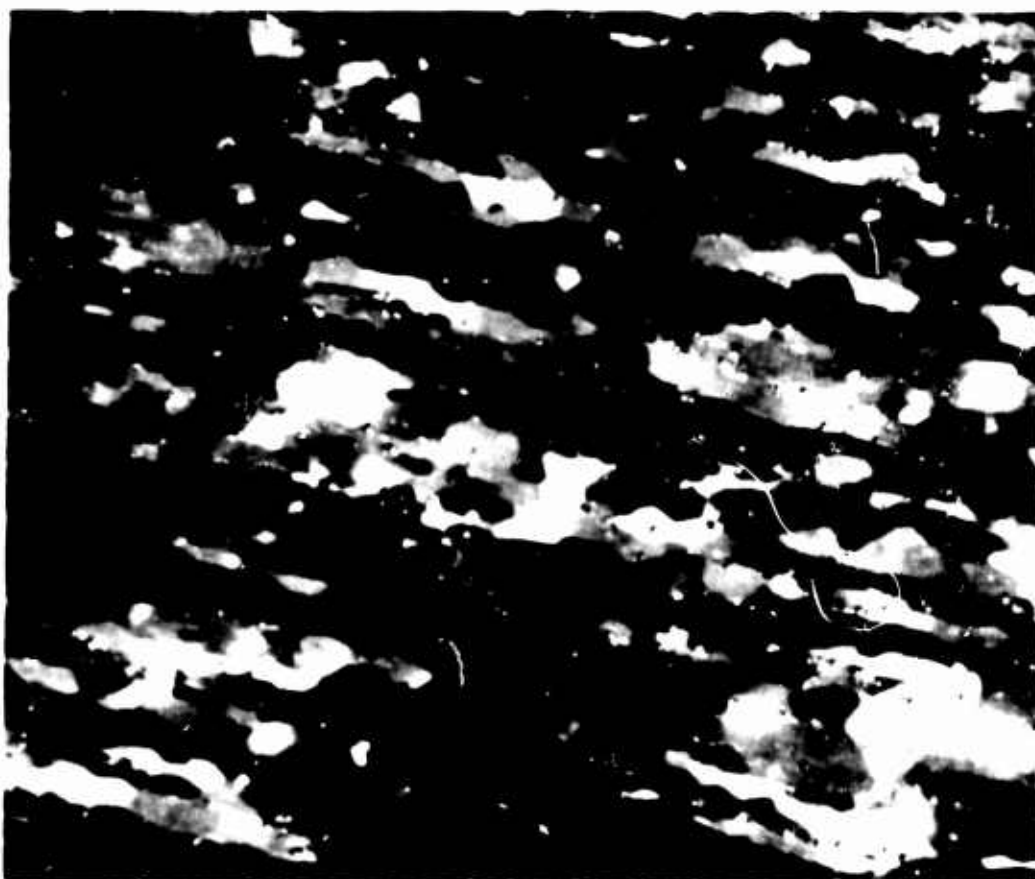


Figure 8 - Longitudinal section of Pechiney extrusion, $d_1 = 6.5$ microns. 500X. Polarized light.

Section 3

RESULTS

3.1 Grain Size Measurements

Results of the measurements of grain size in the hot-pressed and the extruded material are shown in Tables 3 and 4. The grain size values for the Pechiney samples extend only over a small range. As will be seen later, this made it difficult to compare mechanical properties of the Pechiney samples on the basis of grain size. The smallest d values for the Brush and Pechiney materials were sufficiently alike that any differences in properties could probably be attributed to differences in purity.

3.2 Pole Figures

The basal and prismatic pole figures for the -150 +200 mesh Brush extrusion are presented in Figures 9 and 10. The basal pole figure shows a dual texture, with the basal poles concentrated at approximately 45 degrees to the transverse direction. The prism pole figure has a very strong {1010} texture parallel to the extrusion direction, as is normally observed.

The pole figure is assumed to be representative of all of the extrusions. Unfortunately, funds were insufficient for analyses of the other samples.

3.3 Tensile Tests

The study of the ductile-brittle transition in beryllium required testing at several temperatures. The temperatures were selected somewhat arbitrarily, since it was not known beforehand where the transition would occur, if at all. This resulted in the hot-pressed samples being tested from room temperature to 500°C, and the extruded samples from -195°C to 200°C. Subsequent analysis of the data showed that it would be desirable, although not essential, to overlap and extend these regions further to provide a more thorough understanding of the deformation processes in beryllium. Notwithstanding, sufficient information was obtained to permit a reasonable explanation of the nature of the transition.

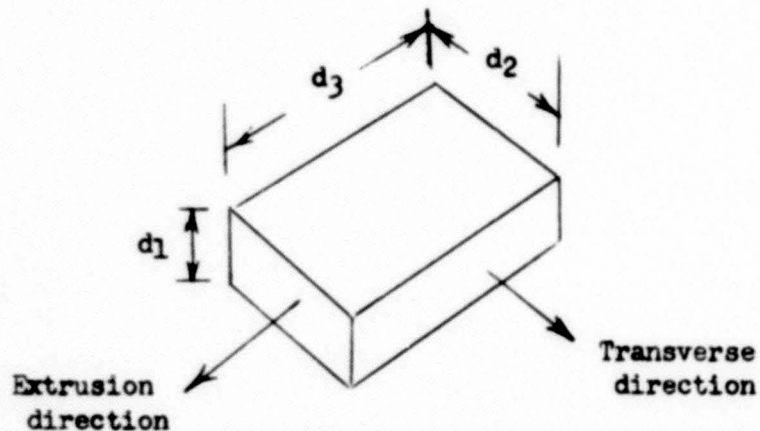
Tensile specimens were tested in two conditions, which will be referred to as unaged and aged. The unaged specimens were essentially in the as-received condition, except for the 700°C stress-relief anneal for the hot-pressed material. In selecting an aging treatment, the idea in mind was not to strengthen the lattice, but to soften it by rejecting impurity atoms from solution, agglomerating them in the form of non-coherent precipitates, and thereby improving ductility. Because of the extensive test program scheduled, there were relatively few specimens available to test the effects of various heat treatments, and it was thought advisable to try aging treatments that previous investigators had successfully used to improve properties. In 1955, Mash (Ref. 22) reported that the ductility of hot-pressed QMV beryllium could be raised from 1 percent to about 5 percent by heating for 6 hours at 800°C and furnace cooling; or by heating at 800°C for 1 hour, air cooling, and then heating at 600°C for 40 minutes. Samples of hot-pressed Brush and Pechiney were therefore

Table 3
GRAIN SIZE FOR HOT-PRESSED BLOCKS

<u>Designation</u>	<u>Source</u>	<u>Nominal Mesh Size</u>	<u>d (μ)</u>
PEC-1	Pechiney	- 50 + 120	13.2
PEC-2	"	-120 + 200	11.0
PEC-3	"	-200 + 350	10.3
QMV-4	Brush	- 60 + 80	26.5
QMV-5	"	-150 + 200	18.9
QMV-6	"	-325	9.7

Table 4
GRAIN SIZE FOR EXTRUDED FLATS

<u>Designation</u>	<u>Source</u>	<u>Nominal Mesh Size</u>	<u>d₁(μ)</u>	<u>d₂(μ)</u>	<u>d₃(μ)</u>
PEC-4	Pechiney	- 50 + 120	8.02	10.6	12.2
PEC-5	"	-120 + 200	8.09	11.6	12.1
PEC-6	"	-200 + 350	6.57	8.23	11.2
QMV-1	Brush	- 60 + 80	14.5	17.6	17.4
QMV-2	"	-150 + 200	9.59	13.2	14.4
QMV-3	"	-325	6.07	8.69	7.87



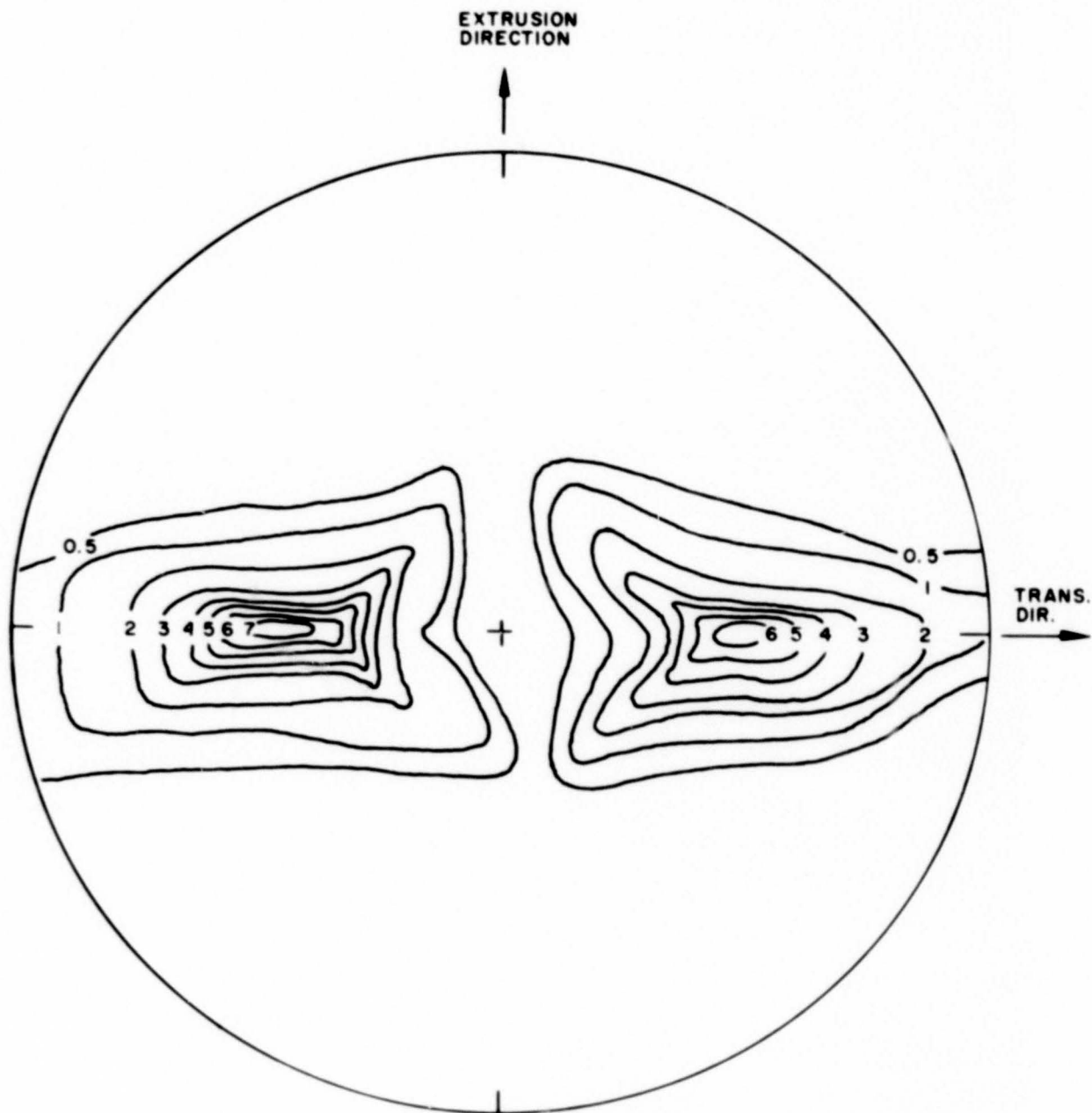


Figure 9 - (0002) pole figure for extrusion fabricated from -150 + 200 mesh Brush QMV powder. Numbers indicate intensity, times random.

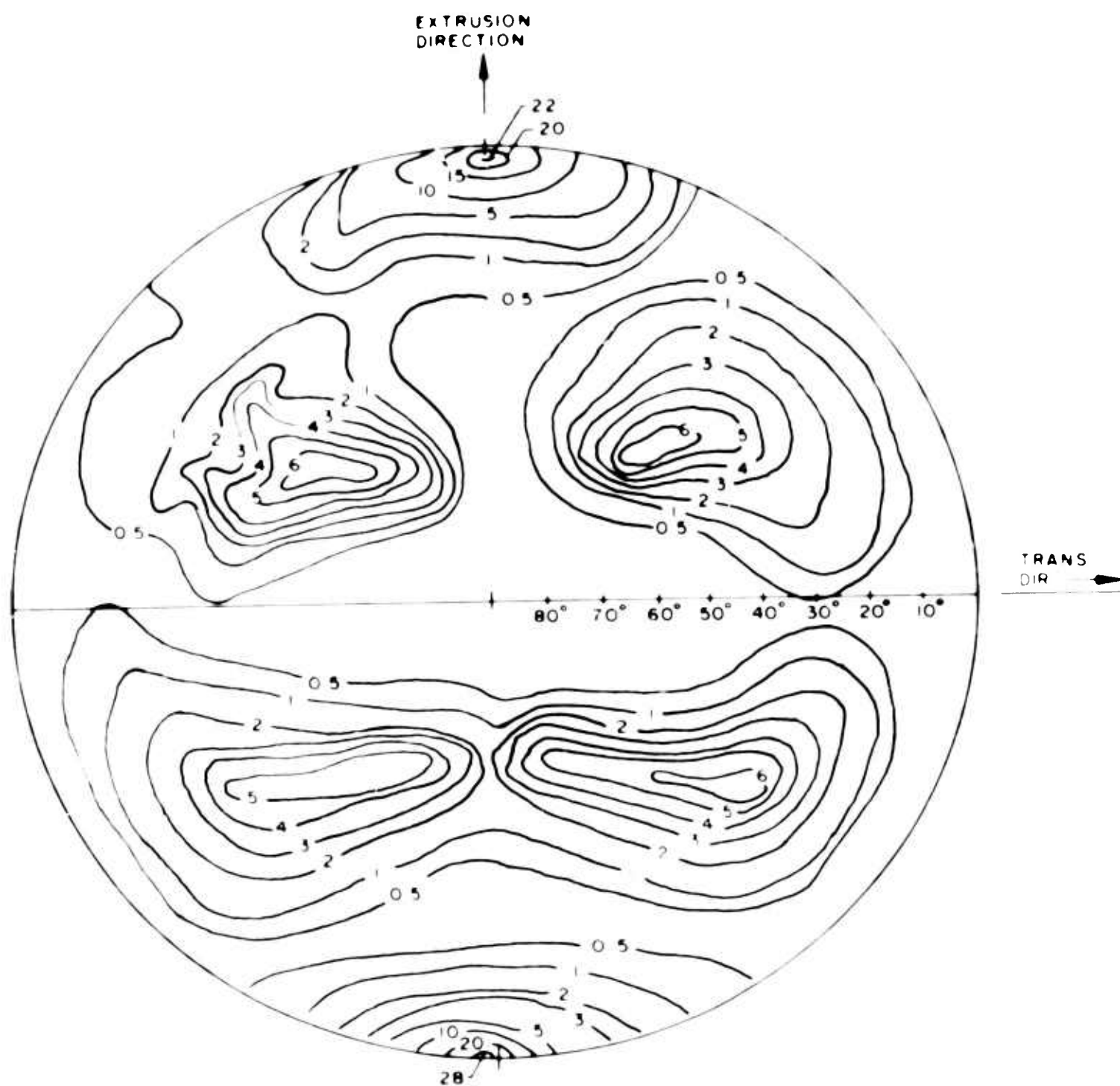


Figure 10 - $(10\bar{1}0)$ pole figure.

treated in this manner in a vacuum annealing furnace maintained at approximately 5×10^{-5} mm of Hg, after which they were polished as described previously and tested in tension at room temperature, with the results shown in Table 5.

Examination of the data reveals that no significant alteration of properties resulted from these heat treatments. Wolff, et al (Ref. 24) found that the ductility of rod extruded from Brush QMV powder was lowered by heating at 1100°C for 1 hour and water quenching; however, ductility could be restored by prolonged aging at 700°C . A similar schedule was therefore applied to the present hot-pressed material. The solution treatment was 1 hour at 1000°C , which was felt to be sufficiently high to dissolve most of the metallic impurities. The samples were cooled rapidly in a stream of argon and then annealed for 96 hours at 700°C . Again, as shown in Table 5, no improvement in ductility was noted.

In an investigation of intermetallic phases in commercial beryllium, Rooksby (Ref. 32) reported that a cubic phase identified as $\text{Be}_5(\text{Fe}, \text{Al})$, with lattice parameter $a_0 = 6.057\text{\AA}$, could be formed by solution treating for 6 hours at 900°C and aging at 700°C . Rooksby also found a Be_{11}Fe structure, which is hexagonal, with $a = 4.13\text{\AA}$ and $c = 10.72\text{\AA}$. Samples in the present investigation were heated for 6 hours at 900°C , rapidly cooled in a stream of argon, and aged for 48 hours at 700°C . Results of tension tests of these samples are also shown in Table 5, and again, there were no improvements in ductility. X-ray diffraction studies of these aged samples revealed the presence of $\text{Be}_5(\text{Fe}, \text{Al})$ in all specimens, and the presence of Be_{11}Fe in the Brush material only. The diffraction patterns also showed several lines with high d spacings that could not be identified with any known beryllium compounds.

Since the aging treatments selected thus far did not improve room temperature ductility, it was decided to see if there were any effects at elevated temperatures. Samples of hot-pressed Brush material with the smallest grain size were given the 6 hr- 900°C , 48 hr- 700°C treatment and tested at 200, 300, and 400°C . Ductilities were substantially higher than for unaged samples tested at the same temperatures, as will be seen subsequently.

Rather than commit any additional samples to experimental heat treatments in the hopes of improving room temperature ductility, the decision was made that all of the hot-pressed and the extruded specimens scheduled for testing in the aged condition would be solution treated for 6 hours at 900°C and aged for 48 hours at 700°C .

3.3.1 Tests on Hot-Pressed Material

The effects of temperature, grain size, and heat treatment on the tensile strength, 0.1% offset yield strength, elongation, and reduction in area at fracture of Brush and Pechiney hot-pressed block tested at a crosshead speed of 0.005 in/min are shown in Figures 11, 12, 13, and 14. Tensile strengths were calculated from the maximum load and the original cross-sectional area. Yield strengths were determined by the 0.1% offset method. The results shown are for single tests, except where indicated. The tensile and yield strengths were generally higher for the smaller grain sizes, and were affected only slightly by aging.

Table 5

EFFECTS OF AGING TREATMENTS ON PROPERTIES OF HOT-PRESSED BLOCK

<u>Material</u>	<u>Grain Size,</u>	<u>Aging Treatment</u>	<u>0.1% Offset Yield Strength, psi</u>	<u>Ultimate Tensile Strength, psi</u>	<u>Elong. in 1.5" per cent</u>
Brush	26.5	None	25,700	28,000	0.7
"	18.9	"	29,900	37,700	1.2
"	9.7	"	39,500	49,900	1.5
Pechiney	13.2	"	24,100	30,300	0.8
"	11.0	"	28,800	39,000	1.2
"	10.3	"	32,700	43,600	1.2
Brush	26.5	6 hr 800°C	28,300	31,800	0.7
"	18.9	"	29,600	35,400	1.1
"	9.7	"	41,200	49,700	1.1
Pechiney	13.2	"	--	29,800	--
"	11.0	"	28,100	30,500	0.7
"	10.3	"	29,900	38,100	1.1
Brush	18.9)	1 hr 800°C	29,900	36,900	1.1
"	9.7)	3/4 hr 600°C	32,100	48,900	1.5
Brush	26.5	1 hr 1000°C	25,300	27,400	0.7
"	18.9	96 hr 700°C	29,400	33,200	0.8
"	9.7	"	38,500	44,800	0.9
Pechiney	13.2	"	27,900	30,500	0.7
"	11.0	"	29,400	33,600	0.8
"	10.3	"	34,400	42,400	1.1
Brush	26.5	6 hr 900°C	25,100	27,600	0.6
"	18.9	48 hr 700°C	27,800	34,700	1.0
"	9.7	"	38,400	45,800	1.1
Pechiney	13.2	"	29,500	31,400	--
"	11.0	"	26,600	28,500	0.6
"	10.3	"	35,400	45,900	1.2

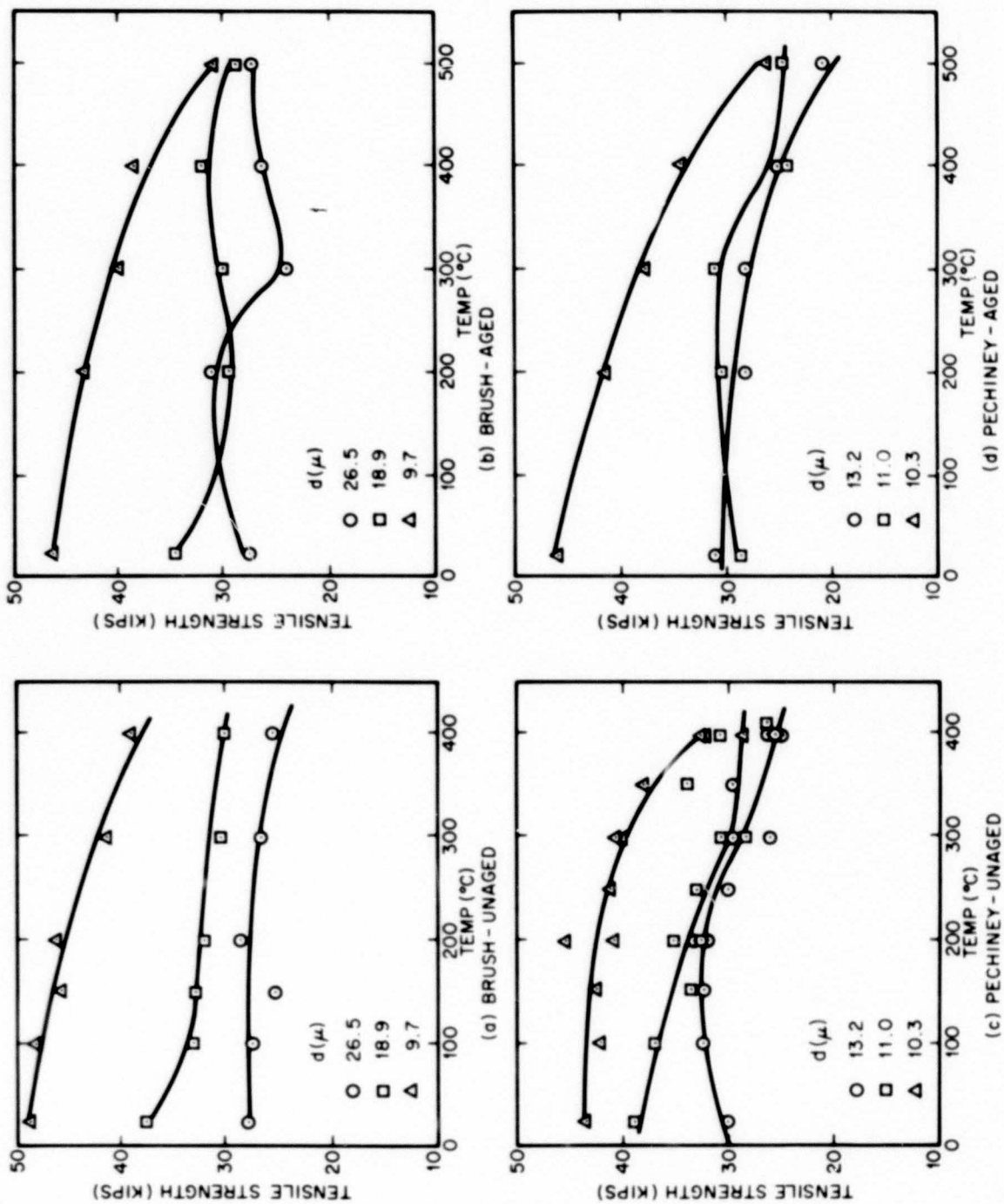


Figure 11 - Tensile strength of hot-pressed beryllium.

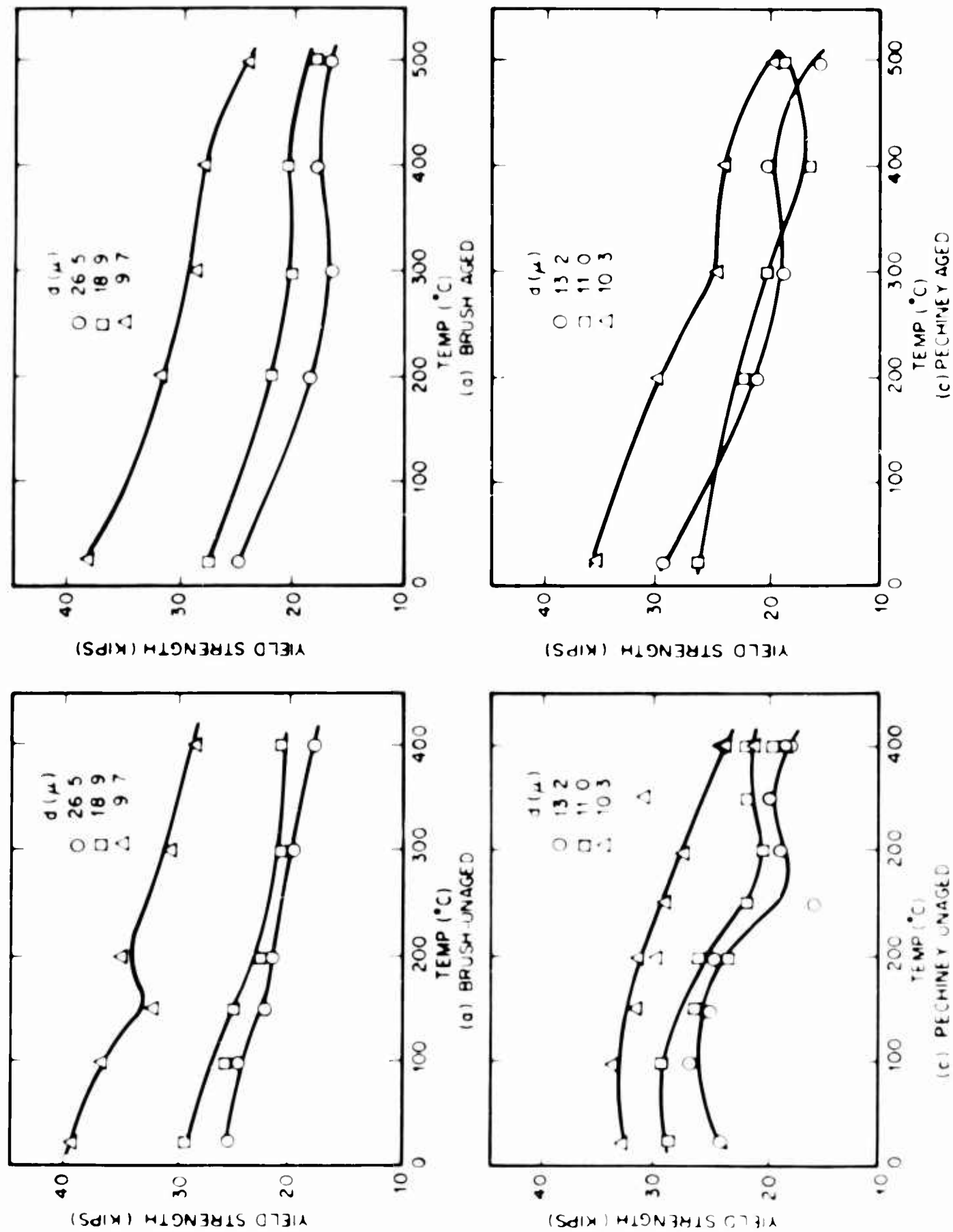


Figure 12 - Yield strength of hot-pressed beryllium.

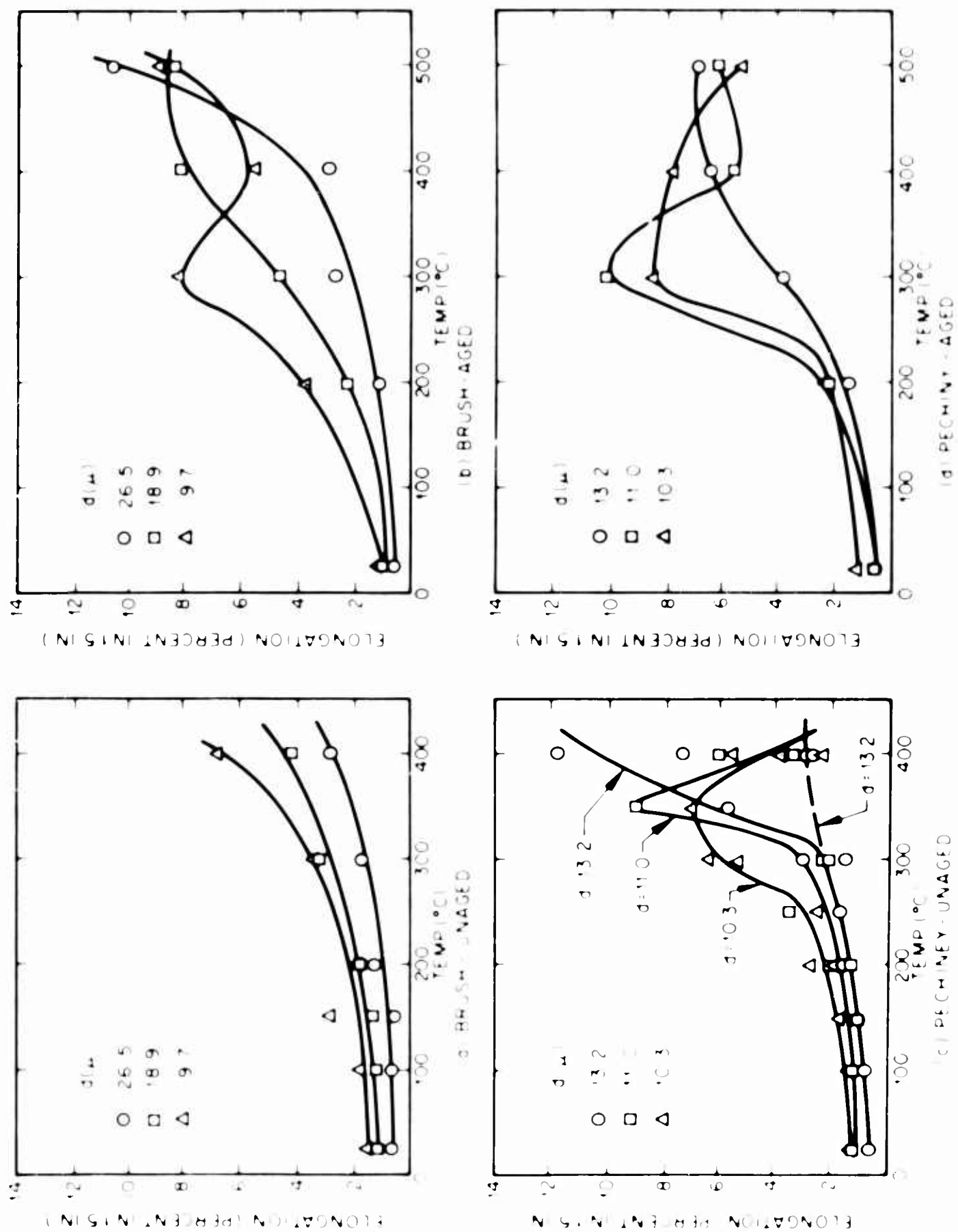


Figure 13 - elongation of hot-pressed beryllium.

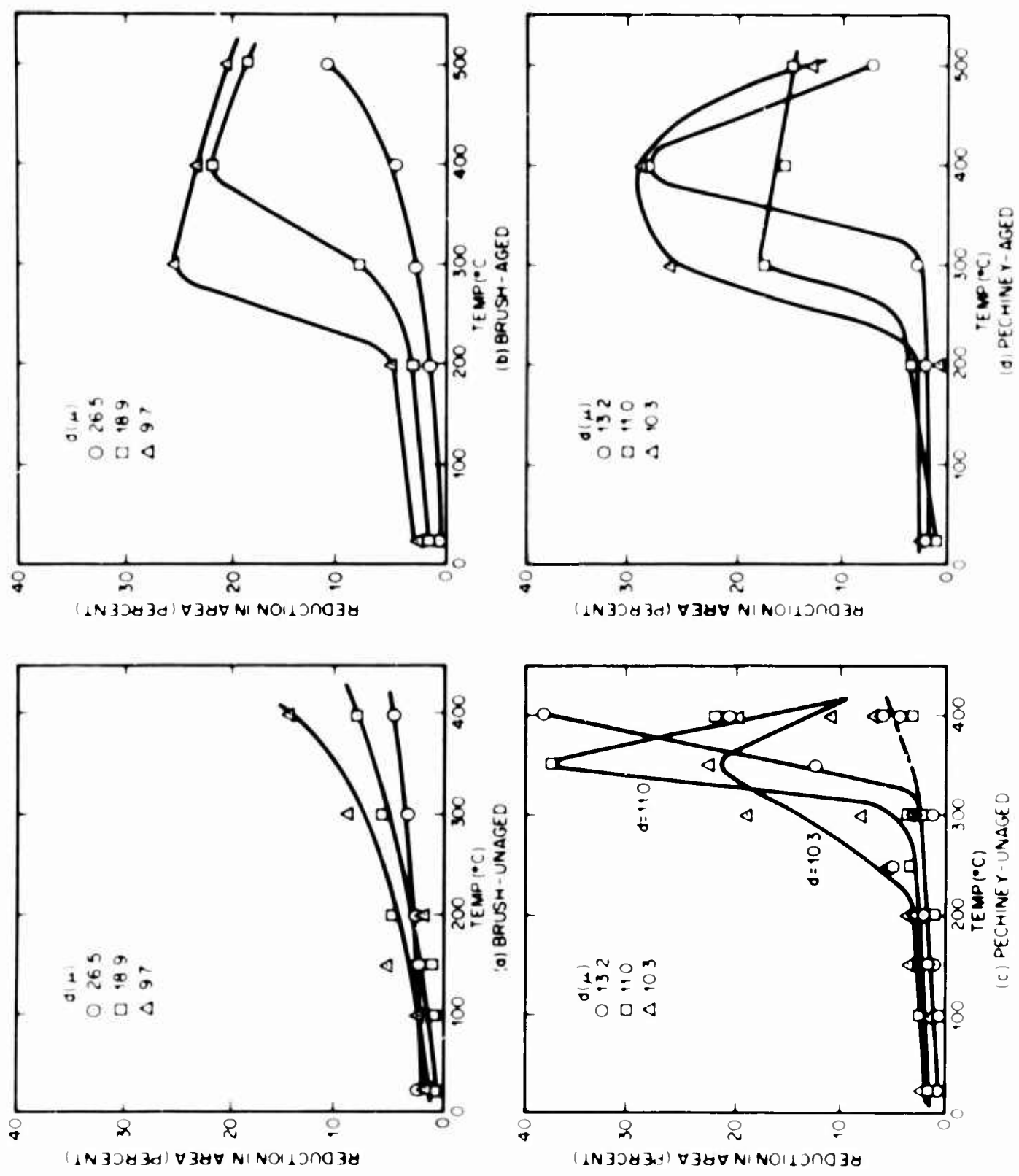


Figure 14 - Reduction in area of hot-pressed beryllium.

Elongation and reduction in area of unaged Brush samples increased gradually with temperature to 400°C; thus, no ductile-brittle transition was observed. There were insufficient specimens to continue the tests to higher temperatures. Aging of the Brush samples introduced marked changes in ductility, with a ductile-brittle transition, as indicated by reduction in area, at about 200°C for the smallest grain size and at 300°C for the medium grain size. Samples with the largest grain size are still increasing in ductility at 500°C, whereas the others have already experienced a maximum. Note that for the aged samples, the test temperature has been extended to 500°C, but that no tests were made at 100°C.

The unaged Pechiney samples exhibited ductile-brittle transitions at about 225°C, 300°C, and 325°C for grain sizes of 10.3, 11.0, and 13.2 microns, respectively. The larger grain sizes tended to have their ductility maxima at higher temperature, and also exhibited higher maximum ductilities. The elongation and reduction in area for the 13.2 micron grain size material showed an extreme range of values at 400°C, with the result that the curves are shown in two sections, one of which is dotted. Materials with a ductile-brittle transition characteristically exhibit both high and low values of ductility in the transition region. Aging did not alter the ductility appreciably, although the transition temperature for the 11 micron material has been lowered about 100 degrees.

A comparison of the mechanical properties of aged Brush and Pechiney samples, with $d = 9.7$ and 10.3 microns, respectively, are shown in Figure 15, where it is apparent that both materials have very similar properties. This is quite interesting, since the ductilities were so markedly different prior to heat treatment.

True stress vs. true strain curves, drawn to the point of maximum load, are shown for the 9.7 micron Brush and 10.7 micron Pechiney samples in Figures 16 and 17, respectively. True stress, σ , was calculated from the relation

$$\sigma = \frac{P}{A_0} (1 + e) \quad (1)$$

where P is the applied load, A_0 the original area, and e the engineering strain. True strain, ϵ , was calculated as

$$\epsilon = \ln(1 + e) \quad (2)$$

The requisite values of P and e were obtained from the load deflection curves. Yield points or yield inflections were not observed on any of the hot-pressed specimens. However, serrated stress-strain curves, characteristic of a Portevin-LeChatelier effect, were observed at 400°C for both aged and unaged Brush samples having grain diameters of 18.9 and 26.5 microns. The stress-strain curves for the aged and unaged samples in Figures 16 and 17 are similar, although the aged material generally exhibits lower rates of work hardening.

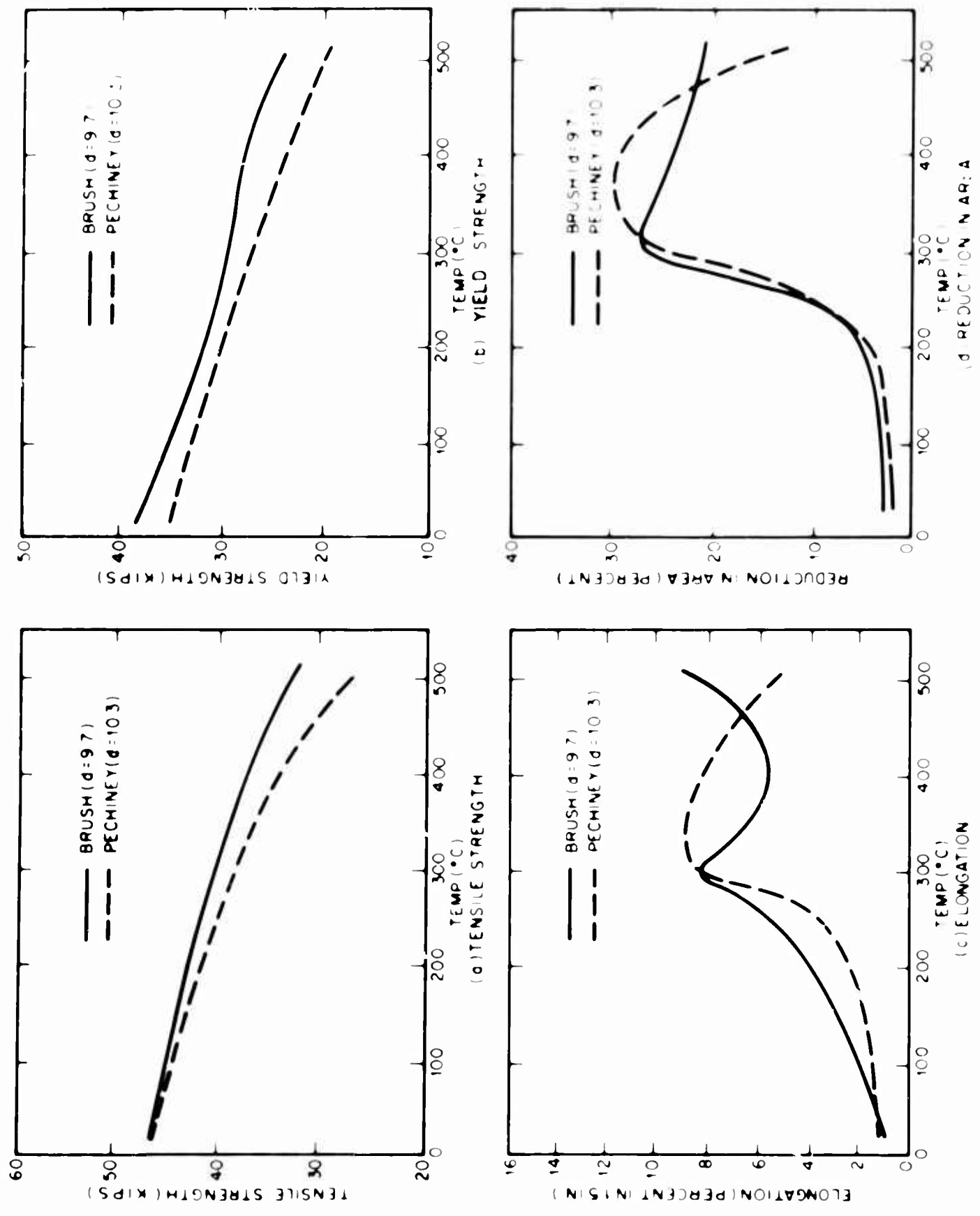


Figure 15 - Comparison of mechanical properties of hot-pressed Brush and Pechiney beryllium in the aged condition.

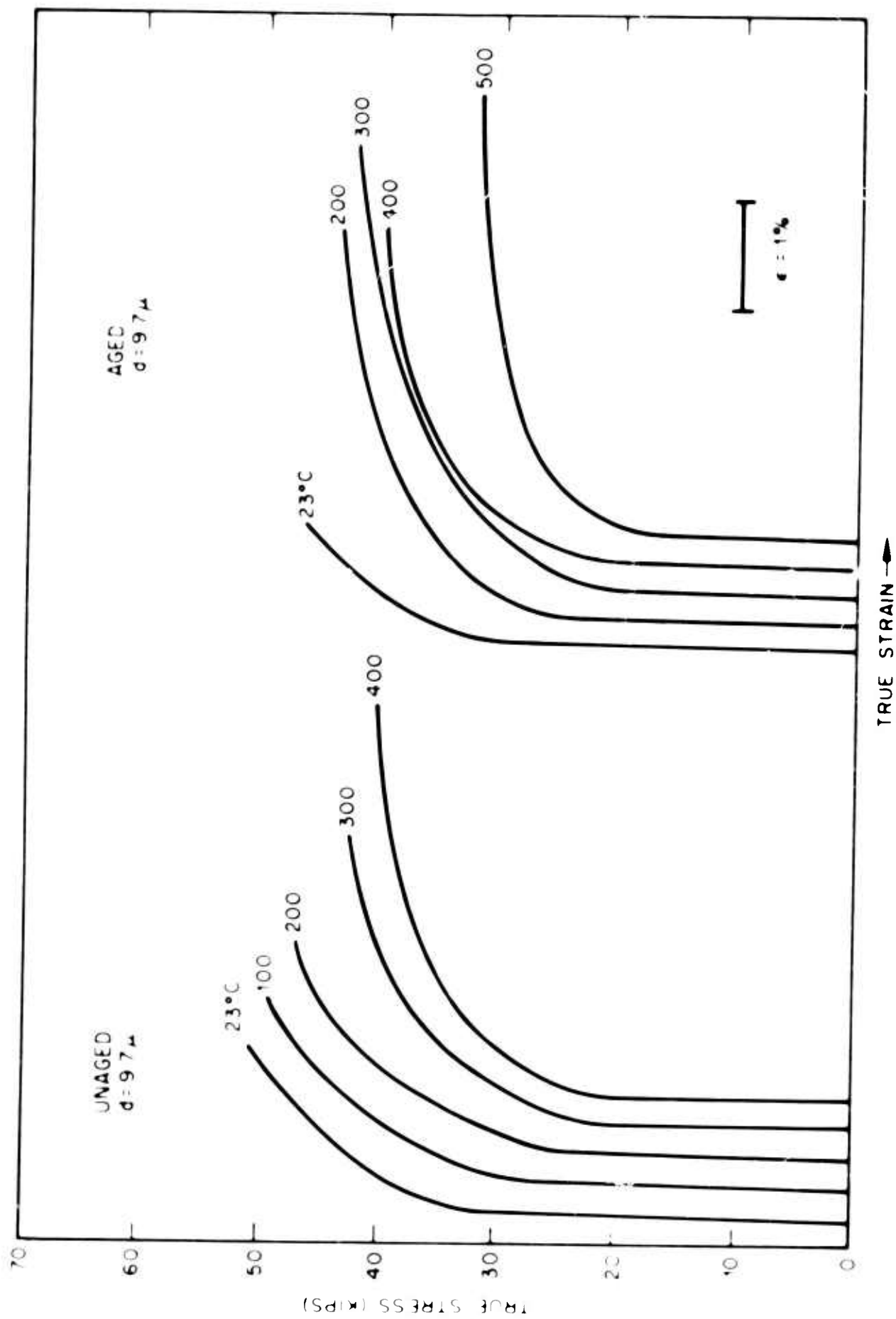


Figure 16 - True stress vs. true strain curves for hot-pressed brush.

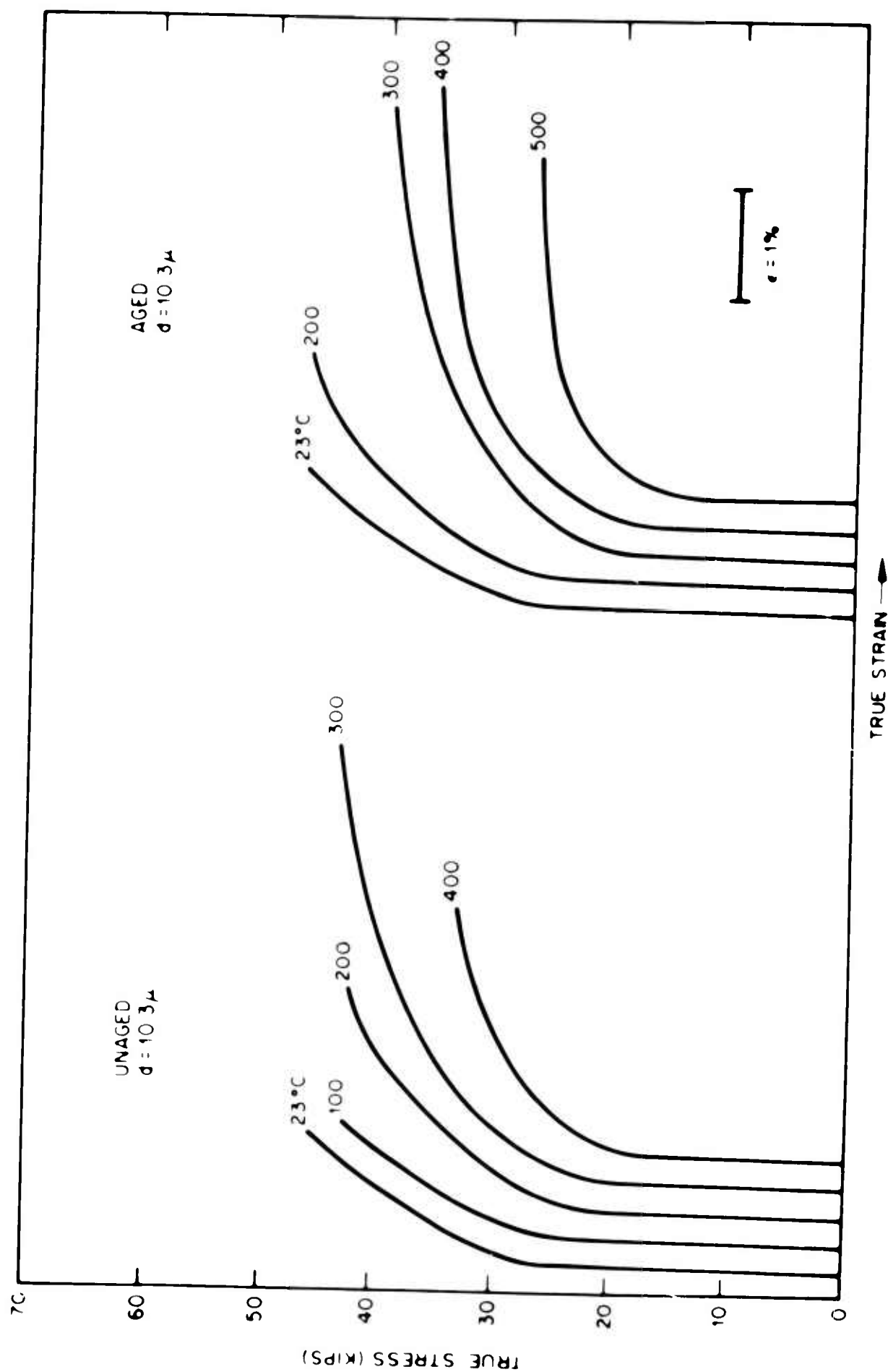


Figure 17 - True stress vs. true strain curves for hot-pressed Pechiney.

The effects of strain rate on the mechanical properties of hot-pressed block at room temperature, 200°C, and 400°C are presented in Tables 7 and 8, Appendix I. Three crosshead speeds were used (i.e., 0.005, 0.05, and 0.5 in/min), giving nominal strain rates of 0.0033, 0.033, and 0.33 per minute.

Figures 18, 19, 20, and 21 show the effects of these strain rates on the properties of the 9.7 micron Brush material and the 10.3 micron Pechiney material. Generally, increasing the strain rate increased the yield and tensile strengths and decreased elongation and reduction in area. The rate of work hardening was also higher for the higher strain rates. Maxima in the curves of elongation or reduction in area vs. temperature were not observed for any of the samples tested at the two highest strain rates, although tests at intermediate temperatures would be required to establish this definitely. It is difficult to define a transition temperature for the higher strain rates with the few points available, but the temperature at which ductility begins to increase sharply for a strain rate of 0.033 is about 100°C higher than for a strain rate of 0.0033. An anomaly was noted in the Pechiney samples in that at 400°C, the highest strain rate resulted in the best ductility. This would be the case if fracture at 400°C were intergranular for the slow strain rate. Metallographic examination showed that for the slow strain rate, fracture was partially intergranular and partially transgranular for both the aged and unaged samples at 400°C.

With the exception of unaged samples tested at 400°C, all specimens tested at the highest crosshead speed (0.5 in/min) exhibited slight instabilities in flow which appeared as stepwise increases in the load-deflection curves during the first 1 or 2 percent deformation. The small increases in load were not followed by a decrease, as would be the case for a yield point, or strain aging.

At 400°C, the aged and unaged 26.5 micron Brush specimens exhibited repeated yielding over the entire plastic region when tested at a crosshead speed of 0.05 in/min, but not when tested at 0.5 in/min. The increases and decreases in load, characteristic of a Portevin-LeChatelier effect, were not as pronounced as in the samples tested at a crosshead speed of 0.005 in/min.

As mentioned in Section 1.1, the effect of prestrain at elevated temperature on room temperature mechanical properties was investigated briefly. The prestrains used were 2% at 400°C and 2% at 200°C, with the results as shown in Table 6. These treatments were obviously unsuccessful in improving ductility, and, in fact, elongation was reduced slightly while yield strength increased.

3.3.2 Tests on Extruded Material

The initial tests on extrusions were made at room temperature. In the transverse orientation, fracture frequently occurred in the shoulder portion of the tensile specimen. The most likely cause for this behavior was the stress concentration at this location, combined with a preferred orientation of cleavage planes. The difficulty was largely eliminated by etching the specimens until the gage section was approximately 0.150 inch in diameter. Incidental to this was the elimination of any residual stresses introduced in the initial machining, since about 0.020 inch of material was removed from the surface. Occasionally, some of the large-grained samples still fractured in the shoulders when tested at subzero temperatures. However, if the test was repeated, and fracture occurred in the gage section, the mechanical properties were not

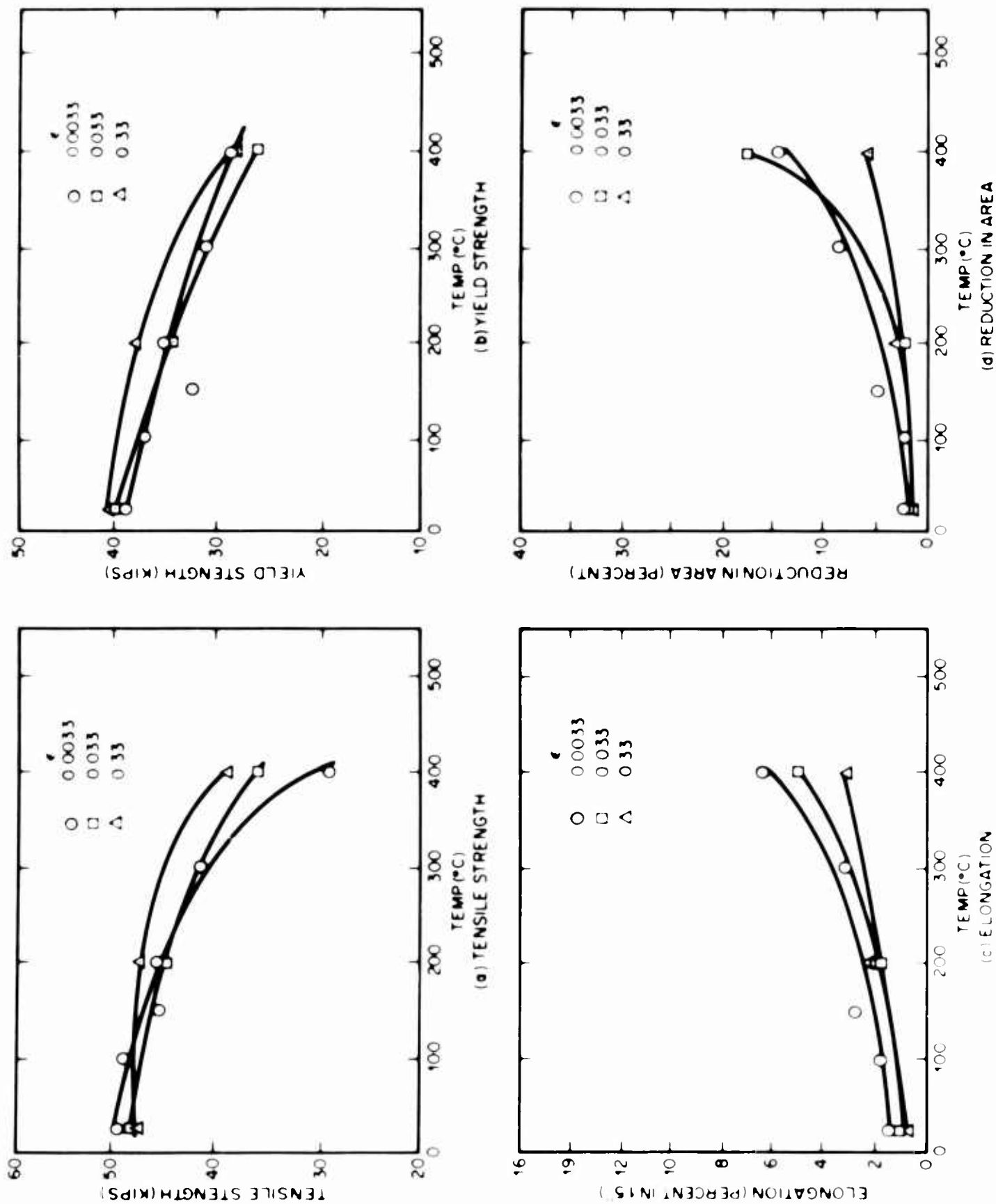


Figure 18 - Effect of strain rate on mechanical properties of unaged, hot-pressed Brush, d = 9.7 microns.

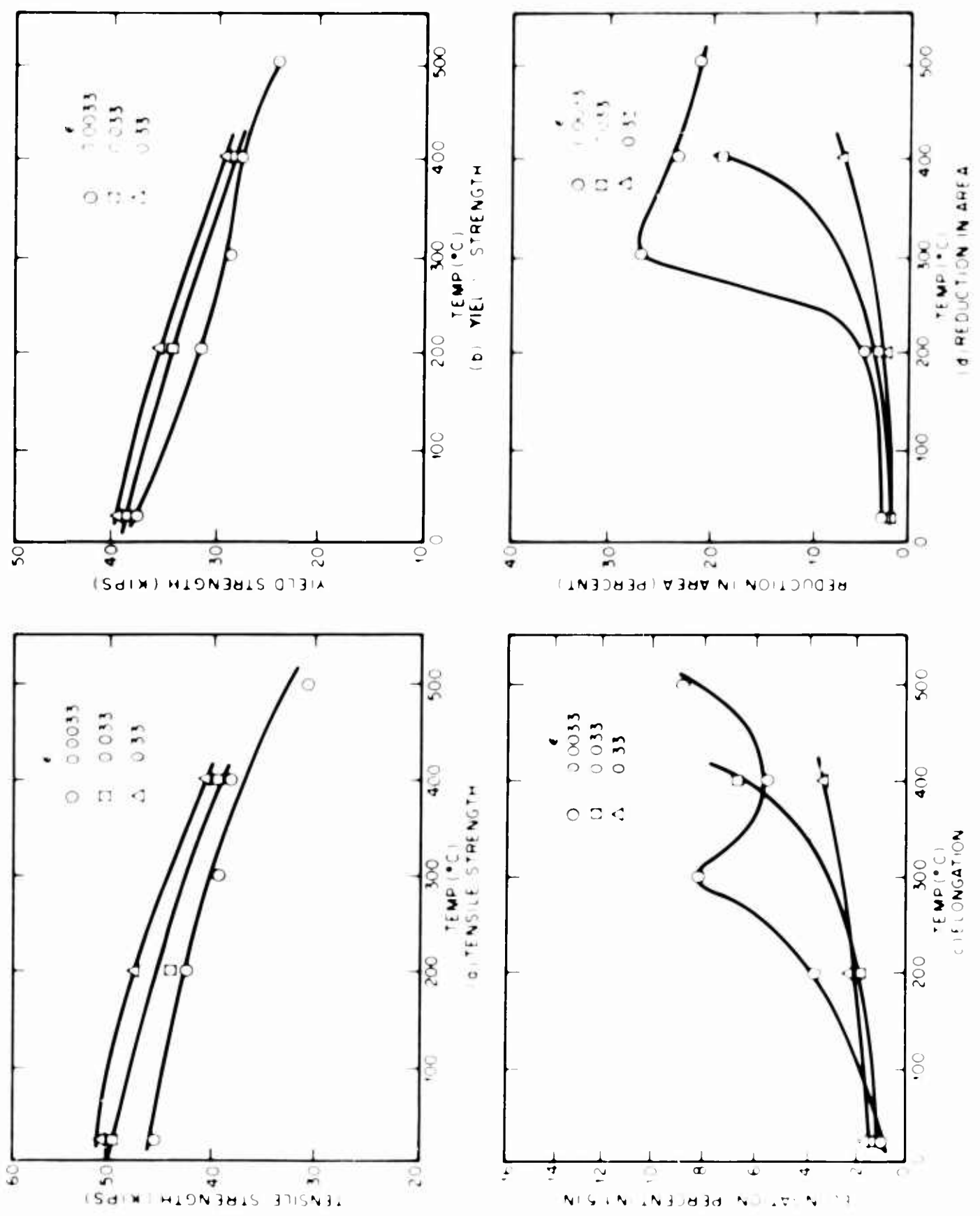


Figure 19 - Effect of strain rate on mechanical properties of aged, hot-pressed Brast, $d = 9.7$ microns.

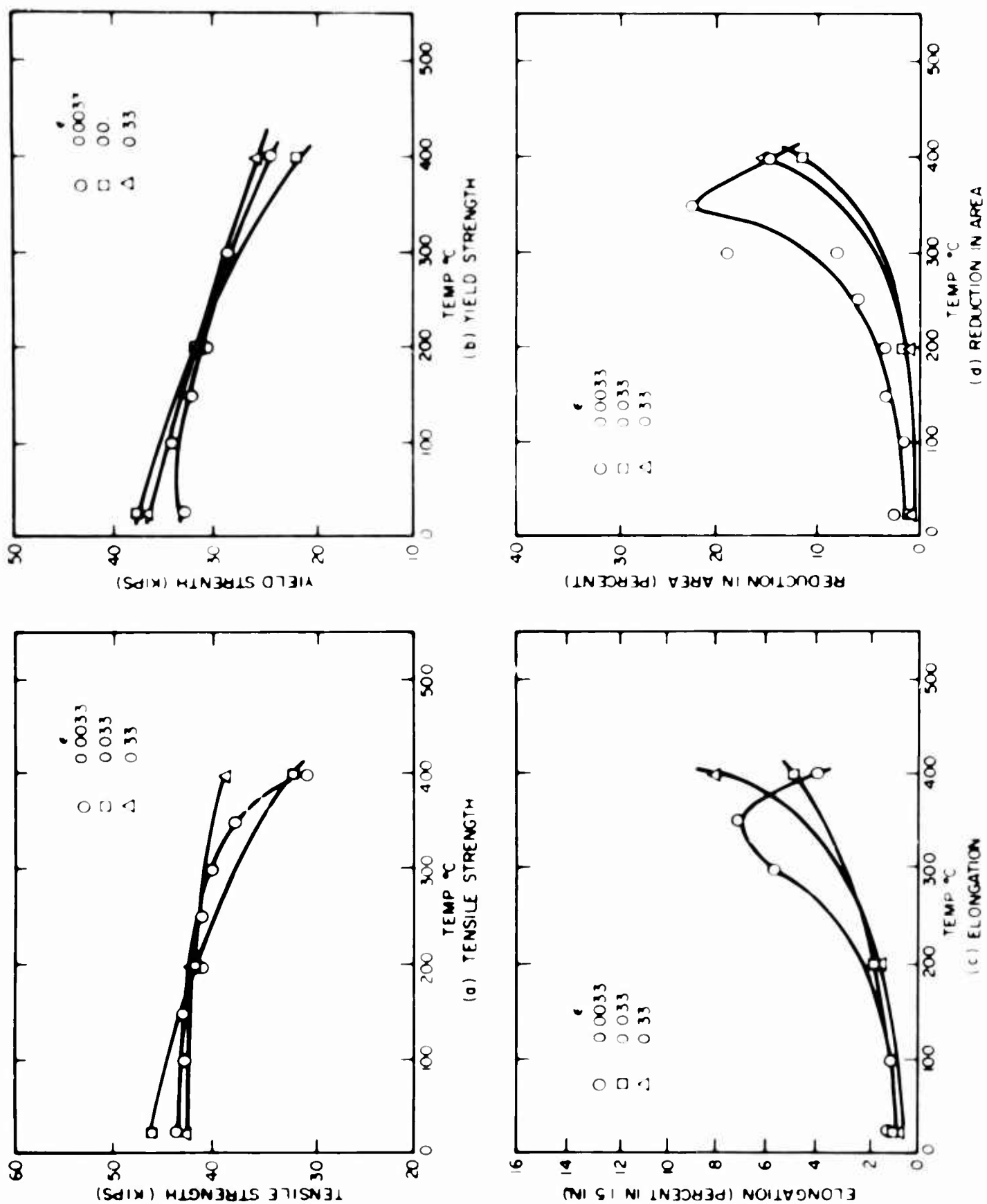


Figure 20 - effect of strain rate on mechanical properties of unaged, hot-pressed Pechiney, d = 10.3 microns.

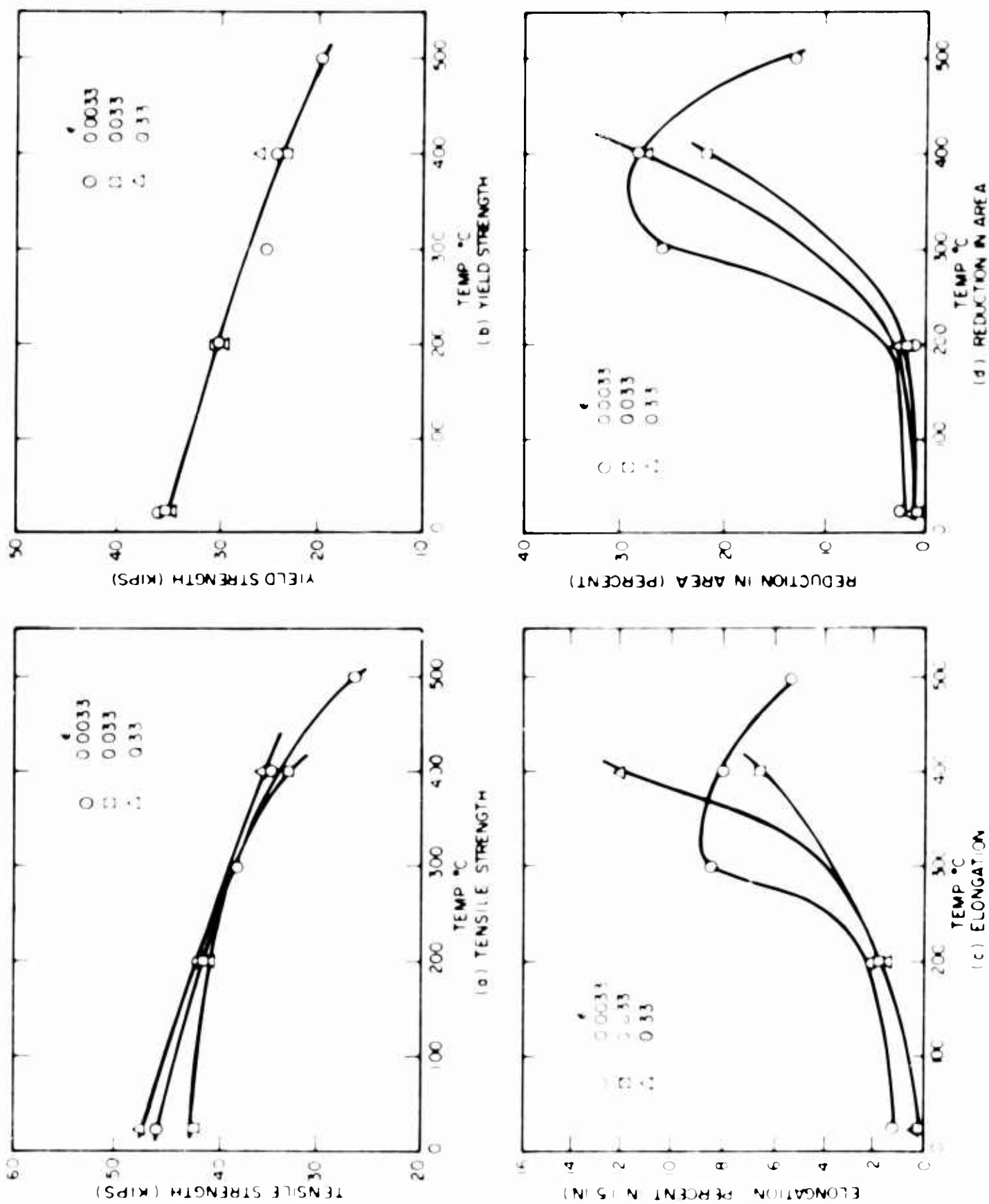


Figure 21 - Effect of strain rate on mechanical properties of aged, hot-pressed Pechiney, d = 10.3 microns.

Table 6

**EFFECT OF PRESTRAIN AT ELEVATED TEMPERATURE ON
ROOM TEMPERATURE MECHANICAL PROPERTIES
OF UNAGED HOT-PRESSED BLOCK**

<u>Material</u>	<u>Grain Size,</u>	<u>Prestrain Treatment</u>	<u>0.1% Offset Yield Strength, psi</u>	<u>Ultimate Tensile Strength, psi</u>	<u>Elong. in 1.5 in., per cent</u>
Brush	26.5	None	25,700	28,000	0.7
"	18.9	"	29,900	37,700	1.2
"	9.7	"	39,500	49,900	1.5
Pechiney	13.2	"	24,100	30,300	0.8
"	11.0	"	28,800	39,000	1.2
"	10.3	"	32,700	43,600	1.2
Brush	26.5	2%, 400°C	30,000	30,400	0.5
"	18.9	"	33,800	34,400	0.5
"	9.7	"	44,300	49,600	1.1
Pechiney	13.2	"	32,500	33,700	0.5
"	11.0	"	31,000	31,000	0.5
"	10.3	"	40,400	42,300	1.1
Brush	26.5	2%, 200°C	31,000	31,000	0.3
"	18.9	"	36,500	37,700	0.6
"	9.7	"	Failed at 2%, 200°C		--
Pechiney	10.3	"	--	42,700	1.0

significantly different. In other words, if the specimens had not fractured in the shoulder portion, they would have fractured in the gage section at about the same load and deformation.

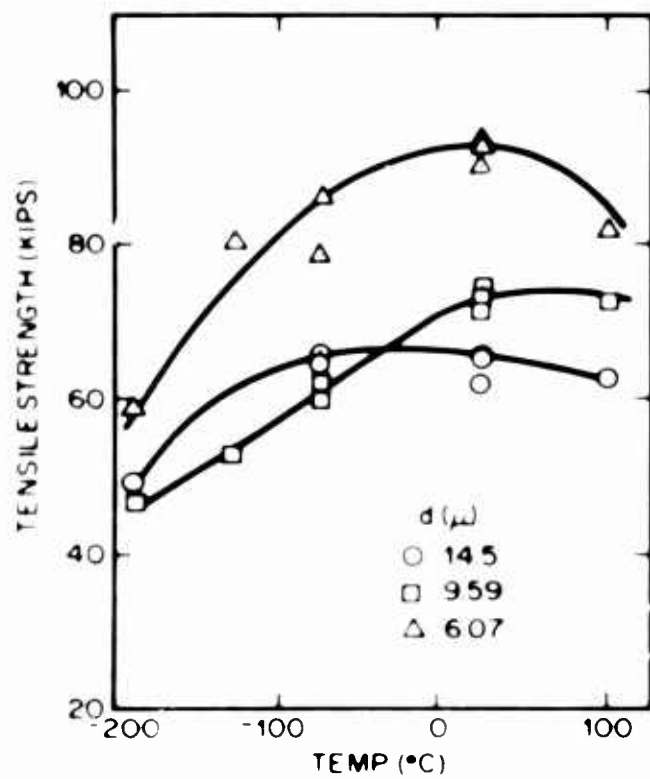
The tensile strength, 0.1% offset yield strength, and elongation of Brush and Pechiney extruded flats are shown in Figures 22 through 27. Reduction in area was not calculated for the extruded samples, since in many cases it was non-uniform, producing an oval-shaped gage section. Each figure shows the data for four conditions: (1) longitudinal-unaged; (2) longitudinal-aged; (3) transverse-unaged; and (4) transverse-aged. The grain size indicated on each figure is d_1 (Table 4), the smallest grain dimension measured in each case.

The data cover the range from -195°C to 100°C for the unaged samples, and -195°C to 200°C for the aged samples. The initial tests were made on unaged extrusions at room temperature, and elongations as high as 13 percent were observed. Tests at subzero temperatures were therefore required to locate the ductile-brittle transition. Some samples did not show extensive elongation at room temperature and tests at high temperatures were necessary. Even at 100°C , some relatively low elongation values were observed, but additional specimens were unavailable for tests at higher temperatures. Tests were made at 200°C , however, on some of the aged samples. There were insufficient longitudinal samples in the aged condition to obtain complete curves.

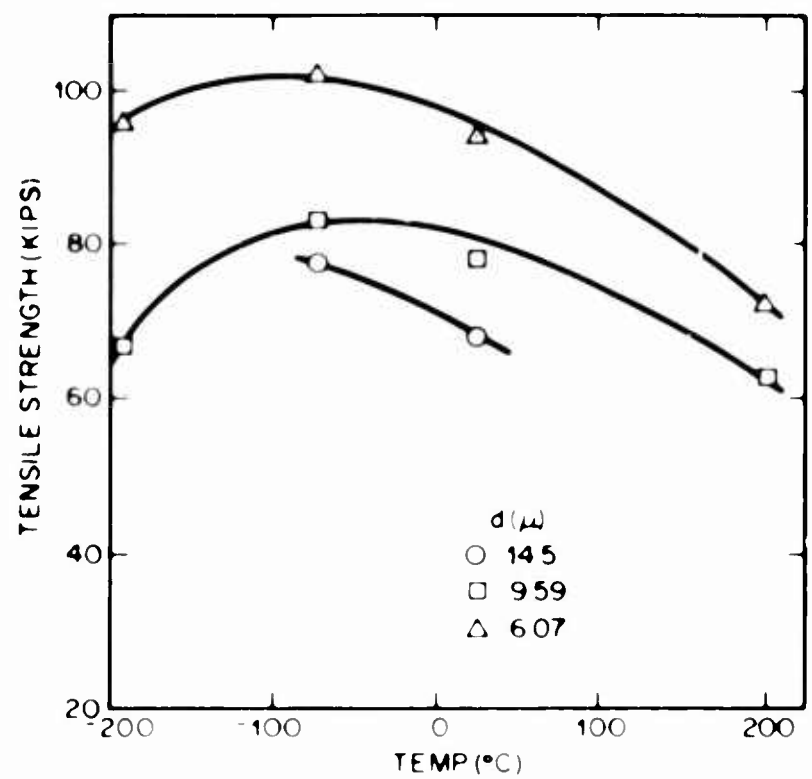
The curves of tensile strength vs. temperature for the Brush extrusions (Figure 22) show that below room temperature tensile strength decreased as temperature decreased for the unaged longitudinal samples, but increased for the transverse samples. Aging generally increased the tensile strength below room temperature for both the longitudinal and transverse orientations, but did not significantly affect the strength at room temperature. At 100°C , the tensile strengths of the aged transverse samples were all slightly higher than the unaged. Also, the strength of all aged transverse samples decreased between -120°C and -195°C . Further discussion of these curves will be deferred to the next section of this report.

Figure 23 shows the tensile strength of Pechiney extrusions. In the unaged longitudinal samples, above room temperature, the tensile strength is highest for the smallest grain size. However, at low temperatures, tensile strength was higher for the larger grain sizes. The tensile strength of the unaged transverse samples did not increase continuously with decreasing temperature, as was the case with the Brush material; rather, the strength reached a maximum and then declined in the -100°C to -195°C range. Tensile strengths were somewhat improved by aging, and again, it was noted that at 100°C , the strength of the aged transverse samples was greater than for the unaged.

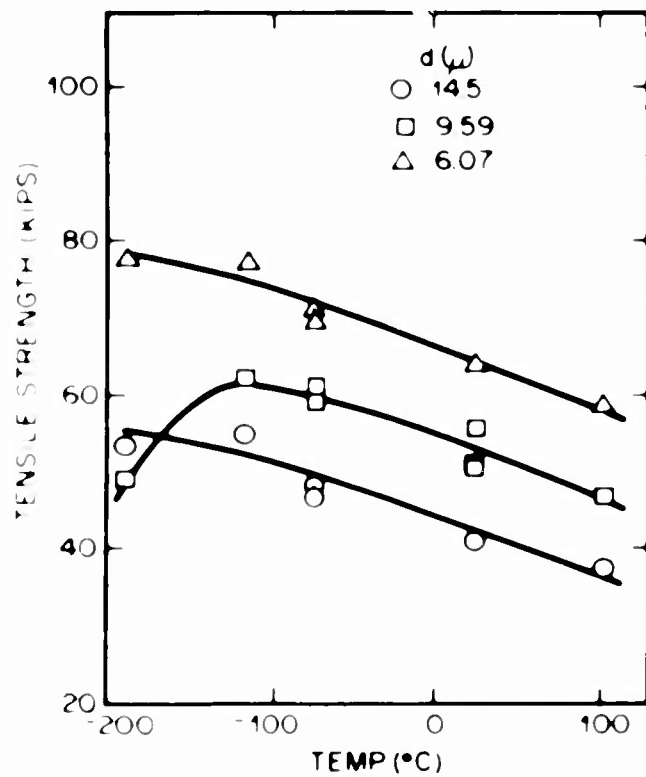
The yield strengths (Figures 24 and 25) followed patterns similar to the tensile strengths, and many of the same comments apply. Aging caused significant improvements in the yield strength of the fine-grained longitudinal Brush samples at all temperatures, and in the fine-grained transverse Brush and Pechiney samples everywhere but at room temperature. Aging also raised the yield strength of the longitudinal Pechiney extrusions. Several of the aged



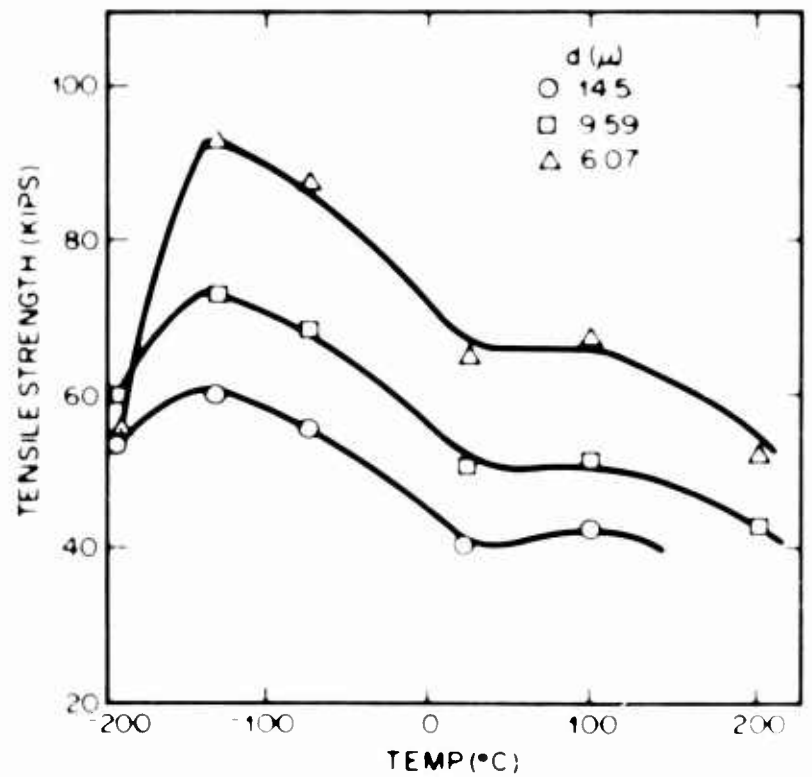
(a) LONGITUDINAL-UNAGED



(b) LONGITUDINAL-AGED



(c) TRANSVERSE-UNAGED



(d) TRANSVERSE-AGED

Figure 22 - Tensile strength of Brush extrusions.

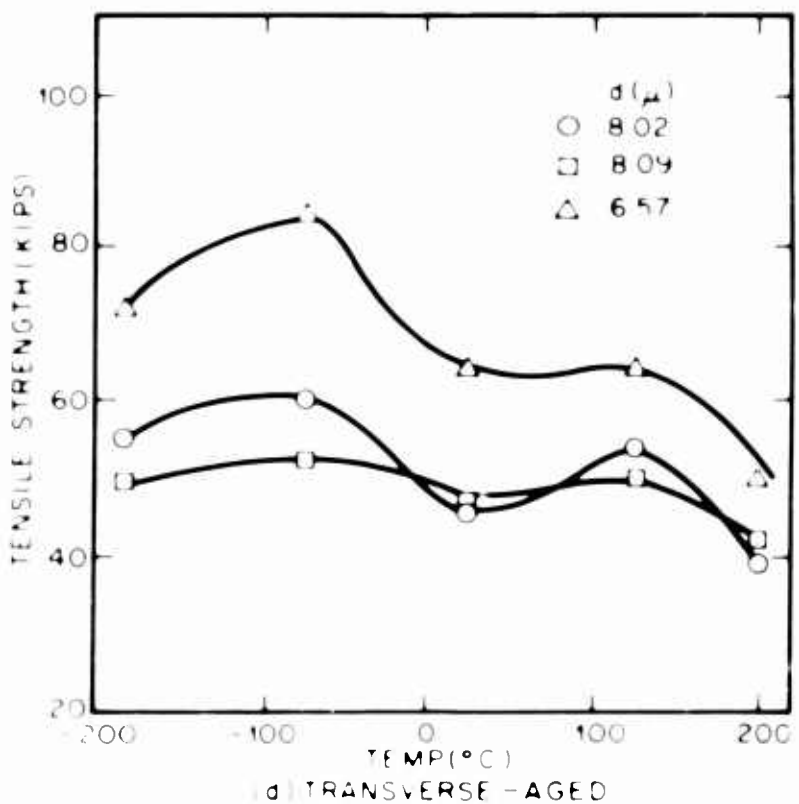
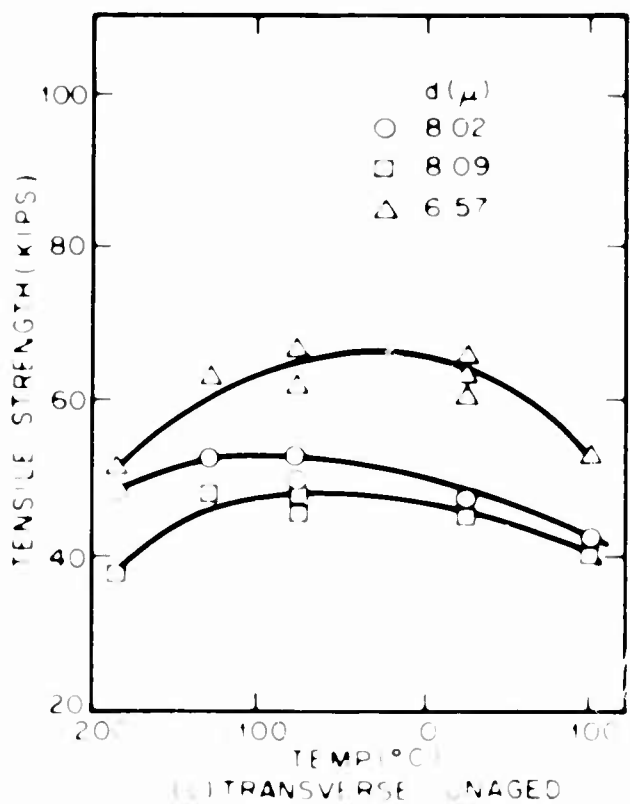
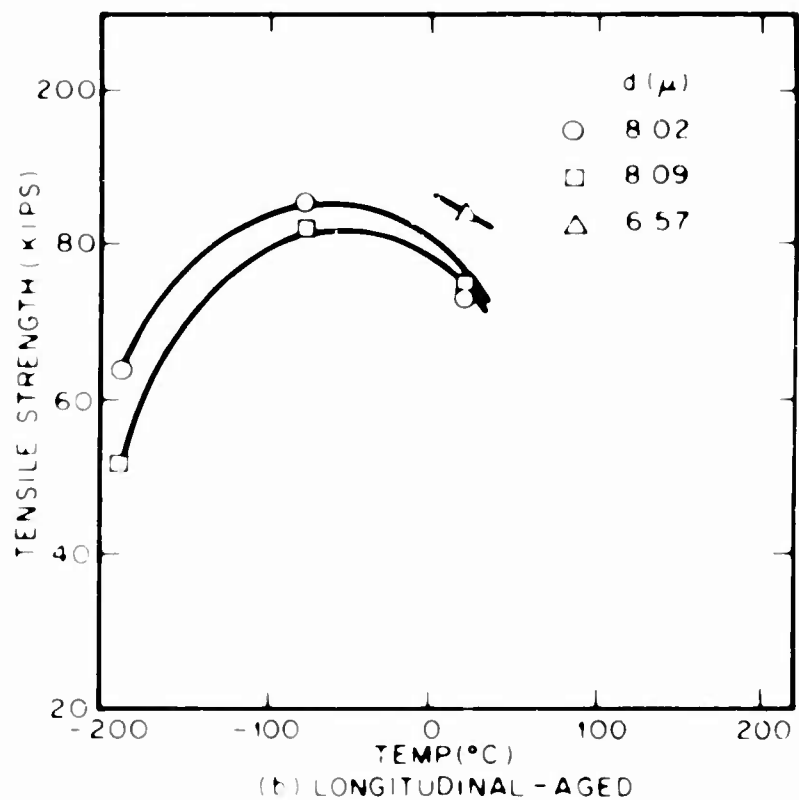
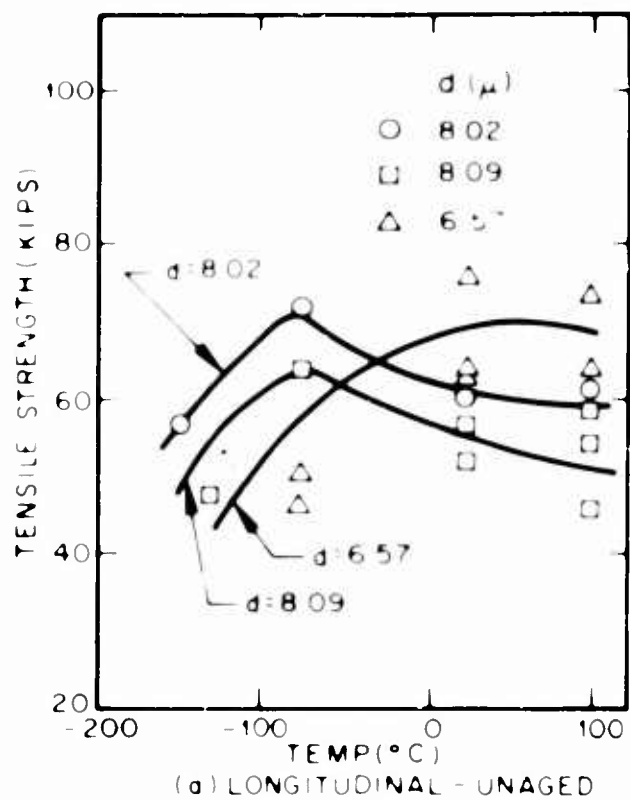
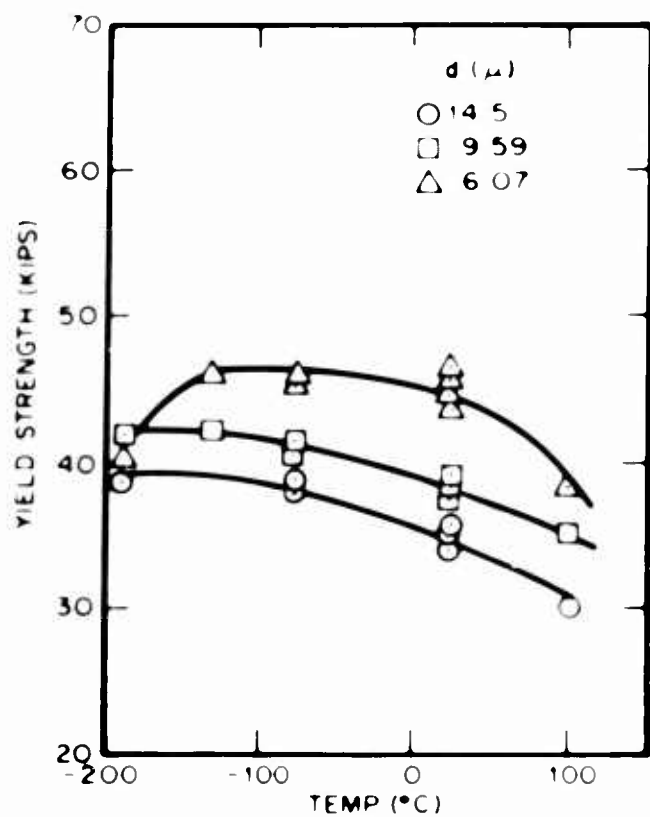
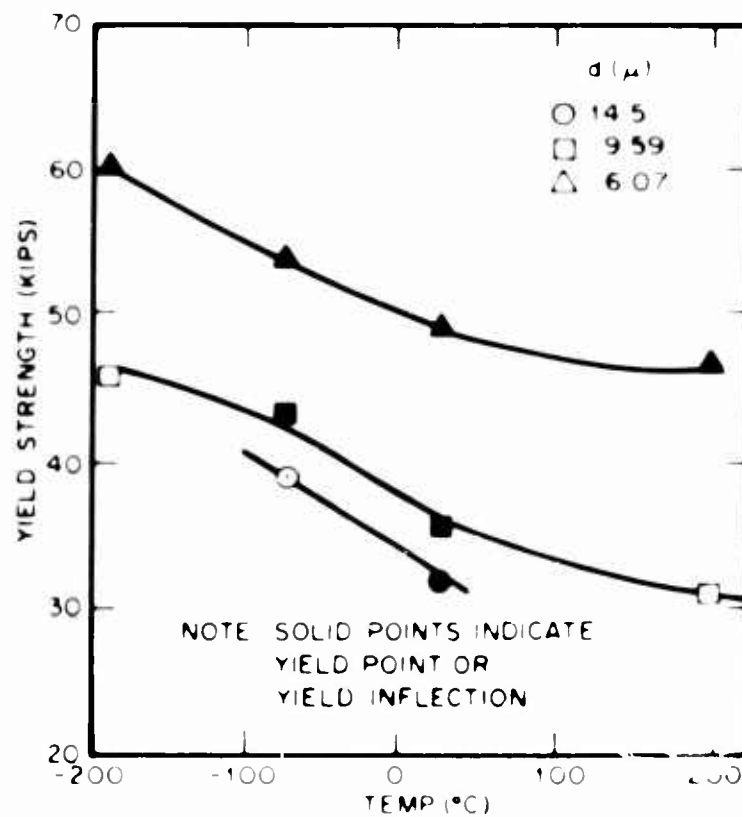


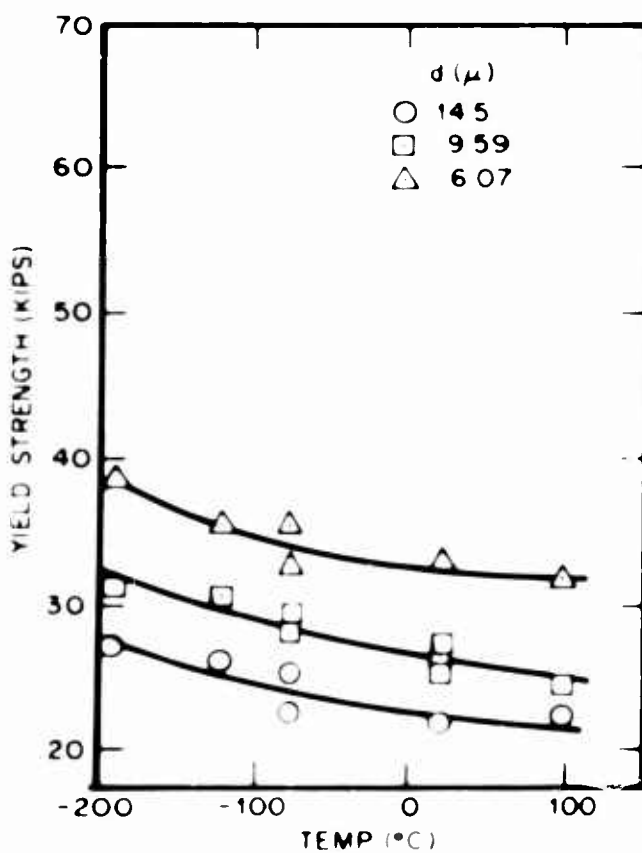
Figure 23 - Tensile strength of Pechiney extrusions.



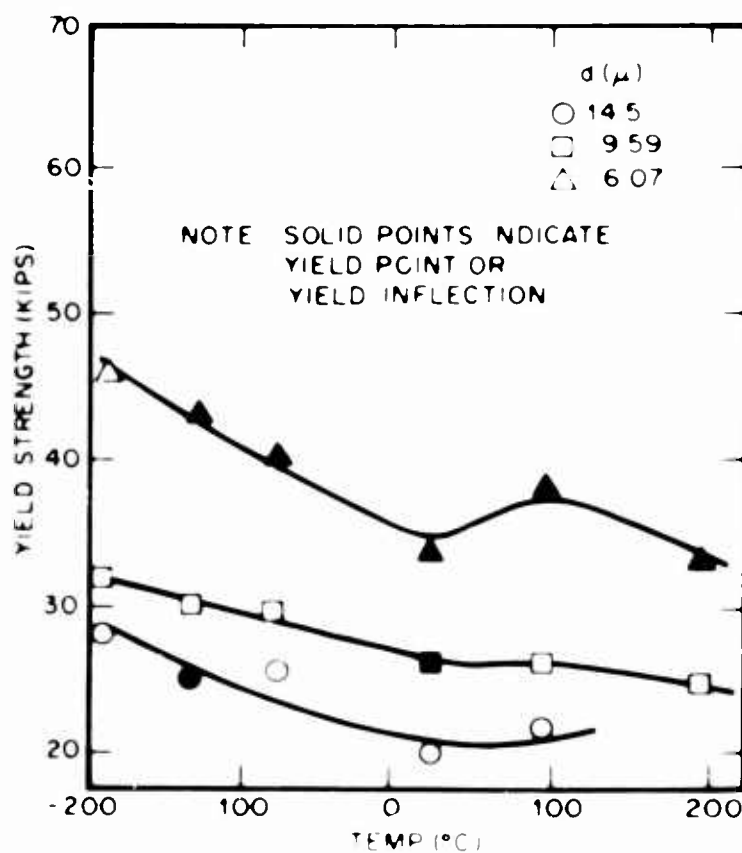
(a) LONGITUDINAL-UNAGED



(b) LONGITUDINAL-AGED



(c) TRANSVERSE-UNAGED



(d) TRANSVERSE-AGED

Figure 24 - Yield strength of Brush extrusions.

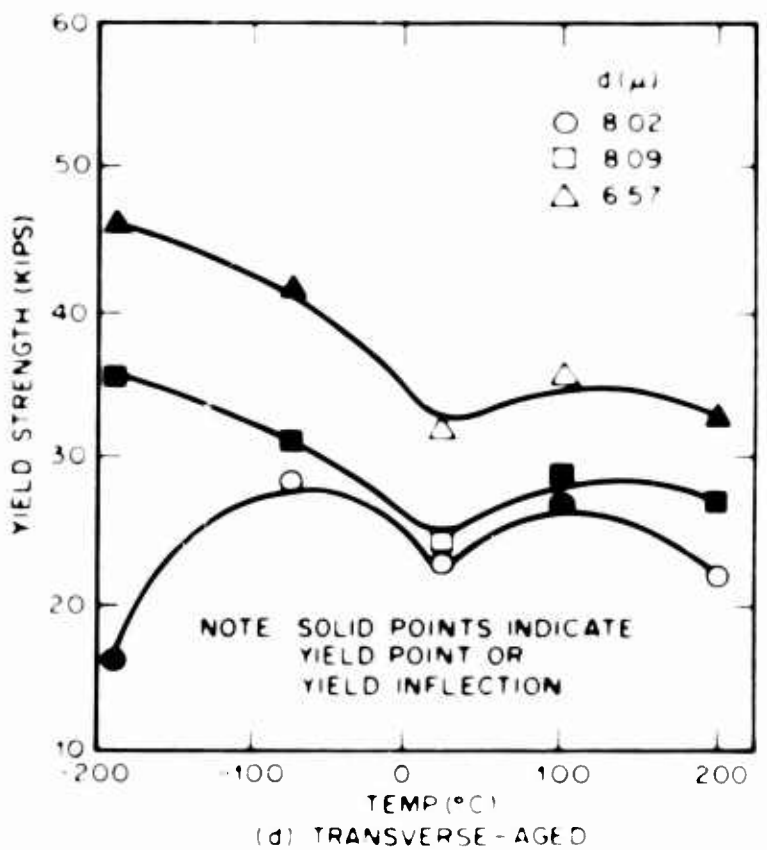
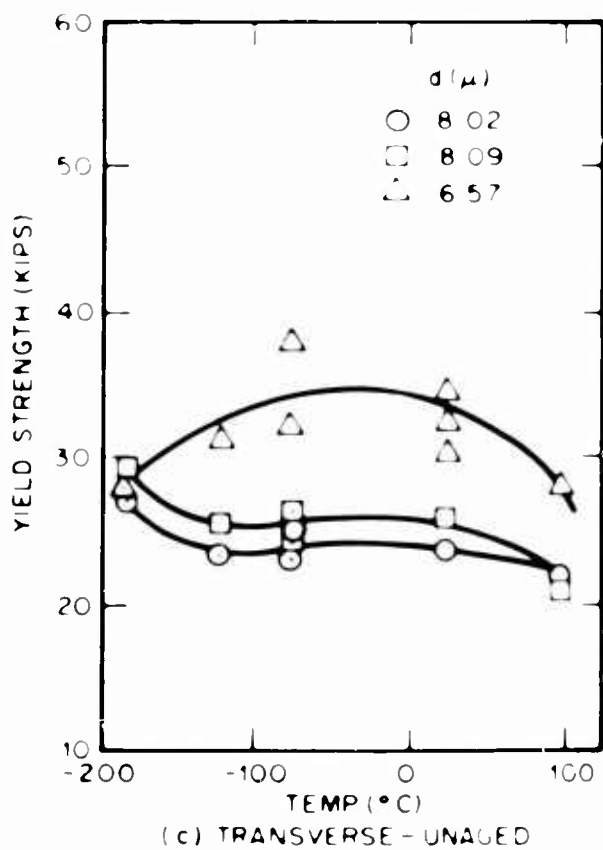
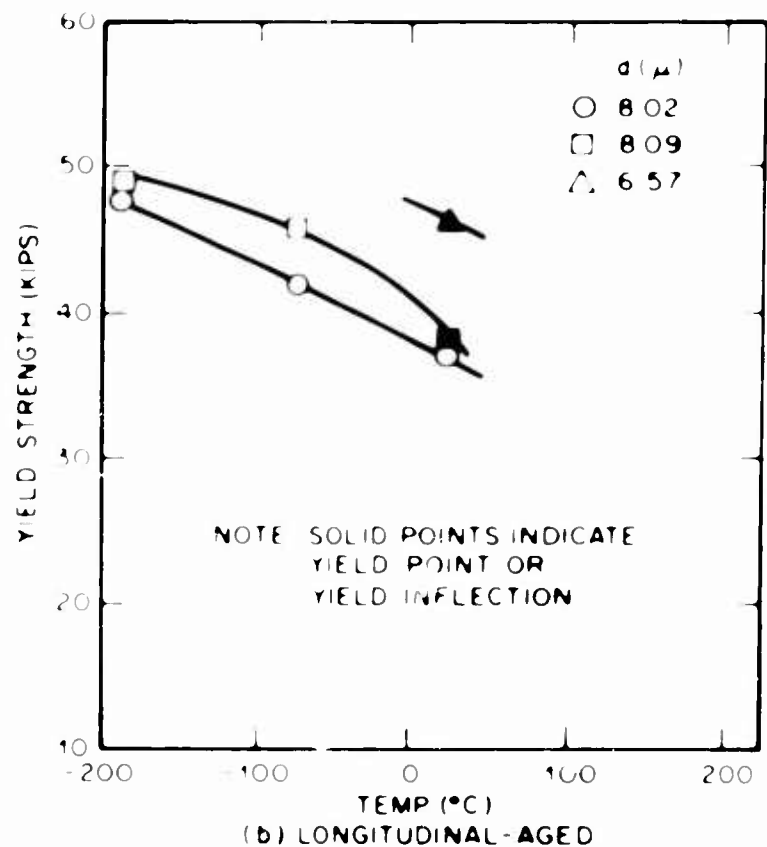
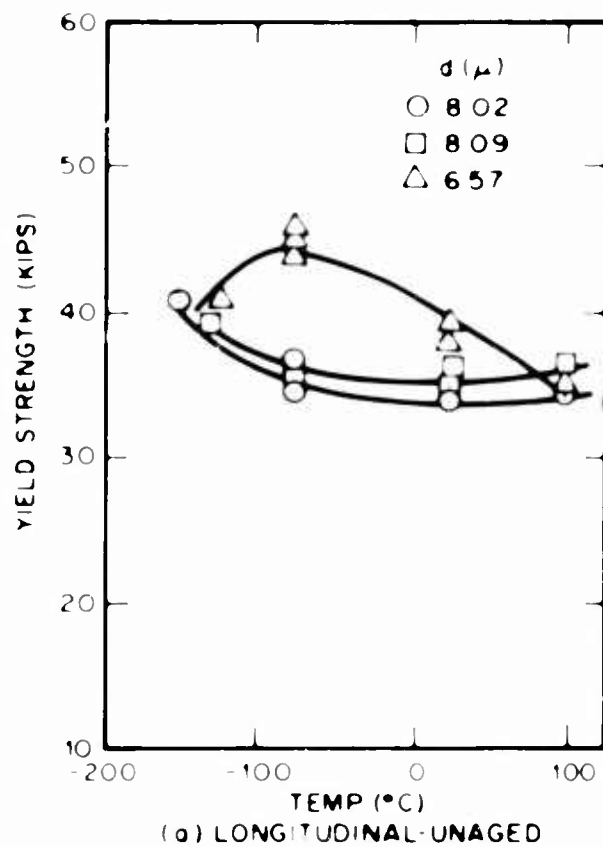
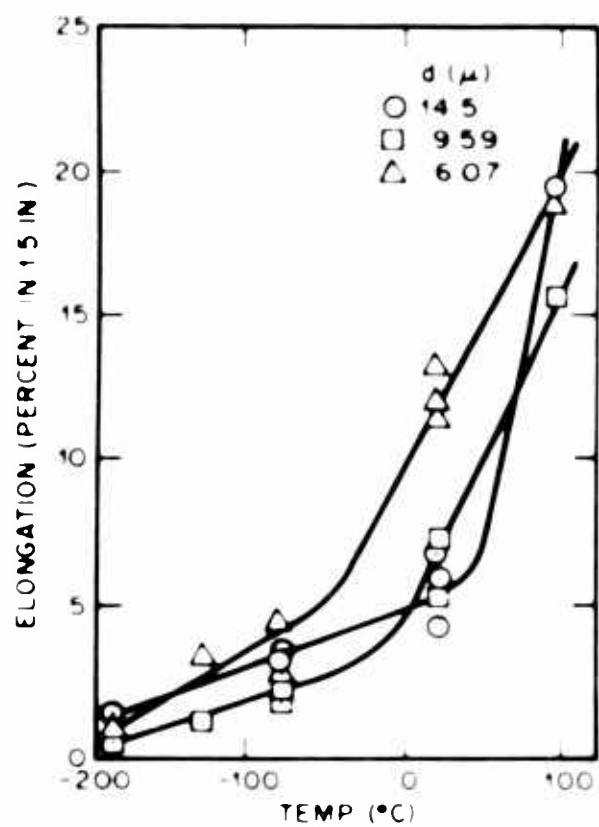
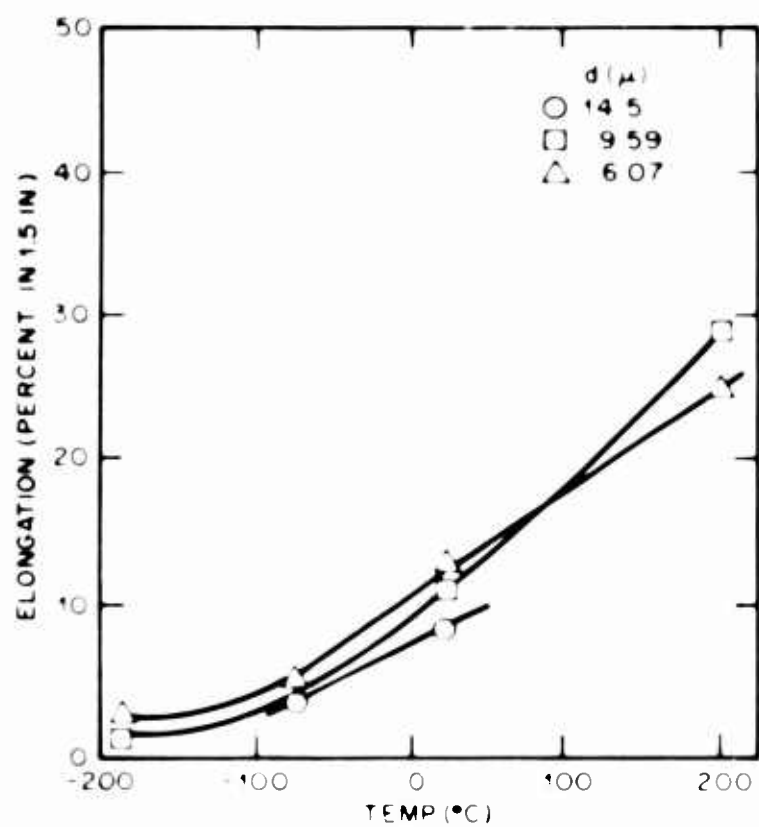


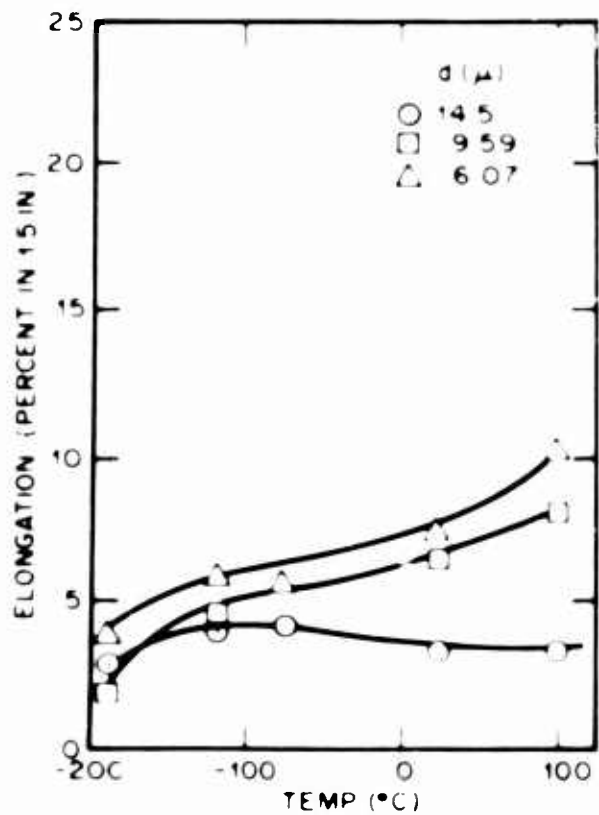
Figure 25 - yield strength of Pechiney extrusions.



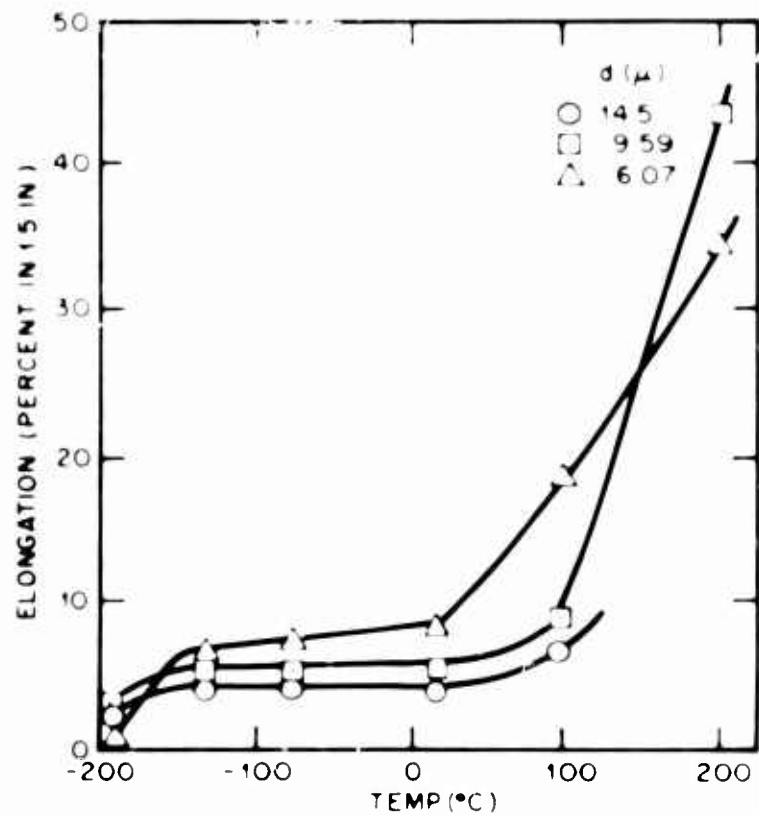
(a) LONGITUDINAL - UNAGED



(b) LONGITUDINAL AGED



(c) TRANSVERSE - UNAGED



(d) TRANSVERSE - AGED

Figure 26 - Elongation of Brush extrusions.

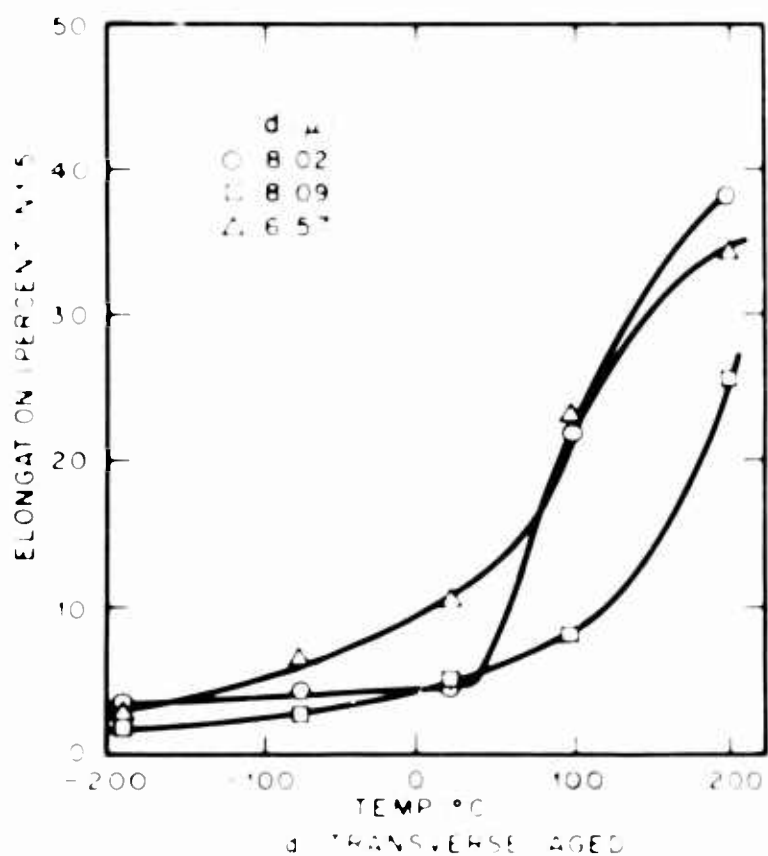
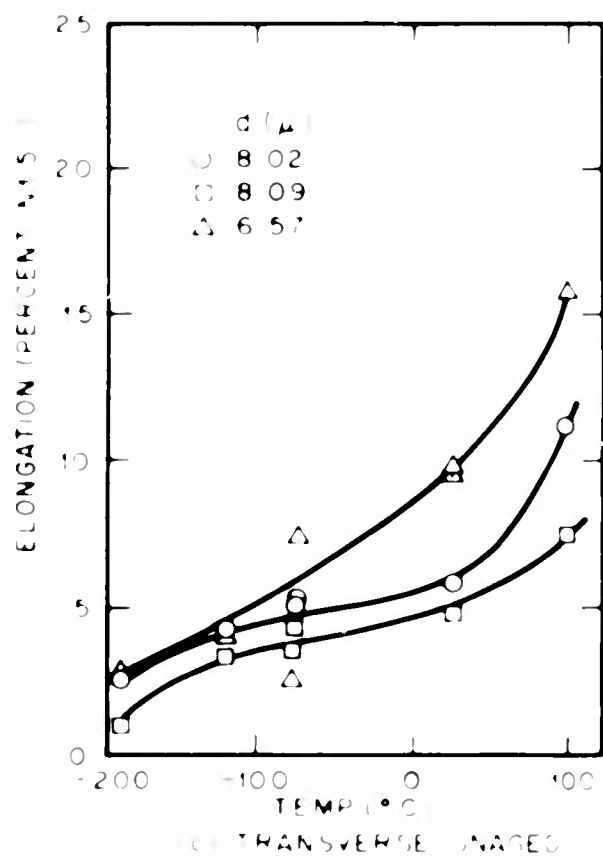
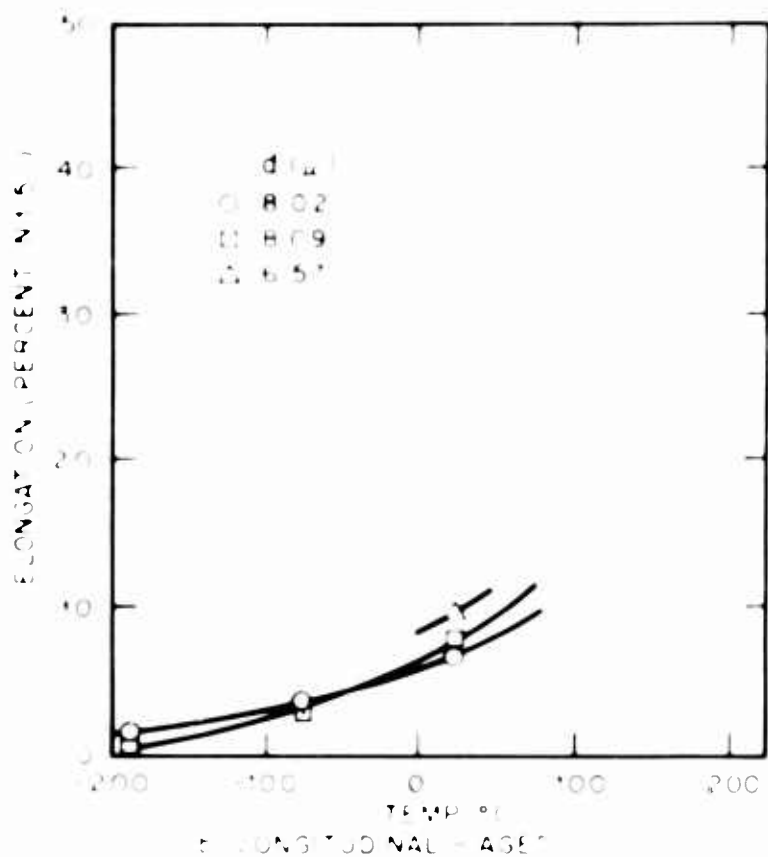
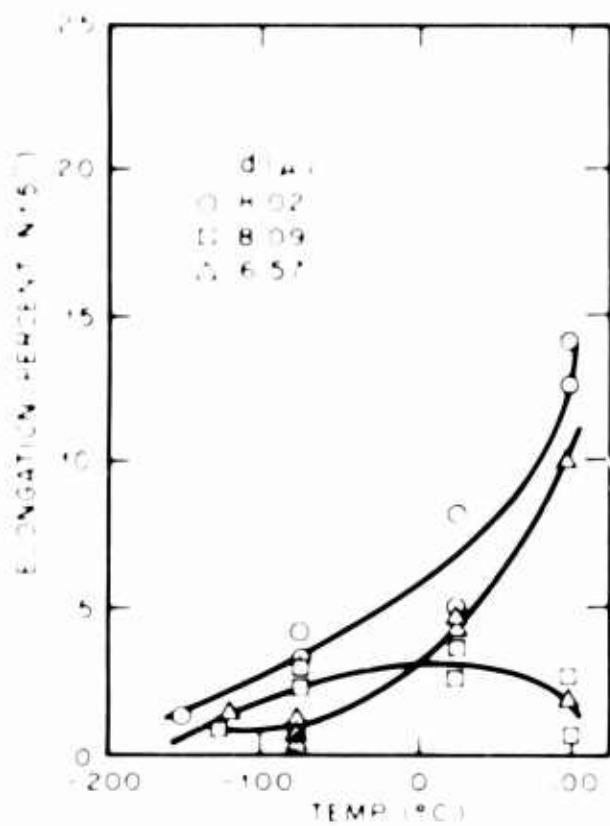


Figure 27 - Elongation of Pechiney extrusions.

samples showed either an upper or lower yield point, or an inflection in the stress-strain curve at yielding. There was no consistency in the appearance of such irregularities, although, as indicated by the solid points in Figures 24 and 25, they were more prevalent in the finer-grained, less pure materials. The appearance and magnitude of an upper yield point is subject to a number of variables, such as alignment, surface condition, and strain rate, and it is possible that those samples showing merely an inflection would have shown an upper and lower yield point under special test conditions.

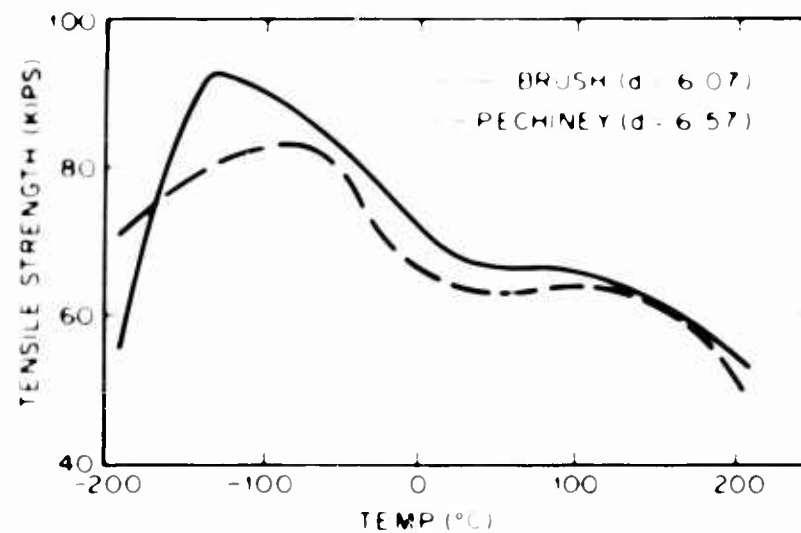
Elongation vs. temperature plots are shown in Figures 26 and 27. In examining these figures, care should be taken to note the change in the ordinate values for elongation in the aged condition when compared to the unaged. For the Brush extrusions, ductile-brittle transitions were observed in the aged and unaged longitudinal samples, and in the aged transverse samples. Such transitions may have been observed in the unaged transverse samples had testing been extended to higher temperatures. Aging generally had little effect on the elongation values, although at 100°C ductility of the fine-grained transverse sample is about twice that for the unaged.

The ductility situation for the Pechiney extrusions is somewhat unclear. In the unaged longitudinal condition, the extrusion with $d = 8.02$ microns, which, incidentally, has the lowest impurity content, had the greatest ductility. This is contrary to the behavior of the Brush extrusion in the same condition, in which the greatest ductility was exhibited by the least pure, smallest grain size material. In the aged condition, only a single, small grain size ($d = 6.57$ microns) sample was tested at room temperature, but the elongation was 10 percent, twice that for the unaged specimens.

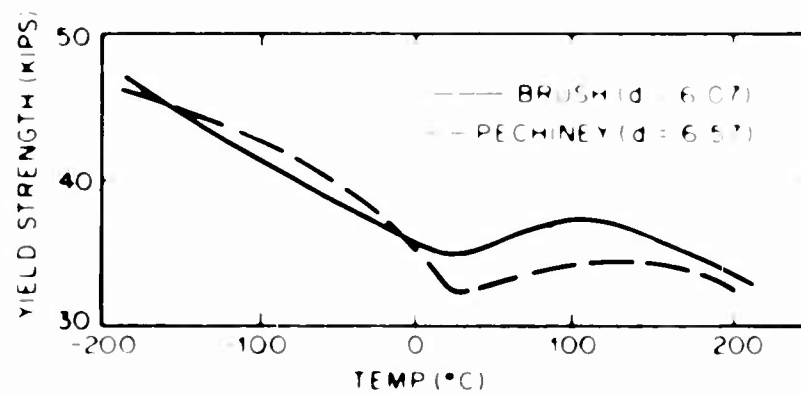
In the unaged transverse condition, the 6.57 micron samples had the best ductility. Aging had little effect below room temperature, but produced a marked improvement in the 6.57 and 8.02 micron samples at 100°C.

A comparison of the mechanical properties of the aged Brush and Pechiney fine-grain size extrusions in the transverse orientation is shown in Figure 28. The marked similarity is apparent, despite the differences that existed prior to heat treatment. There was not enough longitudinal samples to make similar comparison, but where data exist, the properties of the aged 9.59 micron Brush material are very similar to those of the aged 8.02 micron Pechiney material.

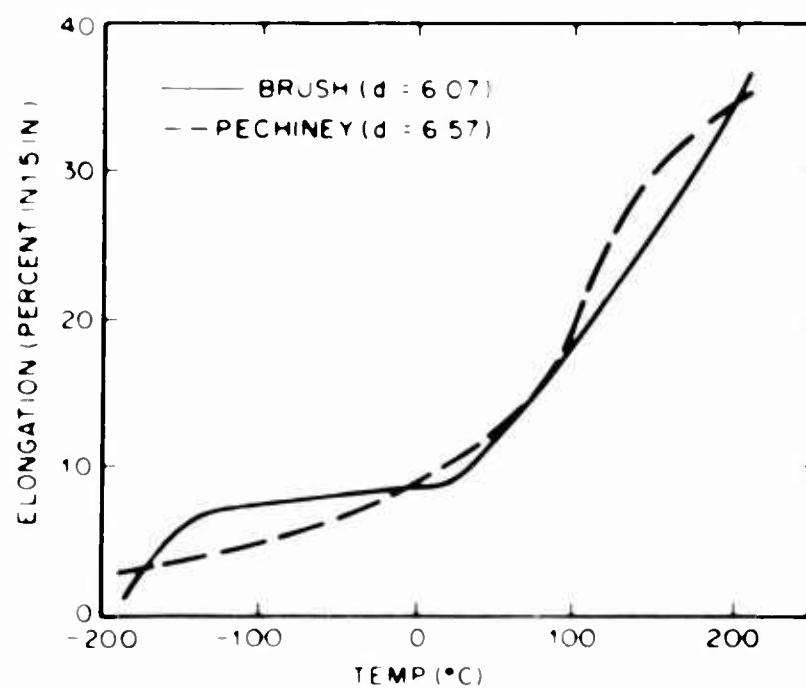
True stress-true strain curves for unaged Brush extrusions tested at room temperature are shown in Figure 29. For comparable strains, the work hardening rates increase as grain size decreases, and are higher for the longitudinal orientation. A similar set of curves is shown for -195°C in Figure 30. These curves are all drawn to the fracture point, making evident the superior strength and ductility of the transverse samples for comparable grain sizes. The serrated curve for the 14.5 micron longitudinal sample is indicative of extensive twinning at low temperature, which was verified metallographically. Although no serrations were visible in the load-extension curves for the 9.59 micron sample, metallographic examination showed a region of twinning along the center of the sample, as shown in Figure 31. Figure 32 shows that similar twinning did



(a) TENSILE STRENGTH



(b) YIELD STRENGTH



(c) ELONGATION

Figure 28 - Comparison of mechanical properties of aged Brush and Pechiney extrusions tested in the transverse direction.

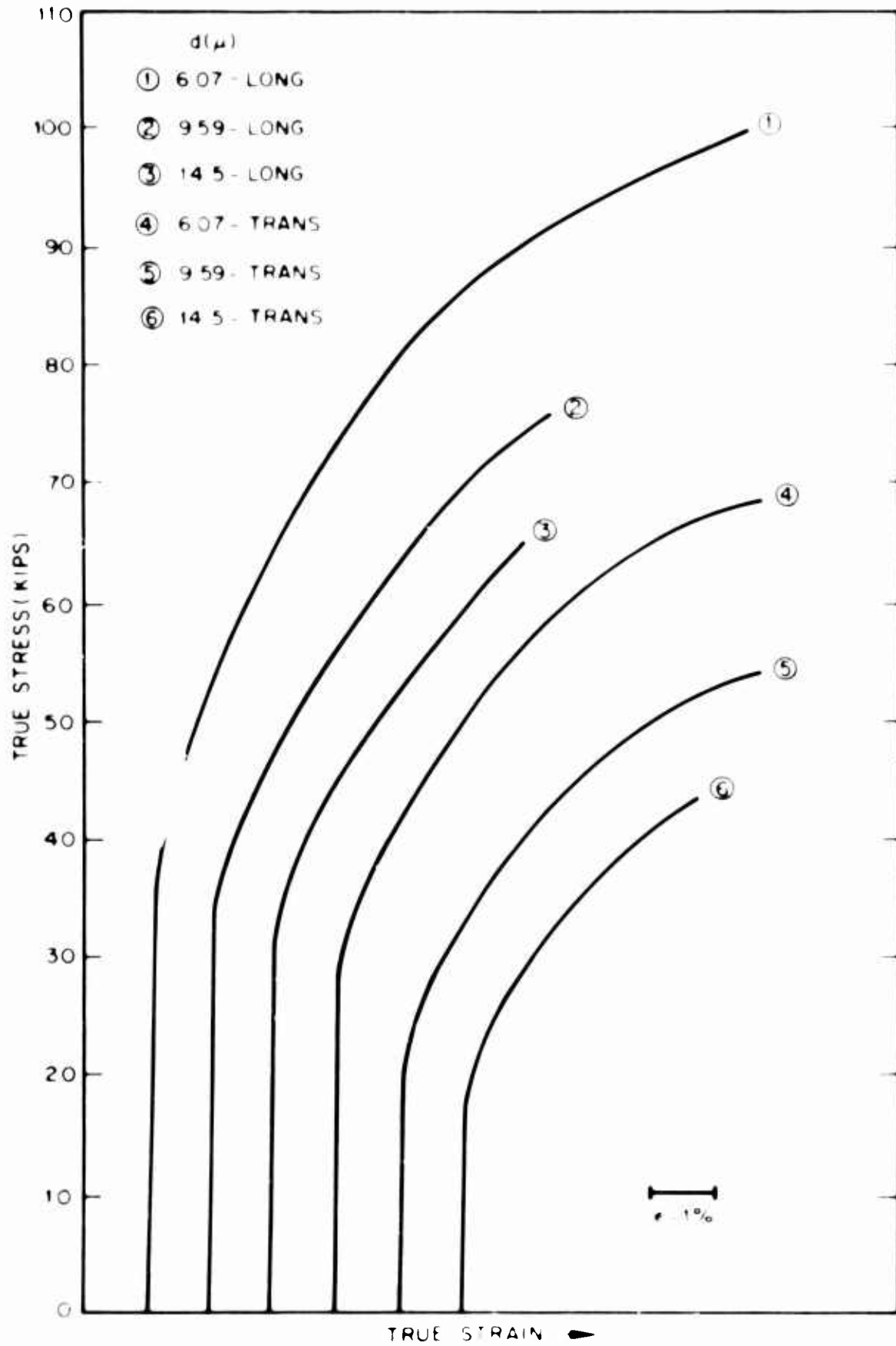


Figure 29 - True stress vs. true strain curves for unaged brush extrusions tested at 23°C.

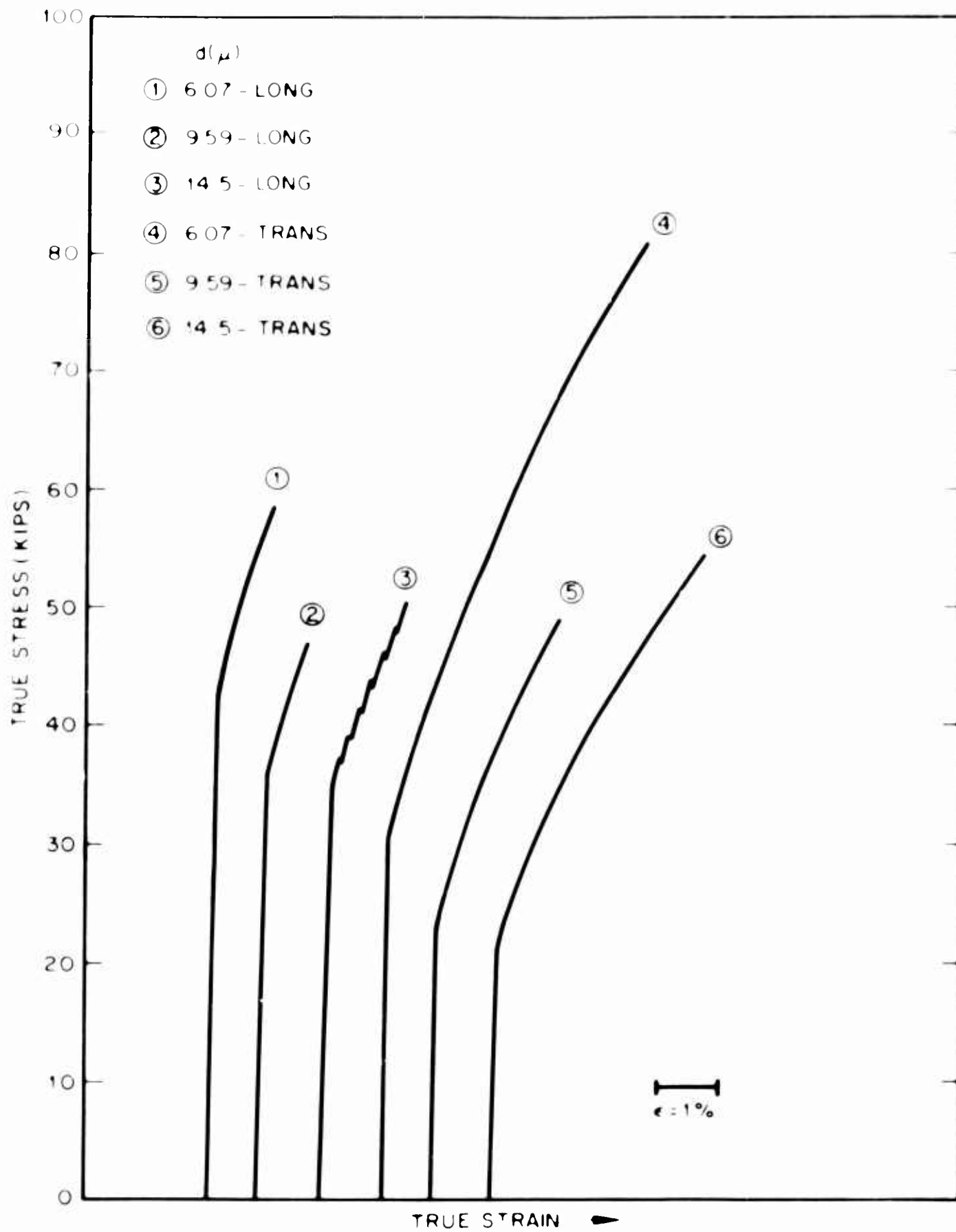


Figure 30 - True stress vs. true strain curves for unaged Brush extrusions tested at -195°C .

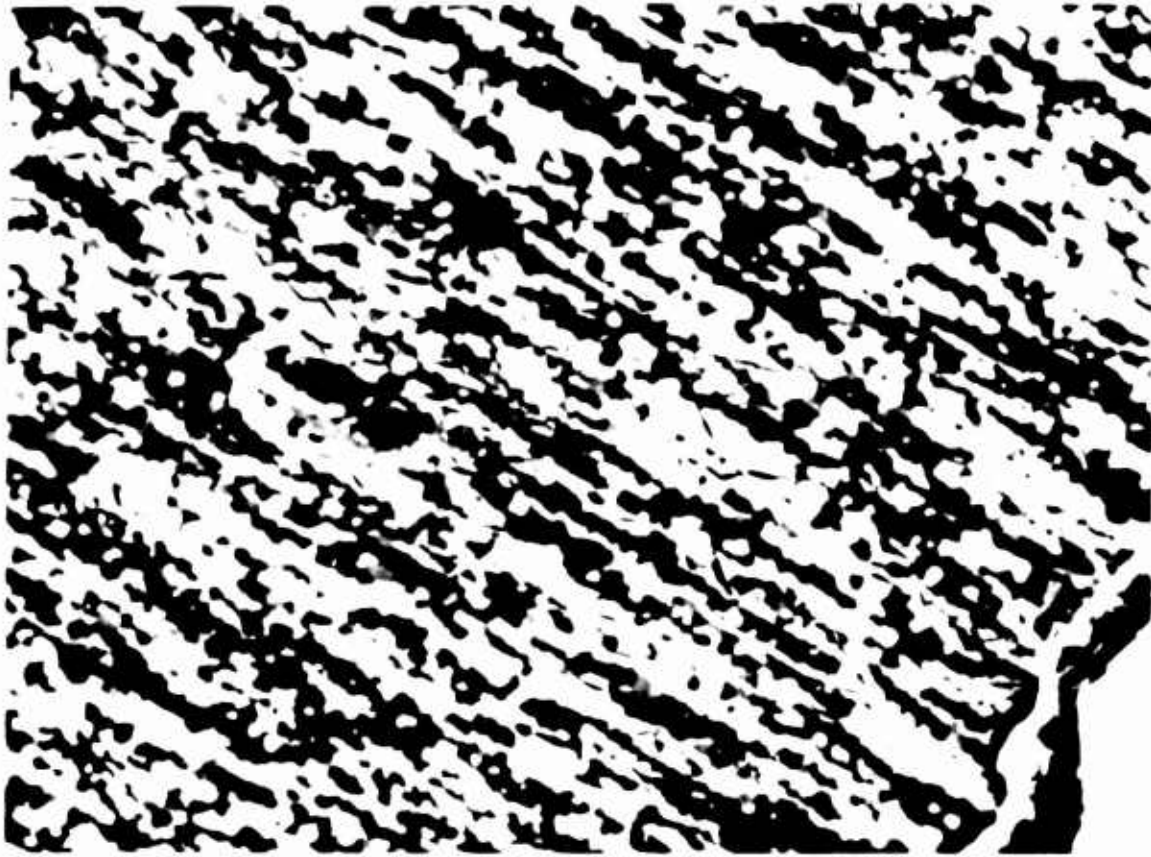


Figure 31 - Twinning in central portion of longitudinal Brush specimen tested at -195°C . 100X. Polarized light.

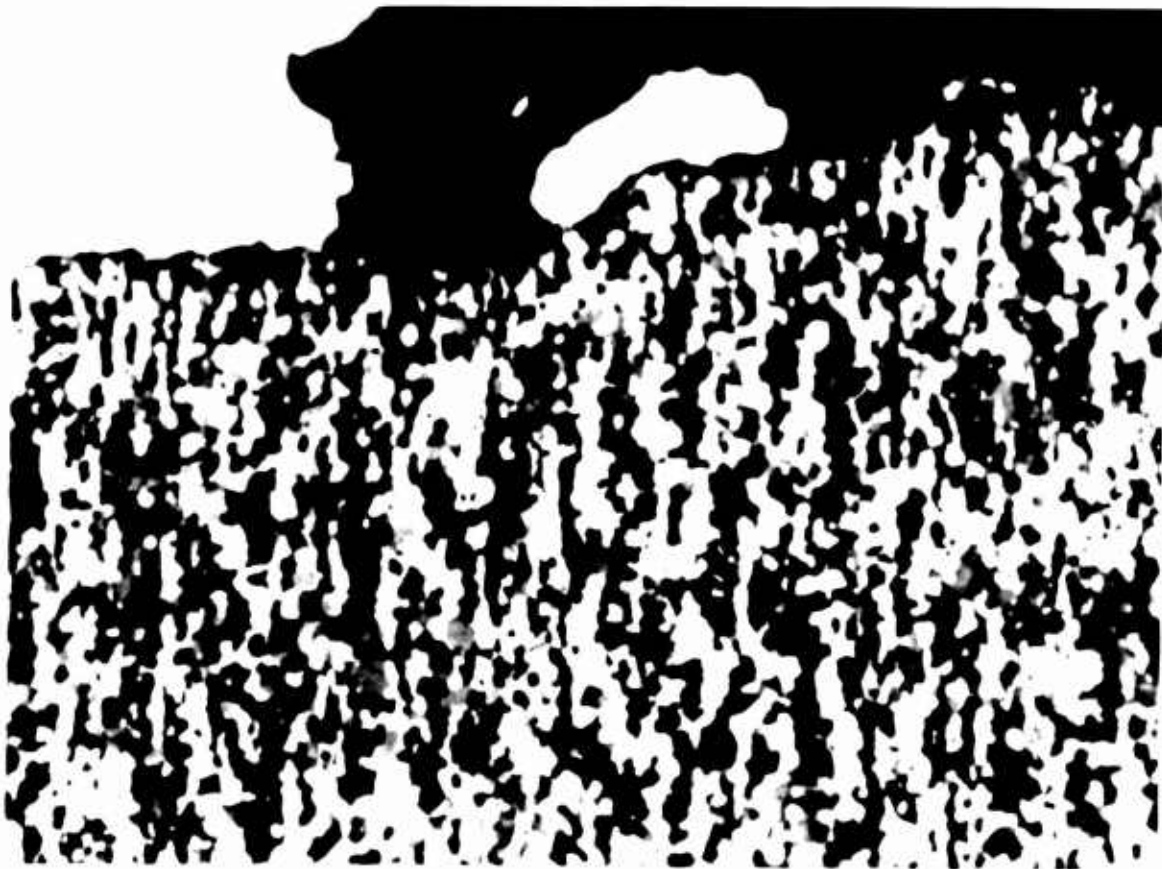


Figure 32 - Central portion of transverse Brush specimen tested at -195°C . 100X. Polarized light.

not exist in the transverse sample of the same grain size. Serrated stress-strain curves were also observed for the 6.57 and 8.09 micron transverse Pechiney samples tested at -120°C , and for a 14.5 micron longitudinal Brush sample tested at -120°C . No serrated stress-strain curves were obtained for extrusions in the aged condition.

Stress-strain curves for the 6.07 micron Brush extrusion tested in various conditions are shown in Figure 33. A typical yield point is indicated for the aged longitudinal specimen tested at 23°C , while a typical yield inflection is indicated for the aged transverse sample at the same temperature. Typical curves for Pechiney extrusions are shown in Figure 34.

The effect of strain rate was not investigated for the extrusions, nor was the effect of prior strain.

Section 4

DISCUSSION OF RESULTS

4.1 General Discussion of Tensile Data

4.1.1 Hot-Pressed Material

The tensile and yield strengths of unaged Brush Beryllium are slightly higher than Pechiney material of comparable grain size, due probably to the higher impurity content of the Brush QMV powder. Aging did not significantly alter strength values for either of the materials. Yield points or yield inflections were not observed in any of the aged or unaged samples, contrary to the results of Mash (Ref. 22), who observed yield inflections even in unaged hot-pressed block. No explanation can be offered for this difference, since grain size, purity, and test conditions appear to be similar. The primary difference is in Mash's specimens, which had a 0.25 x 0.50 in. cross-section.

Ductility of the unaged Brush samples was relatively low at all temperatures. Usually, the ductility of hot-pressed beryllium will increase sharply in the 200-300 $^{\circ}\text{C}$ range (Ref. 1, for example). Since such increases were observed in the unaged Pechiney material, the low ductility of the Brush samples at elevated temperatures appears directly attributable to its high impurity content. This is further demonstrated by the results obtained on aged Brush samples, which showed marked improvements in ductility at the higher temperatures. The X-ray diffraction studies reveal that solute atoms, particularly iron, have precipitated from solid solutions, forming $\text{Be}_5(\text{Fe}, \text{Al})$ and Be_{11}Fe particles that are non-coherent with the matrix. Impurities present as precipitates are evidently less detrimental to ductility than when they are in solid solution. The particles are thought to be non-coherent, since the yield strength was not affected by aging. The lack of an effect of heat treatment on

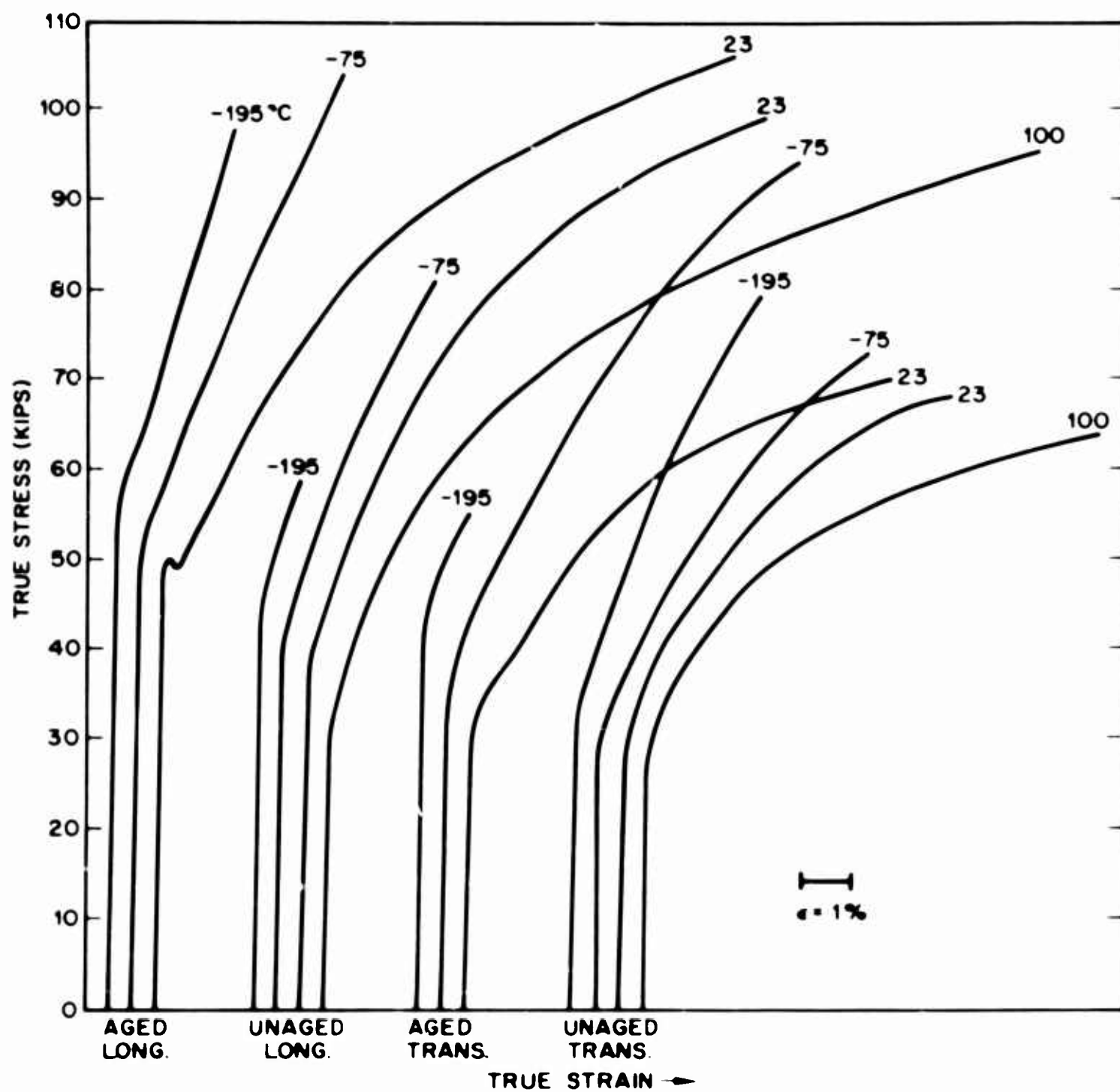


Figure 33 - True stress vs. true strain curves for Brush extrusions at various temperatures, $d_1 = 6.07$ microns.

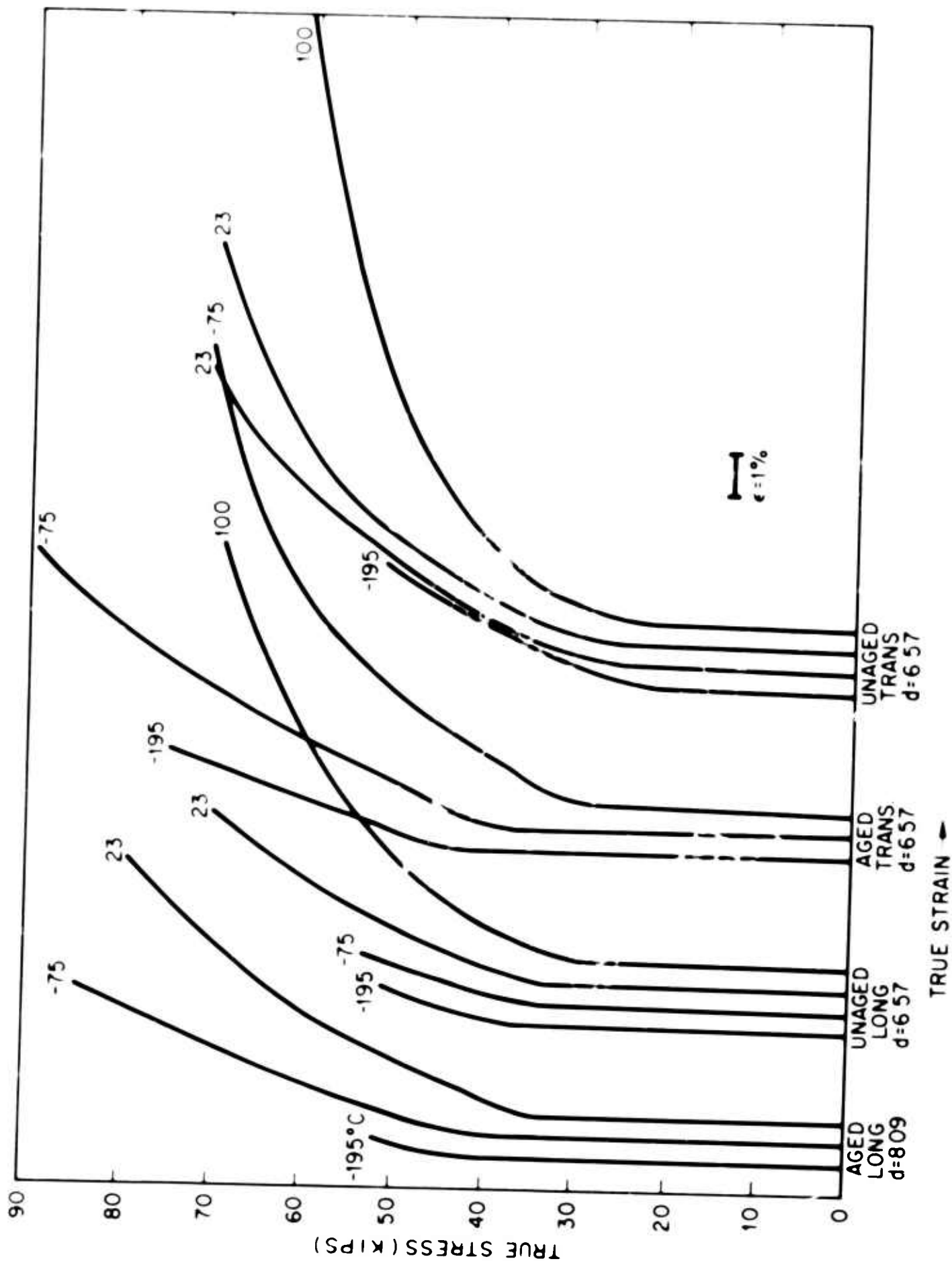


Figure 34 - True stress vs. true strain curves for Peciney extrusions at various temperatures.

yield strength can also be explained by the supposition that softening resulting from solid solution depletion balances or outweighs any hardening due to the precipitate itself (Ref. 35).

The location of the precipitate particles is not definitely known, since metallographic examination at 1000X failed to reveal any difference between aged and unaged structures. Electron microscopy was not employed. According to Adda, et al (Ref. 34), aluminum was present in the grain boundaries of commercial purity beryllium when heated above 650°C. Adda's material contained 1500 ppm of Al, and 400-450 ppm of iron. During heating between 650 and 800°C, iron and silicon dissolved in the aluminum, but above 1000°C, iron returned to the matrix, where it could be retained by quenching. In the present investigation, the Brush material contained some 1500 ppm of iron, which was probably retained in the matrix on cooling from 900°C. A portion of this was subsequently precipitated as Be_{11}Fe on reheating to 700°C. Some of the iron also migrated to the grain boundary, where it dissolved in the aluminum to form $\text{Be}_5(\text{Fe}, \text{Al})$. The Pechiney material contained a maximum of 190 ppm of Al and 300 ppm of Fe. This small amount of iron is soluble in beryllium at 700°C and would not precipitate on thermal treatment, which corresponds to the observation that no Be_{11}Fe was formed in the aged Pechiney samples. However, the iron in solution apparently migrated to the aluminum at the grain boundaries to form the observed $\text{Be}_5(\text{Fe}, \text{Al})$. Precipitation of Be_{11}Fe might be induced in the Pechiney material by long time, low temperature aging treatments.

That some redistribution of impurities did occur in the present study can be inferred from Figures 35 and 36, which show the structure adjacent to the fracture surface of unaged and aged Pechiney specimens tested at 300°C. The unaged specimen contains a few transgranular fractures in grains near the fracture surface. The aged specimen shows several fractures which at higher magnification and under polarized light appeared to be primarily transgranular. Evidently, it was easier to nucleate cracks in the aged material but more difficult to propagate them, permitting greater deformation prior to fracture.

The observation that repeated yielding was observed in the Brush samples tested at 400°C is an indication that even after aging, there are significant amounts of impurities still in solution. Serrated stress-strain curves result at elevated temperatures when strain aging occurs during deformation, i.e., when temperature and strain rate are such that initially a dislocation is torn from its atmosphere, only to regain it later as the dislocation is held up at some obstacle. Repeated yielding has also been observed between 350 and 575°C in large-grained extruded vacuum-cast metal (Ref. 16, p. 418) and in extruded flake and pebble ingot at 300-500°C (Refs. 34, 35). In all cases, it has been attributed to foreign atoms in solution.

Inflections in the curves of tensile and yield strength in the range 300-400°C can be explained by strain aging (Ref. 34). Precipitation during straining at these temperatures apparently acts as a strengthening mechanism.

Increasing the strain rate reduces the magnitude of the repeated yield effect at 400°C. This is in accord with the theory that the repeated yielding

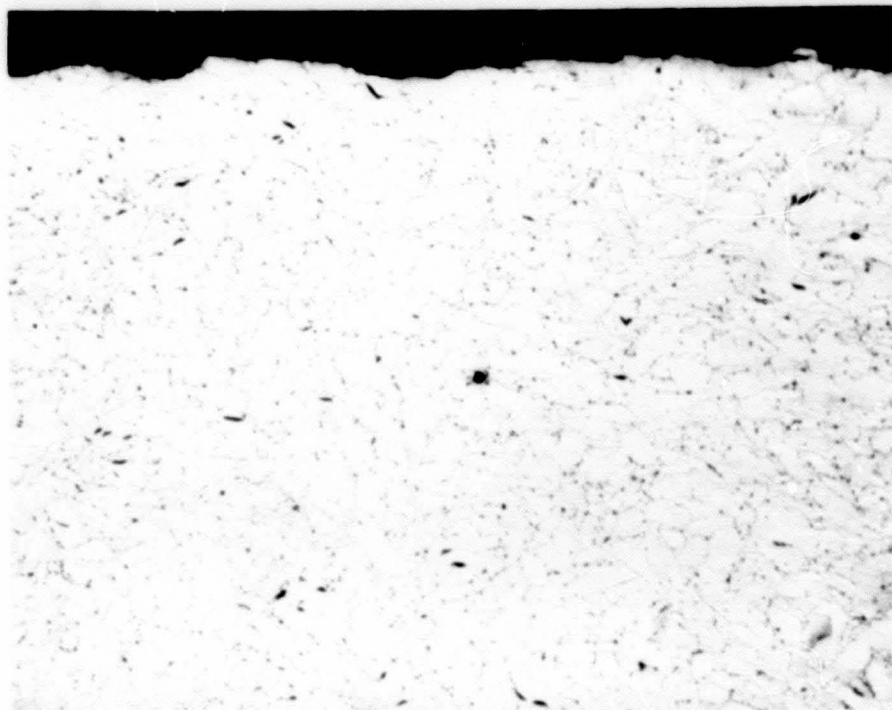


Figure 35 - Region adjacent to fracture surface of unaged, hot-pressed Pechiney specimen tested at 300°C, $d = 10.3 \mu$. 100X.

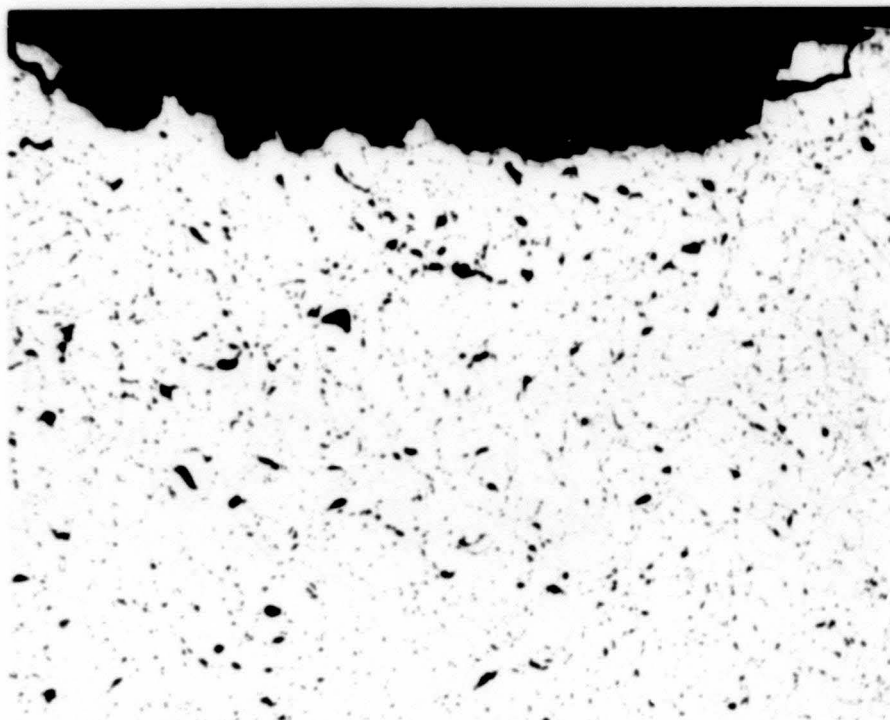


Figure 36 - Region adjacent to fracture surface of aged, hot-pressed Pechiney specimen tested at 300°C, $d = 10.3 \mu$. 100X.

is due to dislocation locking, since at high strain rates the dislocations would be expected to break away from the atmospheres and not be locked again.

The effects of strain rate on tensile and yield strength at all temperatures was only slight. However, ductility decreased markedly with increasing strain rate, displacing the ductile-brittle transition to higher temperatures. This behavior is characteristic of the region in which fracture is transgranular (Ref. 34). It is also what would be expected if the ductile-brittle transition is related to a thermally-activated deformation process, as will be discussed subsequently.

The experiments involving the effects of prior strain at elevated temperature on room temperature properties were prompted by results obtained by Weaver (Ref. 36) on chromium. After 3 percent strain of chromium at 400°C, just above the ductile-brittle transition temperature of 350°C, the material had a room temperature elongation of 66 percent. Presumably, dislocations were unlocked from impurity atoms at the elevated temperature. However, prestrains of 2 percent at 200 and 400°C had a slightly adverse effect on the room temperature ductility of beryllium. On the basis of the previous discussion, it would seem that deformation at 400°C would tend to lock the dislocations rather than free them. However, if this were so, a yield point should appear on testing at room temperature. No such yield points were observed, due possibly to dislocations being freed from their atmospheres by strains induced in cooling from the pre-strain temperature. The anisotropy of the coefficients of expansion of beryllium increases the likelihood that such strains would occur. In any event, the prestrains at 200 and 400°C can be treated simply as warm working operations, which raised the yield strength and lowered the ductility at room temperature.

4.1.2 Extruded Material

Consider first the properties of Brush extrusions. Contrary to expectations, the tensile strength of unaged material in the longitudinal direction decreased as temperature decreased below room temperature. On the other hand, the transverse specimens increased in strength with decreasing temperature, and also exhibited superior ductility below -100°C. This behavior is thought to be related to the extensive twinning that was observed at low temperatures in the longitudinal extrusions. The twins are likely sites for crack nucleation (Refs. 4, 28), particularly at low temperature, where the lack of deformation modes would inhibit, or prevent, the relief of stresses existing at the tip of a twin.

One factor that must be taken into account in this explanation is that the crystallographic orientation of longitudinal samples is unfavorable for twinning. The orientation is such that the c-axes are perpendicular to the extrusion direction, and hence, perpendicular to the direction of the tensile stress. In order to cause twinning in metals with c/a less than $\sqrt{3}$, as in beryllium, it is necessary to apply a tensile stress parallel to the c-axis. This could arise if some of the grains otherwise unfavorably oriented were somehow constrained to twin. One possible mechanism for establishing the necessary constraints has been proposed by Main (Ref. 37). A specimen in tension tends to

elongate in the direction of applied stress and to contract in a perpendicular direction. The outside of the specimen is free to contract, but the center is restrained from doing so by the material around it. This, in effect, produces a tensile stress on material at the center which is actually perpendicular to the applied tensile stress. Thus, there would be a component of tension parallel to the c-axes and twinning could occur.

The situation for aged Brush samples is apparently different, since aging significantly increased tensile and yield strengths, particularly below room temperature. For example, the tensile strength in the longitudinal direction increases with decreasing temperature and only shows a slight decrease below -100°C . Tensile strength of the transverse samples also increases with decreasing temperature, although there is a drop in strength below -130°C . The load-extension curves for the longitudinal samples did not indicate twinning, as was the case for the unaged samples. No metallographic examination of the aged samples was made. The conclusion to be drawn from this is that purification of the matrix by precipitation of impurities from solid solution has decreased the propensity for twinning, and hence, eliminated a premature failure mechanism. According to Garber, et al (Ref. 38), the elimination of impurities from beryllium increases the uniformity of deformation and, consequently, raises the plasticity.

The effect of purity on low temperature properties can also be seen from a consideration of the tensile strength and ductility of longitudinal unaged Pechiney samples. The tensile strengths of the large-grained, but purer, samples are higher than those of the fine-grained samples below -50°C . The elongation of the purest material (extruded from the $-50 + 120$ mesh powder) is highest at all temperatures (Figure 27a). This was not true of the unaged transverse Pechiney samples, where grain size appears to be the dominant factor, at least above liquid nitrogen temperatures.

From the increases in tensile strengths that resulted after aging in both the Brush and Pechiney extrusions, it might be expected that elongation would also increase below room temperature. However, no increase was observed, most probably because the yield strength also increased, and thus, there was no net change in the capacity for plastic flow.

The yield behavior after aging is interesting, and not at all similar to the case for the randomly oriented, hot-pressed samples. Aging served to raise the yield strength, particularly below room temperature, and to introduce yield points or yield inflections in many instances. The presence of a yield point may be due to simple dislocation locking. In hexagonal close-packed metals, an interstitial solute atom produces a non-spherically symmetrical distortion which is capable of interacting with both edge and screw dislocations, and yield points have been observed in cadmium (Ref. 39) and zinc (Ref. 40) crystals which contained nitrogen. Yield points are also frequently observed in beryllium (Refs. 22, 24), but have not been related to any specific impurity element. Since yield points were observed only in the aged alloys, it is possible that precipitate particles prevent significant amounts of dislocation movement until a sufficiently high stress is reached, at which point large numbers of dislocations could move around or through the precipitate particles. In this case,

yielding is a dynamic phenomenon, involving a sudden multiplication of the number of moving dislocations at suitable velocities (Ref. 41). Additional experiments specifically related to the yield point in beryllium would have to be performed if this phenomenon is to be fully understood.

The reason why yield points were observed in the extrusions is believed to be related to their preferred orientation. In the randomly oriented, hot-pressed material, only a relatively few grains are correctly oriented for flow to occur at a particular stress level, and yielding is a gradual process. In the extrusions, there are many grains with suitable orientation, and large numbers of them can yield at a particular stress, giving rise to effects sufficiently large to be measured by the tensile machine.

The increases in yield strength below room temperature after aging are indicative of a dispersed phase hindering dislocation motion. Similar hardening below room temperature has been observed in zirconium containing a dispersion of $ZrCr_2$ (Ref. 42) and Al containing $CuAl_2$ (Ref. 43). The increases in tensile strength result from the elimination of the premature failure mechanism due to purification of the matrix. The premature failure mechanism is believed to be twinning in the case of longitudinal specimens, and bend-plane splitting in the case of transverse specimens.

One additional factor deserves comment in connection with the yield strength data for the extrusions. It is apparent that both the temperature dependence of the yield strength for the longitudinal and transverse samples, as well as the magnitude of the difference in yield strength in the two directions,* bear little resemblance to single crystal data (Ref. 11). This is partly the result of the relatively low extrusion ratio, which prevented development of "pure" textures, and partly due to the inhomogeneities in flow and the constraints that develop in the deformation of any polycrystalline aggregate.

Also of interest in the present study was the relatively high ductility observed in the transverse extrusions, which is contrary to the results of previous investigators (Refs. 1, 12). This again is related to the impure texture and the constraints existing at grain boundaries. Flow undoubtedly commenced on the basal planes, but as stress increased, some prismatic flow probably took place, particularly at grain corners or other areas where stresses could be concentrated.

4.2 Ductile-Brittle Transition Theory

Theories of the ductile-brittle transition in beryllium have been extensively discussed in recent years (Refs. 6, 13, 18) and only a brief summary will be given here. In the review by Martin and Ellis (Ref. 13), the lack of three-dimensional ductility in polycrystalline beryllium at low temperature was ascribed to several factors, all of which may be contributory. These are:

* Magnitudes can be compared directly, in spite of orientation differences. Multiplying the applied stress by 0.43 gives the shear stress on the basal planes in the transverse samples, and also the shear stress on the prism planes in the longitudinal samples.

(1) The restricted number of deformation modes, which make it difficult to transmit slip from grain to grain and to accommodate lattice stresses resulting from slip on a single system.

(2) The absence of slip modes resolvable along the c-axis.

(3) The fact that the basal plane is the predominant slip plane and also the plane of easy cleavage.

(4) The ease with which bend planes form during basal slip, and the inability of these bend planes to be moved by the applied stress, so that further strain promotes basal-plane splitting (Ref. 44).

The rapid increase in ductility above room temperature may therefore be due to:

(1) The rapid drop in the resolved shear stress required for prismatic slip as the temperature is increased.

(2) The onset of pyramidal slip, possibly in a direction that can be resolved along the c-axis.

(3) An increasing ability for basal slide to occur without the formation of bend planes, as the temperature is raised, or an increased ability for bend planes, once formed, to migrate under the influence of the applied stress.

Purity, although not specifically mentioned above, would exert a strong influence on the stresses required for the movement of dislocations in any deformation mode. Theories of the ductile-brittle transition have been extensively investigated for b.c.c. metals, and equations have been developed that explain the transition with some fair amount of success. These theories have already been described in detail (Ref. 45) and only the salient points will be mentioned here, along with the attempts to fit the data obtained in the present program to the existing theories.

4.2.1 Theory of Cottrell (Ref. 46)

The yield stress of b.c.c. metals generally fits the equation (Ref. 5):

$$\sigma_y = \sigma_1 + k_y d^{-\frac{1}{2}} \quad (3)$$

in which σ_y is the yield stress, σ_1 a lattice friction stress, k_y is a constant relating to the stress required to unpin a dislocation, and d the grain diameter. From this, the following equation, relating change in transition temperature to grain size, can be derived:

$$\frac{\delta T}{\delta d^{\frac{1}{2}}} = - \frac{\sigma_1 k_y d^{-\frac{1}{2}}}{\sigma_y - \frac{k_y}{T} + k_y \frac{\partial \sigma_y}{\partial T}} \quad (4)$$

In the transition region, values can be found for the parameters in Eq. 4 and a value of $\delta T / \delta d^{\frac{1}{2}}$ calculated. From this, the effects of changes in d on the transition temperature can be determined.

The quantities on the right-hand side of Equation 4 can all be determined from plots of σ_y vs. $d^{-\frac{1}{2}}$, provided such plots are linear. Figures 37 and 38 show the effect of grain size on the yield strength of Brush hot-pressed block and Brush extrusions, respectively. The linear relation is obeyed, except for the aged extrusions. The quantity σ_1 , supposedly representing a lattice friction stress, is obtained by extrapolation of the data to the stress axis, where a positive value should be obtained. In Figure 37b, the physical significance of curves that extrapolate to negative values of stress is difficult to assess. Thus, before any calculations are even made, it can be seen that there are problems in attempting to fit the data to Cottrell's theory.

Notwithstanding, the case for longitudinal unaged extrusions will be analyzed as the transition temperatures are rather sharply defined and good linear plots are obtained (Figure 38). The value of σ_1 is approximately 20,000 psi, or 14 kg/mm². The slope, k_y , is similar for all curves and is 1.4 kg/mm^{3/2}. The variation of k_y with temperature is slight, so $\partial k_y / \partial T = 0$. The variation of yield strength with temperature, $\partial \sigma_y / \partial T$ is obtained from Figure 24a, and is -2.8×10^{-2} kg/mm² per degree for the middle grain size in the vicinity of the transition temperature. Substituting these values into Equation 4 gives

$$\frac{\delta T}{\delta d^{\frac{1}{2}}} = + \frac{14 \text{ kg/mm}^2 \times 1.4 \text{ kg/mm}^{3/2} \times 10.1 \text{ mm}^{-\frac{1}{2}}}{1.4 \text{ kg/mm}^{3/2} \times 2.8 \times 10^{-2} \text{ kg/mm}^2/\text{deg}} = 5050 \text{ deg/mm}^{\frac{1}{2}}$$

To determine the experimental value of $\delta T / \delta d^{\frac{1}{2}}$, the following information is obtained from Figure 26a:

$d(\text{mm})$	$d^{\frac{1}{2}}(\text{mm}^{\frac{1}{2}})$	$T_c(\text{deg K})$
14.5×10^{-3}	12.0×10^{-2}	318
9.59×10^{-3}	9.8×10^{-2}	263
6.07×10^{-3}	7.8×10^{-2}	223

If $d^{\frac{1}{2}}$ is plotted against T_c , a straight line is obtained with slope 2250 deg/mm^{1/2}. This is slightly less than half the value calculated on the basis of Cottrell's theory. However, it is obvious that difficulties would be encountered in applying this theory to some of the other data. For example, for Figure 36a, σ_1 would be nearly zero, and $\delta T / \delta d^{\frac{1}{2}}$ would be very small. The other cases shown could not be treated at all. In summary, Cottrell's theory is not considered to be applicable to beryllium.

4.2.2 Stroh's Theory of Probability of Brittle Fracture (Ref. 47)

Stroh developed a theory for the ductile-brittle transition based on the assumption that piled-up groups of dislocations form. Although he considered

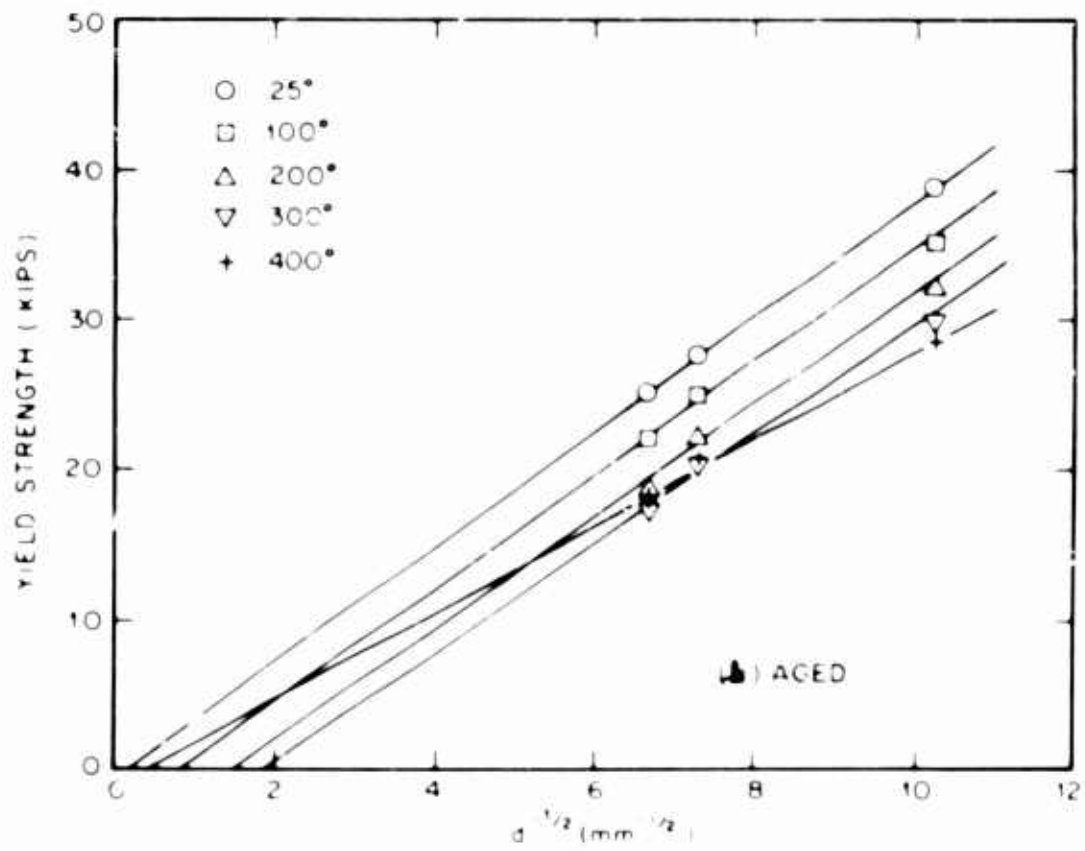
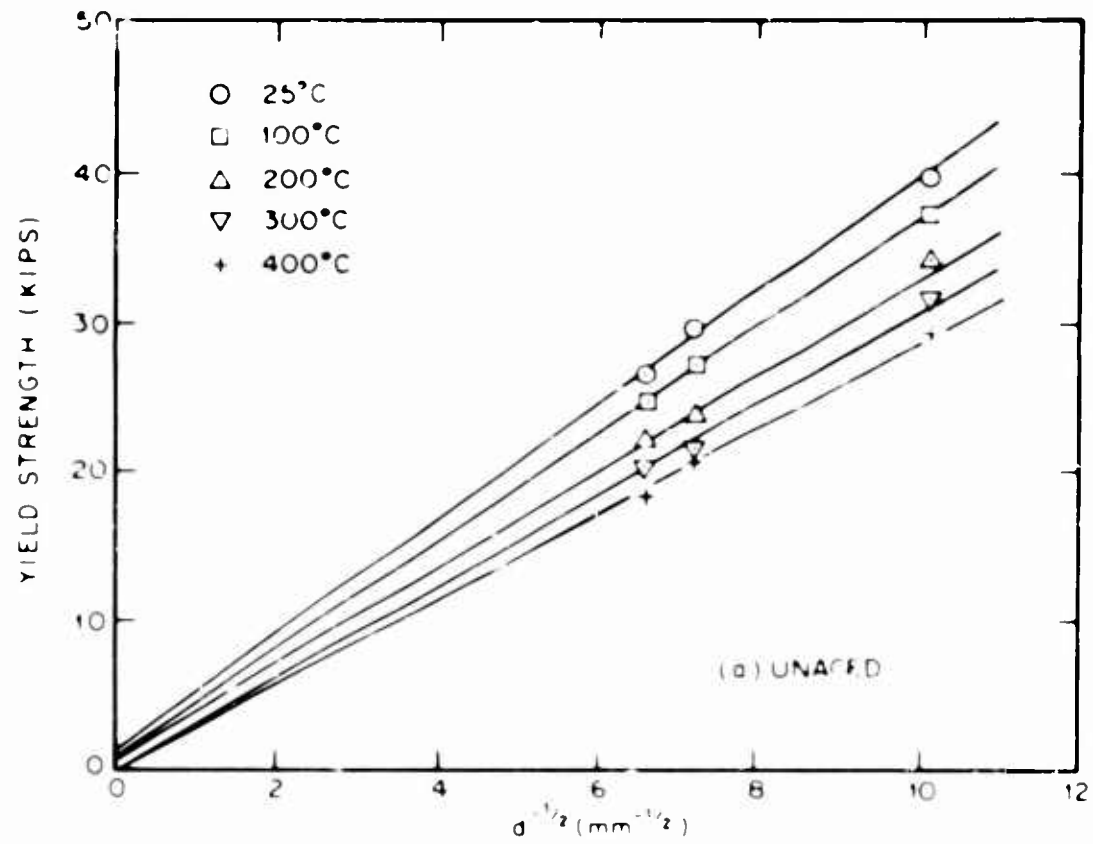


Figure 37 - effect of grain size on yield strength of not-pressed Brush tensile specimens.

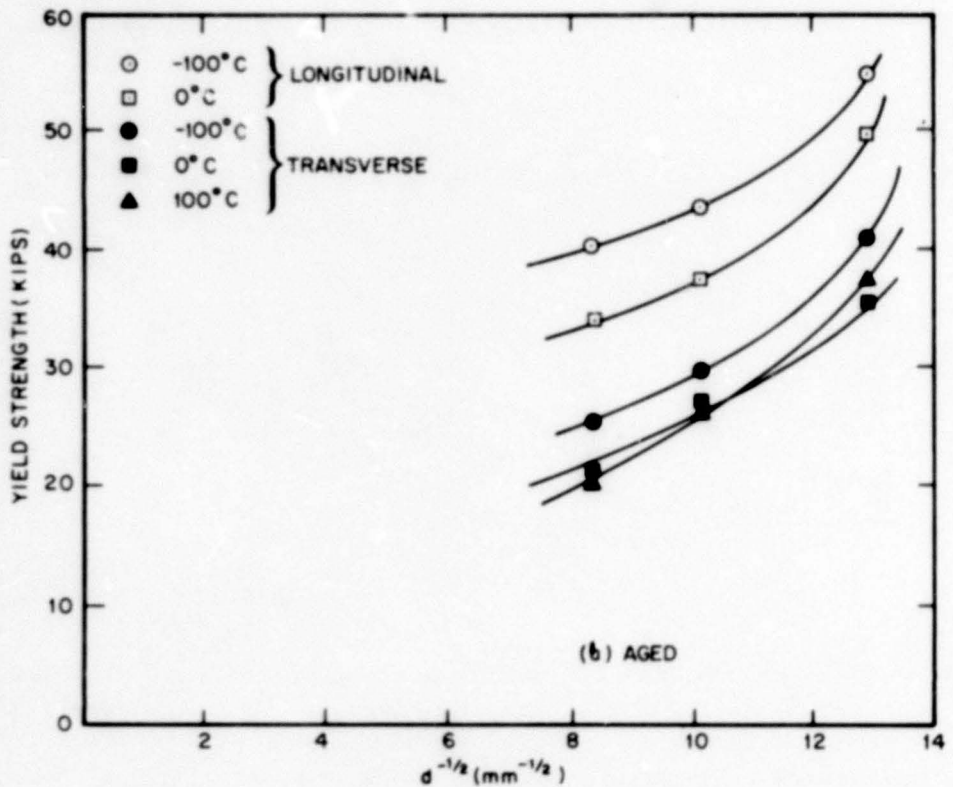
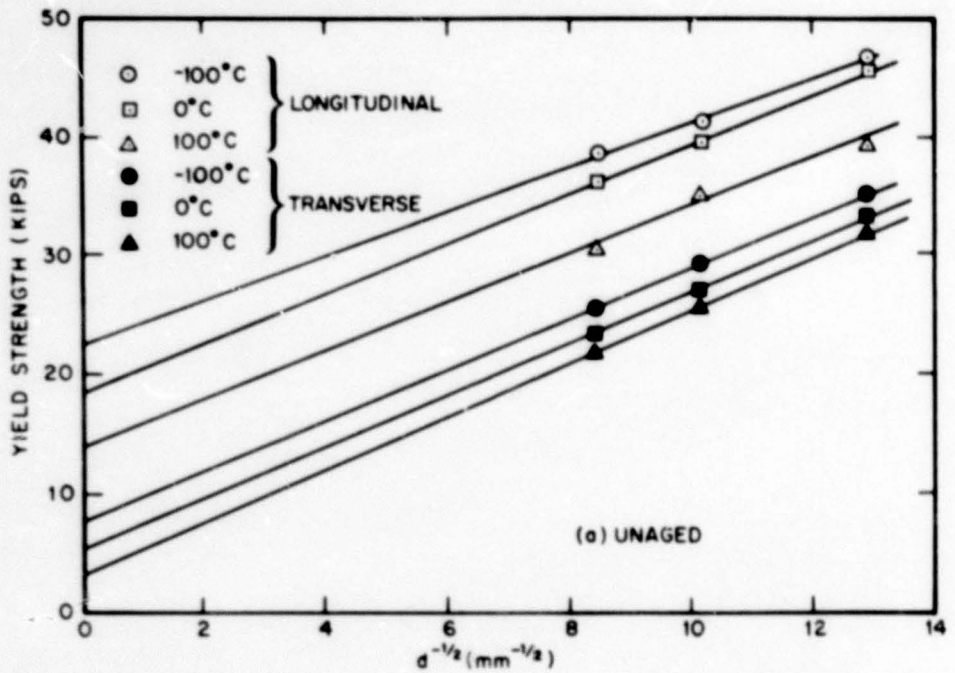


Figure 38 - Effect of grain size on yield strength of extruded Brush tensile specimens.

this case specifically, his method is applicable to any situation in which dislocations are aided in their movement by thermal activation. Stroh assumes that if locked dislocations around a piled-up group can be freed by thermal fluctuations, the metal is ductile; however, if the temperature is too low to permit a sufficient amount of thermal fluctuation, the stresses around a piled-up group become high enough to initiate a crack, and the metal is brittle. Therefore, the probability of brittle fractures is identified with the probability that the dislocations near a piled-up group will not be released.

Stroh's equation defining the probability, p , that a locked dislocation will not be released by a stress dependent activation energy, $U(\sigma)$ is:

$$p = \exp \left[-\nu t \exp \left\{ -U(\sigma)/kT \right\} \right] \quad (5)$$

where ν is a constant of dimensions of frequency, t is the time for which the stress on the dislocation is near the value σ , k is the Boltzmann constant, and T is the absolute temperature. As a result of the double exponential, this function changes rapidly from 0 to 1 near a critical temperature, T_c , which is taken as the transition temperature. The model thus reproduces the sharp increase in elongation at the transition temperature. Because p increases from 0 to 1 over a short temperature range, it can take almost any positive value between 0 and 1, and is here assumed equal to $1/e$. Therefore,

$$T_c = \frac{U(\sigma)}{k \ln \nu t} \quad (6)$$

Grain size affects the transition temperature in the following manner. It is assumed that as long as slip can occur in at least one grain, deformation can continue; however, if slip is halted in all grains, the stress at the head of a piled-up group of dislocations may be sufficient to nucleate a crack and cause brittle fracture. The probability of a grain yielding at any time is the product of the number of grains considered and the probability $\nu \exp(-U/kT)$ of a given grain yielding. In a sample of uniform grain size, the number of grains in any region is proportional to d^{-3} ; thus, ν can be redefined to include a factor proportional to d^{-3} . Since t was shown by Stroh to be proportional to d^{-2} , then $\nu t \propto d^{-5/2}$. If this is inserted into Equation 6,

$$\frac{1}{T_c} = -7/2 \frac{k}{U(\sigma)} \ln d + C \quad (7)$$

where C is a constant that takes into account the unknown proportionality constant. The activation energy, $U(\sigma)$, where is a function of the applied stress, is the energy needed to operate a Frank-Read source some distance ahead of the piled-up group.

Allen and Moore (Ref. 6) plotted $1/T_c$ vs. $\ln d$ for beryllium sheet rolled from electrolytic flake ingot and obtained a value of 0.48 e.v. (1 e.v. = 23,000 cal) for $U(\sigma)$. In the present study, similar plots were made for those

Brush samples for which a transition was observed. Figure 39 shows that the linear plots were obtained, from which the following activation energies were calculated:

<u>Condition</u>	<u>U (e.v.)</u>
Hot-pressed, aged	0.36
Extruded transverse, aged	0.27
Extruded longitudinal, unaged	0.19

These are somewhat less than the value quoted by Allen and Moore, but indicate that the basic Stroh theory can be applied to beryllium. The following section of this report will discuss this in some detail. The small difference in grain size between Pechiney samples precluded a similar analysis.

In an earlier report (Ref. 45, p. 12), reference was made to the possibility of distinguishing between a pile-up mechanism and a split bend plane mechanism as being the primary cause of fracture. Unfortunately, no such distinction could be made, as the data obtained in this study fit either case.

4.2.3 Proposed Theory of the Ductile-Brittle Transition in Beryllium

The theory to be developed arose from a consideration of the reasons for the improvements in ductility that resulted from aging. For example, there were only very slight differences in the tensile and yield strengths of aged and unaged hot-pressed Brush samples but marked increases in ductility above a certain temperature. Examination of the stress-strain curves indicated that the primary difference between the two conditions was a lower rate of work hardening for the aged samples. Consideration was given to the fine-grained material, and the slope of the stress-strain curves was measured at 1 percent strain for several temperatures, with the result shown in Figure 40. The work hardening rates for the aged samples are significantly lower in the range from about 100-400°C, commensurate with the improved ductility of the aged samples in this region (see Figures 13 and 14). Note that both the ductilities and the work hardening rates are similar at 400°C for the two conditions. Figure 40 also shows a curve for aged Pechiney material. The curve for unaged Pechiney is not shown, but is almost identical. Again, correlations can be made with the improved ductility and lower work hardening rate as compared to the unaged Brush beryllium.

These results are emphasized in Figure 41, which shows the flow stress at strains of 0.05 and 1.0 percent for the fine-grained Brush specimens. The flow stresses at 0.05 percent are very similar for the aged and unaged conditions, but the aged samples show significantly lower flow stresses at percent strain in the 100-400°C region.

Similar correlations between ductility and work hardening rate were attempted for transverse specimens from Brush and Pechiney extrusions, with only partial success. For example, at room temperature, the work hardening rate for aged, fine-grained, Brush samples dropped below that for unaged, corresponding to the sharp increase in ductility in the aged condition at that temperature.

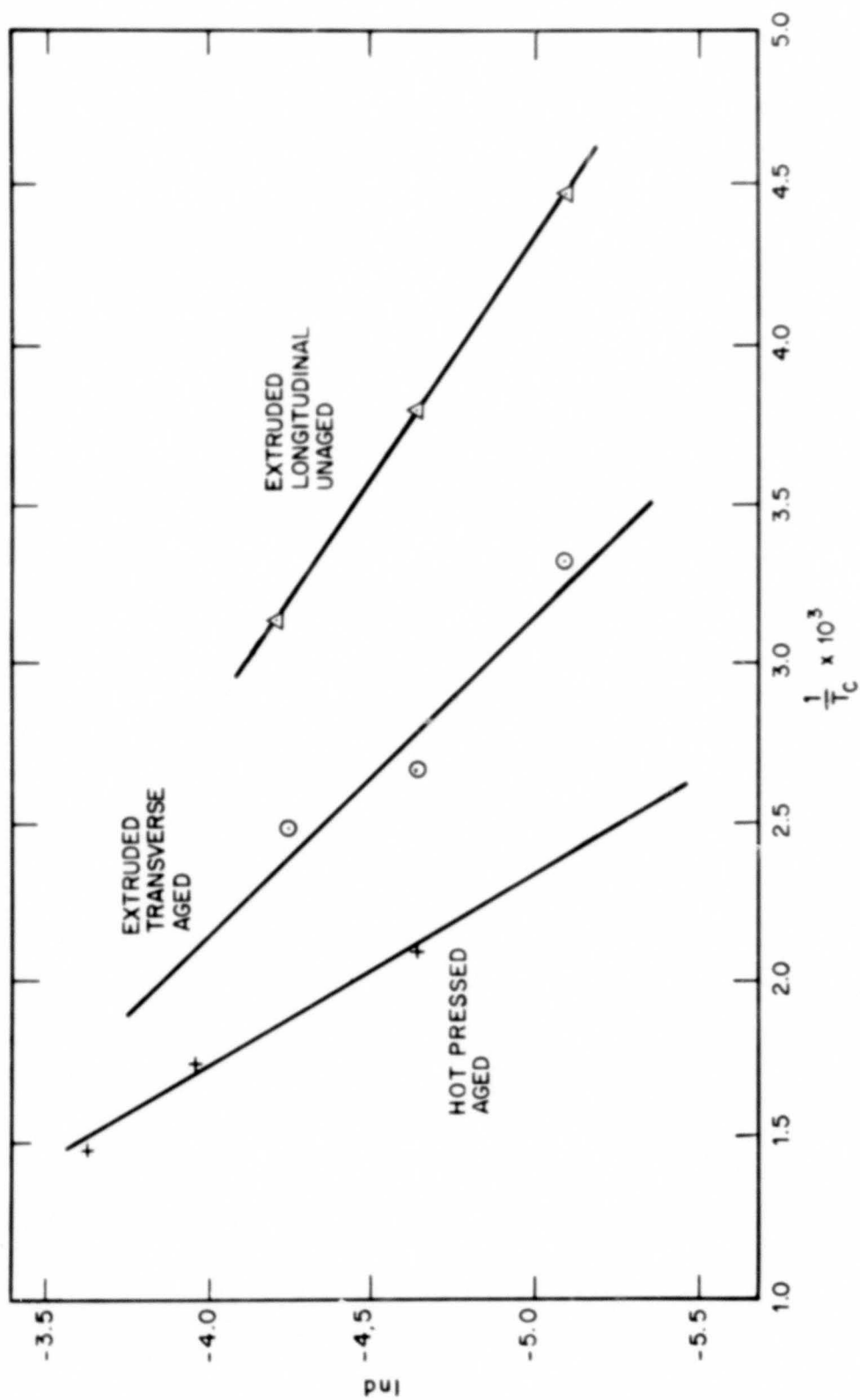


Figure 39 - $\ln d$ vs. $1/T_c$ plots for Brush beryllium.

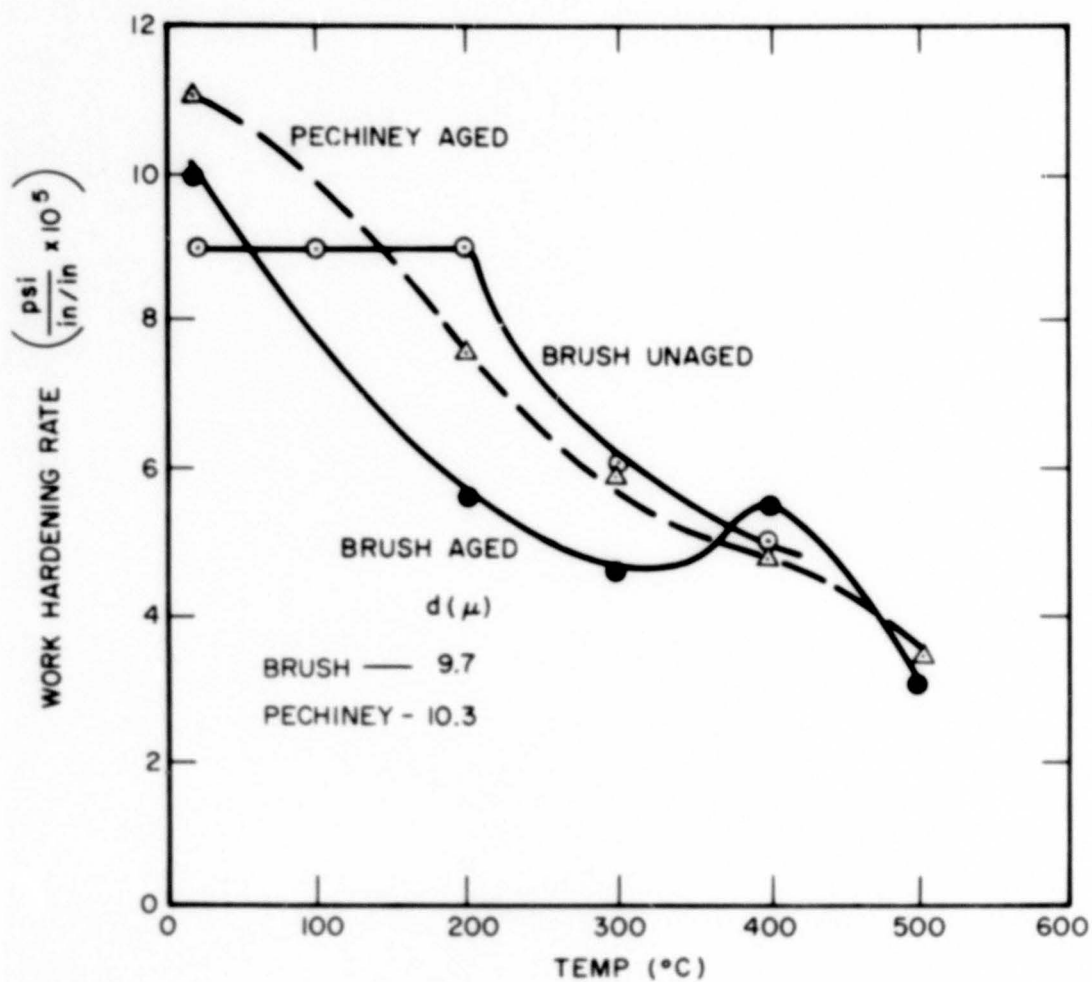


Figure 40 - Work hardening rates at 1 per cent strain for hot-pressed beryllium.

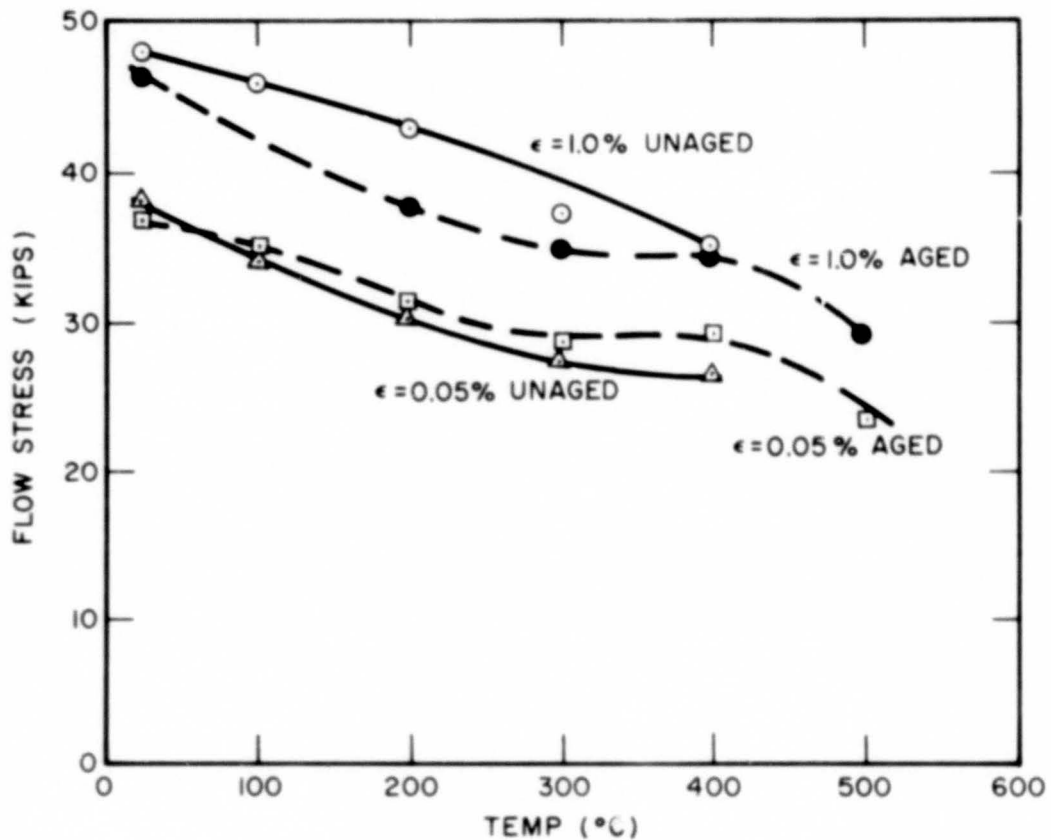


Figure 41 - Flow stress at 0.05 and 1.0 per cent strain for hot-pressed Brush, $d = 9.7$ microns.

However, in some cases material with a high work hardening rate had better ductility. The comparisons may be complicated by textural variations within an extrusion and also be possible textural differences between Brush and Pechiney extrusions of similar grain size. Figure 42 shows the data obtained.

Since there was some indication that good ductility could be correlated with low work hardening rates, theories of work hardening were investigated. A recent review of this subject has been made by McLean (Ref. 48, Chap. 5). The lowest rates of work hardening are found in metals with high stacking fault energy (γ). For example, silver, with a stacking fault energy of less than 20 ergs/cm², has a much higher rate of work hardening than aluminum, with $\gamma = 200$ ergs/cm². The low work hardening rate of beryllium would indicate a high stacking fault energy. Wilsdorf and Wilhelm (Ref. 49) state that beryllium has a high stacking fault energy and Friedel (Ref. 50), citing measurements by Saulnier on extended nodes in a beryllium dislocation network, actually calculates a value of $\gamma = 5 \times 10^{-3}$ Gb, which is 166 ergs/cm².

The reason that metals with high stacking fault energy have low rates of work hardening is that cross slip is easier. Cross slip results when an extended dislocation, blocked by a pile-up or a dislocation tangle, forms a constriction, which bows out and slips on another plane. In metals of high stacking fault energy, the extended dislocations are not very wide, and a relatively small amount of energy is required to form the constriction necessary for cross slip. Obviously, the easier it is to accomplish this, the easier dislocations can move out of pile-ups or tangles, and the lower the rate of work hardening will be. Friedel (Ref. 51) described a thermally activated process whereby screw dislocations, split on the basal plane of a hexagonal metal, recombine to cross slip into a prismatic or pyramidal plane. Flynn, Mote, and Dorn (Ref. 52) successfully applied Friedel's theory to magnesium.

Magnesium is believed to have a high stacking fault energy, since stacking fault ribbons have not been observed, although they have for zinc and cadmium (Ref. 53). The fact that stacking fault ribbons have not been observed in beryllium is further evidence that the stacking fault energy is high, and that cross slip should be easy.

It is therefore proposed that the ductile-brittle transition in beryllium is due to a sudden increase in the probability that cross slip will occur. The applicability of Stroh's theory (Sec. 4.2.2) now becomes apparent, provided certain modifications are made. Assume that dislocations are prevented from moving, either because they are in a pile-up or in a tangle. The latter is more likely, since pile-ups have only been observed rarely in beryllium. If no dislocations can be freed, fracture will occur. However, if additional dislocation motion can be obtained, say by cross slip, then fracture will be delayed. Assuming that constrictions have already occurred as the result of the applied stress acting on the blocked dislocations, we relate the probability of brittle fracture to the probability that a constriction will not bow out and cause additional slip. The constriction here takes the place of the Frank-Read source in Stroh's theory. In fact, it is very similar to a Frank-Read source, in that it is a length of dislocation pinned at the ends. Equation 5 now applies to the constriction in an extended dislocation. The activation energy

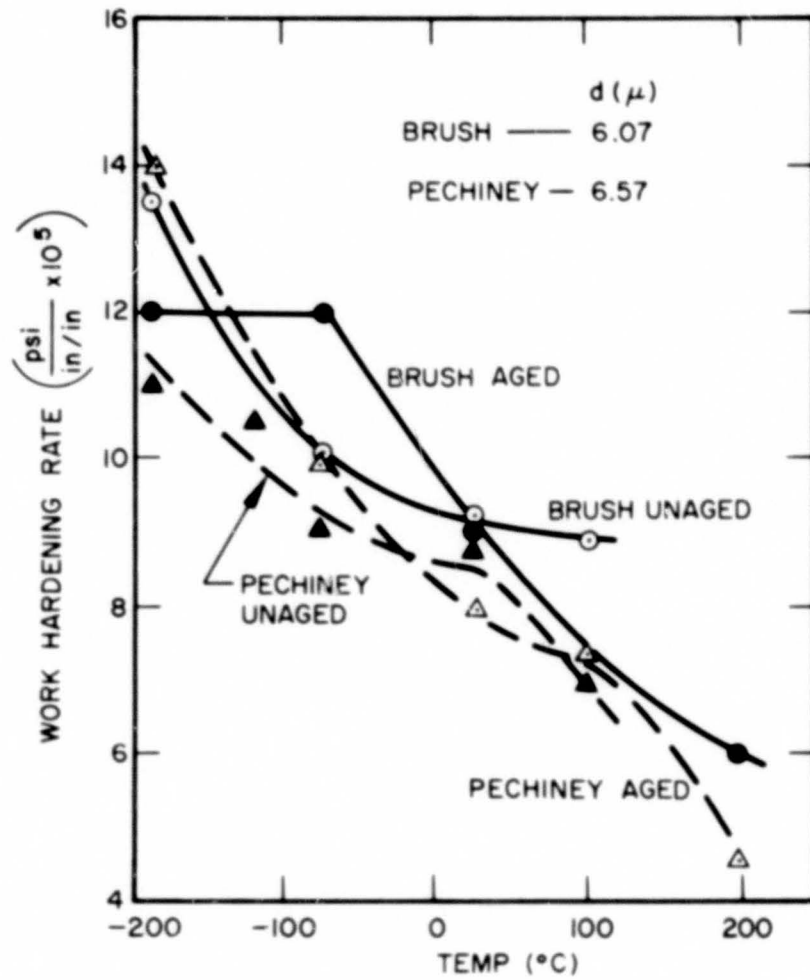


Figure 42 - Work hardening rates at 1 per cent strain for extrusions tested in the transverse direction

refers to the energy required to bow out a constriction. The total activation energy would be the sum of the energy required to cause the constriction to occur plus the energy to bow out the constriction.

We now must inquire as to whether or not the activation energies calculated in Section 4.2.2 are reasonable. For aluminum, which has high stacking fault energy, the energy for bowing out a constriction is 0.95 e.v., whereas for copper, with low stacking fault energy, the energy required is 9.2 e.v. (Ref. 54). From the data given for magnesium (Ref. 52), a value of 0.12 e.v. can be calculated. The activation energies for beryllium (0.19 to 0.36 e.v.) are therefore the correct order of magnitude for a metal with a high stacking fault energy.

It should be possible to obtain verification of the assumption that thermally activated cross slip is responsible for the ductile-brittle transition in beryllium by measuring the temperature and strain rate dependence of the flow stress of single crystals. The data obtained from such studies should make it possible to identify the thermally activated strain-rate-controlling dislocation process at various temperatures. Other thermally activated processes that could control slip are the Peierls mechanism or the dislocation intersection mechanism.

However, assuming that the proposed mechanism does operate to control the transition, the experimental data obtained in the present study can now be rationalized.

Effect of purity. The lower work hardening rates observed for aged material (or for unaged Pechiney samples compared to unaged Brush samples) indicate that cross slip is easier in the aged, or purer, condition. Alloy additions are known to lower the stacking fault energy, and thus make cross slip more difficult (Ref. 48, Chap. 6). Although the unaged beryllium might contain amounts of impurities sufficient to cause a significant reduction in stacking fault energy, this is unlikely. However, Seeger (Ref. 55) proposes another mechanism whereby strains around solute atoms can inhibit cross slip. Dislocations can only cross slip when they are pure screw. The elastic and electrical strains present around solute atoms can make a dislocation line wavy, so that additional energy would be required to straighten it before cross slip could occur. In any event, the probability of cross slip is greater for the material with the least amount of impurity in solid solution, and, consequently, such material should exhibit a lower transition temperature.

Effect of grain size. The reason that the transition temperature is lower for the fine-grained material may be explained simply by Stroh's argument that the more grains there are in a given volume, the greater the probability that one is capable of deforming, in this case, by cross slip. Another possibility is that for any given temperature and amount of strain, the flow stress is always higher for the smaller grain sizes (see for example Figure 29). Since the activation energy is stress dependent, this means that when the stress on the constriction is high, less thermal energy would be required to cause cross slip.

It can also be argued that large grained samples are more susceptible to twinning and bend plane deformation, which would serve to initiate premature failure.

Effect of strain rate. If deformation is controlled by any thermally activated process, then an increased strain rate would tend to reduce the amount of deformation that could be sustained before fracture. Also, the rate of work hardening would be higher for the faster strain rates. Both of these effects were observed in the present study.

Effect of orientation. The ductile-brittle transition temperatures were lower for extruded material than for hot-pressed block. This is a consequence of there being a larger number of grains suitably oriented for flow in the oriented samples. For hot-pressed block, deformation beings in a few suitably oriented grains. As the stress increases, more and more grains contribute to the total deformation, but by this time the applied stress becomes high enough to initiate fracture in the grains that deformed first.

On the basis of the discussion thus far, it might be thought that a ductile-brittle transition should occur only where basal slip is predominant, i.e., in hot-pressed block or in the transverse direction of extruded material. However, Friedel's theory (Ref. 51) assumes that if prismatic slip takes place, then dislocations containing edge components can glide on the prism plane until they combine with dislocations of opposite sign or become blocked. Such blocking can occur in the vicinity of screw dislocations which automatically dissociate with a decrease in energy into their partials on the basal plane. Continued slip therefore requires recombination of the partials on the basal plane to form screw dislocations on the prism plane.

Effect of temperature. The obvious effect of temperature is that cross slip should become easier as temperature increases because of the increased thermal energy available. However, according to Equation 5, a critical temperature, T_c , must be reached before there is a sharp increase in the probability that significant amounts of cross slip will occur and that ductile behavior will result.

The preceding discussion has considered the case for cross slip onto prism planes only. However, there is no reason why the same argument could not be applied to dislocations cross slipping onto a pyramidal plane. Emphasis should be given here to the point that the proposed theory is not based on the initiation of prismatic or pyramidal slip in the ordinary sense, but rather on the thermal activation of cross slip from the basal plane onto either the prismatic or pyramidal plane.

Little discussion has been made of fracture mechanisms in relation to the ductile-brittle transition. The details of the fracture process are not particularly pertinent, since we are concerned primarily with the events leading up to fracture. It will suffice to say that fracture occurs because there is no capacity for plastic flow, and plastic flow ceases when dislocations are no longer free to move.

Section 5

SUMMARY AND CONCLUSIONS

The ductile-brittle transition in beryllium has been investigated from experimental and theoretical standpoints. It has been shown that in two grades of commercial purity beryllium the transition can occur over a wide temperature range, depending on purity, orientation, grain size, and strain rate. Prior to heat treatment, better ductility was observed at certain temperatures for the purer Pechiney CR beryllium than for the relatively impure Brush QMV. However, after an aging treatment, both materials exhibited similar properties. The aging treatment caused the precipitation of impurities from solid solution in the form of compounds, thereby purifying the matrix and increasing the capacity for slip.

The aging treatment of 6 hours at 900°C, followed by 48 hours at 700°C was not an optimum treatment for either material, as strain aging was observed at 400°C in both aged and unaged Brush samples. This indicates that even after precipitation, the matrix was still saturated with impurities. Also, the effects of aging on the Brush material were much greater than on the Pechiney, indicating that a different heat treatment might have been more satisfactory for the latter.

The principal impurity precipitated from solid solution is believed to be iron, since the compounds $\text{Be}_5(\text{Fe}, \text{Al})$ could be identified in all samples, and Be_{11}Fe in the Brush material only, which was initially higher in iron.

Dislocation locking is not believed to be a factor limiting the ductility of randomly oriented beryllium, since treatments which would have freed locked dislocations from impurity atmospheres, i.e., prior strain at elevated temperature, did not improve ductility.

The properties of unaged extrusions at low temperature were contrary to expected behavior in that the longitudinal specimens failed prematurely by twinning, leading to low strength and ductility. Aging resulted in significant improvements in low temperature strength, apparently by reducing the tendency to twin.

The ductile-brittle transition was examined and an attempt was made to explain the transition as being due to the thermally activated cross slip of dislocations from the basal plane into a prismatic or pyramidal plane. The proposed theory was in reasonable agreement with the experimental facts.

This investigation raised several questions that should be the subject of further study. An effort should be made to verify the cross slip theory by studying the temperature and strain rate dependence of flow stress of single crystals. Along with this, work hardening mechanisms should be examined in beryllium, and related to such factors as purity, grain size, strain rate, temperature, and orientation. Further tests should be made at subzero temperatures to establish the conditions better under which beryllium could be used at these temperatures. Consideration should be given to heat treatments that might further improve the ductility of commercial beryllium.

Section 6

REFERENCES

1. W. Beaver and K. G. Wikle, Trans. AIME, 200 (1954) 559.
2. A. R. Kaufmann, E. Gordon, and D. W. Lillie, Trans. ASM, 42 (1950) 785
3. W. Beaver, "Development of Wrought Beryllium Alloys of Improved Properties" Prog. Rep. No. 2, Jan 1958, USAF, D.O. 33(616)-57-19.
4. M. I. Jacobson and F. M. Almeta, "Tensile Failure of QMV Beryllium From Room Temperature to 870°C", Conference on Phys. Met. of Be, London, Oct. 1961.
5. W. D. Bennett, "Recent Beryllium Research in Canada", ibid.
6. B. Allen and A. Moore, "The Tough-Brittle Transition in Beryllium", ibid.
7. J. C. Guest and M. J. Hudson, "Tensile Properties of Hot Extruded Beryllium Rod and Tubing", ibid.
8. P. Cotterill, R. E. Goosey, and A. J. Martin, "An Evaluation of the Hydrogen Content of Commercially Pure Beryllium and its Effect on the Ductile-to-Brittle Transition Temperature", ibid.
9. P. Vachet and M. Logerot, "Mechanical Properties of Extruded Beryllium at Elevated Temperature", ibid.
10. A. J. Meredith and J. Sawkill, "A Precipitation Reaction in Commercially Pure Be", ibid.
11. G. Greetham and A. J. Martin, "The Effect of Purity and Orientation on the Deformation of Beryllium Single Crystals", ibid.
12. J. E. Bunce and R. E. Evans, "A Study of the Effects of Grain Size, Temperature, and Annealing Treatment in the Properties of Wrought Beryllium Ingot", ibid.
13. A. J. Martin and G. C. Ellis, "The Ductility Problem in Beryllium" ibid.
14. R. F. Bunshah, "A Fresh Look at Problems in Beryllium Metallurgy" ibid.

15. C. Gase, "A Study of Mechanical Anisotropy and Heterogeneity in Beryllium Sheets", ibid.
16. J. L. Klein, et al, "The Metal Beryllium", ASM, Cleveland, Ohio, 1955, p.425.
17. G. E. Darwin and J. H. Buddery, "Beryllium", Academic Press, 1960, p. 134.
18. A. P. Green and J. Sawkill, J. Nuclear Materials, No. 1, 1961, p. 101.
19. J. Greenspan, "Ductility in Beryllium Related to Orientation and Grain Size", NMI-1174, Aug. 1957.
20. F. M. Yans, "Third Dimensional Ductility and Crack Propagation in Beryllium Sheet", NMI-1212, March 1959.
21. D. A. Barrow and R. L. Craik, "Fabrication of Beryllium by Hot-Upset Forging ", Conf. on Phys. Met. of Be, London, Oct. 1961.
22. D. R. Mash, Trans. AIME, 203 (1955) 1235.
23. S. H. Gelles, et al, J. Metals 12 (1960) 789.
24. A. Wolff, et al, "Aging Effects in Commercially Pure Be", Beryllium Research and Development Program, ASD-TDR-62-509, Vol. 2., April 1963.
25. M. Herman and G. E. Spangler, "The Flow and Fracture Characteristics of Zone-Melted Beryllium" Conf. on Phys. Met. of Be, London, Oct. 1961.
26. K. L. Edwards and A. J. Martin, "The Purification of Beryllium by Distillation and Zone Melting", ibid.
27. N. A. Hill, "The Effects of Various Treatments Upon the Tensile Properties of Beryllium Sheet", ibid.
28. M. I. Jacobson, F. M. Almeter, and E. C. Burke, "Surface Damage in Beryllium", Beryllium Research and Development Program, ASD-TDR-62-509, Vol. 1, 1962.
29. B. D. Cullity, "Elements of X-Ray Diffraction", Reading, Mass. Addison-Wesley, 1955, pp. 285-295.
30. G. F. Decker, et al, J. App. Phys. 19 (1948) 382.
31. M. Field and M. E. Merchant, J. App. Phys. 20 (1949) 741.
32. H. P. Rooksby, J. Nuclear Materials 7 (1962) 205.

33. Y. Adda, et al, Compt. Rend. 254 (1962) 1052
34. A. B. Brown, F. Morrow, and A. J. Martin, J. Less Common Metals, 3 (1961) 62.
35. J. Sawkill, J. E. Meredith and E. Parsons, "A Precipitation Reaction in Commercially Pure Beryllium", Tube Investments Res. Lab. Rep. 127, 31 Jan 1963.
36. C. M. Weaver, Nature, 180 (1957) 806.
37. S. A. Main, Iron and Steel, Oct. 1958, p. 479.
38. R. I. Garber, I. A. Gindin, and Yu V. Shubin, Soviet Physics JETP, 36, (1959) 260.
39. A. H. Cottrell and D. F. Gibbons, Nature 162 (1948) 488.
40. L. H. Wain and A. H. Cottrell, Proc. Phys. Soc. B63, (1950) 339.
41. G. T. Hahn, Acta Metallurgica, 10 (1962) 727.
42. J. H. Keeler, Trans. Amer. Soc. Metals, 48 (1956) 825.
43. R. B. Shaw, et al, Trans. Amer. Soc. Metals, 45 (1953) 249.
44. G. L. Tuer and A. R. Kaufmann, "The Metal Beryllium", ASM, Cleveland, 1955, p. 409.
45. M. I. Jacobson and E. C. Burke, Beryllium Research and Development Program, QPR for 1 April 1962 through 30 June 1962. NMI-9522, p.9.
46. A. H. Cottrell, Trans. AIME 212 (1958) 192.
47. A. H. Stroh, Advances in Physics 6 (1957) 418.
48. P. McLean, "Mechanical Properties of Metals", J. Wiley and Sons, New York, 1962.
49. H. G. F. Wilsdorf and F. Wilhelm, "On the Behavior of Dislocations in Beryllium", Conf. on Phys. Met. of Be, London, 1961.
50. J. Friedel, in "Electron Microscopy and Strength of Crystals", Interscience, New York, 1963, p. 633.
51. J. Friedel, in "Internal Stresses and Fatigue", Elsevier, Amsterdam, 1959, p. 220.
52. P. W. Flynn, J. Mote and J. E. Dorn, "On the Thermally Activated Mechanism of Prismatic Slip in Magnesium Single Crystals" 7th Tech. Rep., Dec. 1, 1960.

53. P. B. Price, in "Electron Microscopy and Strength of Crystals", Interscience, New York, 1963, p. 41.
54. G. Schoeck and A. Seeger, in "Defects in Crystalline Solids", The Physical Society, London, 1955, p. 340.
55. A. Seeger, in "Dislocations and Mechanical Properties of Crystals", J. Wiley, New York, 1957, p. 243.

APPENDIX I

EFFECT OF STRAIN RATE ON MECHANICAL PROPERTIES OF HOT-PRESSED BLOCK

Table 7

EFFECT OF STRAIN RATE ON MECHANICAL PROPERTIES OF BRUSH HOT-PRESSED BLOCK

Grain Size, μ	Condition	Temp, $^{\circ}\text{C}$	Strain rate, per min.	Ultimate Tensile Strength, Kips	0.1% Offset Yield Strength Kips	Elong. % in 1.5 in.	Reduction in Area, %
26.5	Unaged	23	0.0033	28.0	25.7	0.7	1.7
18.9	"	"	"	37.7	29.9	1.2	1.1
9.7	"	"	"	49.9	39.5	1.5	1.4
26.5	Aged	"	"	27.6	25.1	0.6	0.0
18.9	"	"	"	34.7	27.8	1.0	1.2
9.7	"	"	"	45.8	38.4	1.1	1.5
26.5	Unaged	200	"	28.3	22.0	1.3	2.2
18.9	"	"	"	31.8	22.0	1.8	4.4
9.7	"	"	"	46.1	35.3	1.9	2.3
26.5	Aged	"	"	31.1	18.5	1.2	1.2
18.9	"	"	"	29.4	21.8	2.3	2.0
9.7	"	"	"	43.2	32.2	3.8	4.6
26.5	Unaged	400	"	25.6	17.9	2.9	4.4
18.9	"	"	"	30.1	21.0	4.1	7.8
9.7	"	"	"	38.9	28.8	6.6	14.5
26.5	Aged	"	"	26.6	18.1	3.0	4.6
18.9	"	"	"	32.4	20.4	8.2	21.8
9.7	"	"	"	38.8	28.6	5.6	23.3
26.5	Unaged	23	0.033	31.9	29.6	0.7	1.2
18.9	"	"	"	38.7	31.5	1.3	0.8
9.7	"	"	"	47.8	40.2	1.1	2.0
26.5	Aged	"	"	31.0	26.4	1.0	1.1
18.9	"	"	"	37.9	29.4	1.4	2.0
9.7	"	"	"	50.2	39.7	1.5	1.9
26.5	Unaged	200	"	26.0	20.7	1.06	0.8
18.9	"	"	"	32.2	24.4	1.6	2.0
9.7	"	"	"	45.1	34.8	1.9	2.0
26.5	Aged	"	"	26.3	21.1	1.2	1.1
18.9	"	"	"	32.5	24.2	1.7	2.0
9.7	"	"	"	44.4	34.8	2.1	3.0
26.5	Unaged	400	"	26.4	18.5	3.1	4.3
18.9	"	"	"	27.2	17.5	3.2	6.3
9.7	"	"	"	36.0	25.8	5.2	17.5
26.5	Aged	"	"	26.5	17.9	3.7	5.4
18.9	"	"	"	28.9	17.7	9.3	18.3
9.7	"	"	"	40.3	28.5	6.8	18.9
26.5	Unaged	23	0.33	33.8	30.4	0.8	1.2
18.9	"	"	"	36.5	30.9	0.9	1.6
9.7	"	"	"	47.3	41.2	0.9	2.1
26.5	Aged	"	"	28.9	25.9	0.6	1.1
18.9	"	"	"	37.9	28.6	1.5	2.4
9.7	"	"	"	51.0	39.3	1.7	2.3
26.5	Unaged	200	"	27.4	22.0	1.1	0.8
18.9	"	"	"	33.3	25.0	1.4	2.0
9.7	"	"	"	47.8	38.2	2.3	3.3
26.5	Aged	"	"	27.7	21.5	1.2	1.2
18.9	"	"	"	33.3	24.8	1.8	1.2
9.7	"	"	"	47.8	35.8	2.4	2.4

Table 7 (Continued)

Grain Size μ	Condition	Temp., °C	Strain rate per min.	Ultimate Tensile Strength, Kips	0.1% Offset Yield Strength Kips	Elong. % in 1.5 in.	Reduction in Area, %
26.5	Unaged	400	0.33	26.6	18.7	2.1	3.6
18.9	"	"	"	28.9	19.7	2.7	5.1
9.7	"	"	"	39.1	28.4	3.3	6.2
26.5	Aged	"	"	23.4	16.7	2.5	4.2
18.9	"	"	"	27.6	17.7	4.7	9.8
9.7	"	"	"	40.7	28.7	3.5	7.1

Table 8

EFFECT OF STRAIN RATE ON MECHANICAL PROPERTIES OF PECHINEY HOT-PRESSED BLOCK

Grain Size,	Condition	Temp., °C	Strain rate, per min.	Ultimate Tensile Strength Kips	0.1 % Offset Yield Strength Kips	Elong. % in 1.5 in.	Reduction in Area %
13.2	Unaged	23	0.0033	30.3	24.1	0.8	0.0
11.0	"	23	"	39.0	28.8	1.2	1.1
10.3	"	"	"	43.6	32.7	1.2	2.2
13.2	Aged	"	"	31.4	29.5	-	2.0
11.0	"	"	"	28.5	26.6	0.6	1.1
10.3	"	"	"	45.9	35.4	1.2	2.1
13.2	Unaged	200	"	31.9	24.8	1.6	2.2
11.0	"	"	"	32.1	23.8	1.4	1.1
10.3	"	"	"	45.4	31.8	2.8	3.3
13.2	Aged	"	"	28.2	21.4	1.5	2.1
11.0	"	"	"	30.5	22.0	2.2	3.3
10.3	"	"	"	41.4	30.0	2.2	0.8
13.2	Unaged	400	"	26.7	18.9	7.4	20.0
11.0	"	"	"	31.0	22.6	6.1	22.0
10.3	"	"	"	31.0	24.5	4.0	14.5
13.2	Aged	"	"	25.3	20.6	6.4	23.4
11.0	"	"	"	24.7	16.4	5.7	15.8
10.3	"	"	"	34.4	24.2	7.9	28.6
13.2	Unaged	23	0.033	33.9	31.1	0.7	0.0
11.0	"	"	"	37.3	32.7	0.9	0.0
10.3	"	"	"	45.7	37.4	1.1	1.2
11.0	Aged	"	"	38.3	30.9	1.1	0.8
10.3	"	"	"	42.5	35.3	0.9	0.0
13.2	Unaged	200	"	32.1	24.8	1.4	0.8
11.0	"	"	"	32.7	24.8	1.6	0.8
10.3	"	"	"	41.7	31.5	1.8	1.6
11.0	Aged	"	"	36.1	26.3	2.2	2.3
10.3	"	"	"	41.7	30.4	1.7	1.6
13.2	Unaged	400	"	26.8	17.1	11.9	33.1
11.0	"	"	"	26.3	18.3	3.8	6.5
10.3	"	"	"	32.5	21.9	4.9	11.4
11.0	Aged	"	"	28.3	18.7	11.8	25.4
10.3	"	"	"	32.5	22.8	6.7	22.2
13.2	Unaged	23	0.33	21.6	-	0.3	0.0
11.0	"	"	"	36.1	31.5	1.0	0.0
10.3	"	"	"	42.5	36.8	0.9	0.8
10.3	Aged	"	"	47.6	35.0	1.1	0.8
13.2	Unaged	200	"	25.7	24.9	0.5	1.2
11.0	"	"	"	36.1	37.4	1.4	1.4
10.3	"	"	"	42.0	31.1	1.6	1.2
11.0	Aged	"	"	37.2	27.2	1.6	0.8
10.3	"	"	"	41.1	29.6	1.5	2.3
13.2	Unaged	400	"	25.3	17.5	2.5	3.5
11.0	"	"	"	32.5	20.8	7.4	11.4
10.3	"	"	"	38.9	25.8	8.0	15.1
11.0	Aged	"	"	30.9	19.1	12.3	23.8
10.3	"	"	"	35.5	26.4	12.1	27.0